Study on dispersion of lead-zinc-bearing mine wastes by considering local weather conditions and waste properties in the Kabwe mine, Zambia

ザンビア国カブウェにおける気象条件および鉱滓性状を考慮した鉛・亜鉛系鉱山廃棄物飛散に関する研究

Shinsaku Nakamura

Division of Sustainable Resources Engineering
Graduate School of Engineering
Hokkaido University, Japan

March 2022

Abstract

Mining is a key industry in Zambia. Lead (Pb), zinc (Zn), cobalt, and copper were mined and smelted in Kabwe, Zambia between 1902 and 1994. Mine tailings from these activities have been littered at the dumping site, and it has huge impacts on environmental and human health issues through heavy metal contamination. Impacts and circumstances have been studied and analyzed, but the mechanisms of heavy metal dispersion and deposition by the local weather factors in Kabwe have not been evaluated well. In this study, for elucidating the mechanisms of heavy metal dispersion by winds and other weather conditions, dispersion models were designed and applied to the Kabwe mine. Environmental factors, such as local weather data and water condition in soils were analyzed for understanding their own impacts on the heavy metal contamination in Kabwe.

In Chapter 1, the importance, methods, and the study site for evaluating mechanisms of heavy metal dispersion and deposition were described through discussion on environmental impacts and issues by heavy metal contamination in Kabwe by introducing the background of mining activities and current situations of heavy mental contamination and its impacts on human health especially children and infants.

In Chapter 2, dispersion of Pb-bearing tailings (ISF-slag) was simulated for reproducing Pb contamination of soil in Kabwe. Local weather data of the year 2019 were monitored in situ and used for the simulations. The plume model, weak puff model, and no puff model were adopted for calculation of Pb dispersion under different wind conditions. The results showed that Pb dispersion from the Kabwe mine was directly affected by wind directions and speeds in the dry season, although it was not appreciably affected in the rainy season. This may be because the source strength is lower in the rainy season due to higher water content of the surface. This indicates that Pb-bearing soil dispersion patterns depend on the season. In addition, the distribution of the amount of deposited Pb-bearing soils around the mine corresponded to the distribution of measured Pb contents in soils. These results suggest that Pb contamination in soils primarily results from dispersion of mine tailings, in particular finer wastes.

In Chapter 3, the effects of local weather factors on mechanisms of heavy metal contamination were analyzed based on the results in Chapter 2. Weather in Kabwe was calm through the year, but there were significant differences of solar radiation, barometric pressure, humidity, and air temperature between rainy and dry seasons. Correlation between wind speed and solar radiation was inversely proportional, and affected the accumulated amounts deposited by simulations. Although high wind speeds had huge impacts on Pb-bearing tailing dispersion on the playground in shorter distance from the source, high and low wind speeds did not affect the accumulated amounts deposited at certain distances from the source. Wind directions had large impacts on

dispersion and deposition areas. These results indicate that not only wind speeds and directions but also complicated relationships among weather factors cause Pb-bearing mine tailing dispersion and deposition.

In Chapter 4, for evaluation of dispersing situations and impacts of ponding water at Pb-bearing Zn plant leach residue site, which is often found in the mine throughout a year, simulation of Pb dispersion from the plant leach residue site was performed with modified normalized difference water index (MNDWI) under the actual weather conditions in the year 2019. The MNDWI was demonstrated by data analysis of Sentinel-2 datasets, which were acquired in the year 2019. The index was an indicator for monitoring the soil condition of the source and it is one of parameters necessary for estimating Pb dispersion. Ponding water is an effective inhibiting factor on windborne Pb dispersion. Wind speeds and directions had large impacts on windborne Pb dispersion when MNDWI indicated negative values. Analyzing and understanding environmental conditions that can be factors for windborne Pb dispersion are crucial for countermeasures on Pb dispersion and remediation of soil contamination.

In Chapter 5, all results in this dissertation were summarized, and the expected practical utilization of the results and methods were proposed.

日本語要旨

ザンビアにおいて鉱山は重要な産業である。鉛 (Pb)、亜鉛 (Zn)、コバルト、銅は 1902 年から 1994 年の間にザンビア国カブウェで採掘され、精錬された。これらの活動による鉱滓は集積場に 放置され、重金属汚染源として環境や人々の健康に大きな影響を及ぼしている。重金属汚染の影響 や被害は分析、評価されているが、カブウェの地域的気象要因による重金属の飛散および沈積のメ カニズムは十分に評価されていない。そこで本研究では、風やその他の気象条件による重金属飛散 のメカニズムを解明するために、飛散シミュレーションモデルを構築し、カブウェ鉱山に適用し た。さらに、カブウェにおける重金属汚染に対する影響を明らかにするため、気象データや土壌中の水分分布など環境要因を評価した。

第 1 章では、カブウェにおける採掘活動の背景や重金属汚染の現状、子どもや幼児の健康への 影響についての文献調査をとおして、重金属の飛散および沈積のメカニズムを分析する重要性、方 法、研究地点について記述した。

第 2 章では、鉱滓に含まれる Pb の飛散量を評価するモデルを開発し、カブウェにおける土壌の Pb 汚染の状況を再現した。2019 年の現地気象データを収集し飛散シミュレーションに適用した。 風速にあわせて 3 つのシミュレーションモデル (plume model、weak puff model、no puff model) を 採用した。カブウェ鉱山からの Pb 飛散量は、ISF-スラグ集積場を煙源の束と仮定し計算した。そ の結果、乾季においては風向と風速に大きな影響を受けることが明らかになった。一方で雨季にお いてはこれらの影響をあまり受けないことがわかった。これは、雨季には地表の水分量が多いこ とから、煙源から舞い上がる鉱滓量 (煙源強度) が低かったためである。このことは、Pb 飛散のパターンが季節によって異なることを示唆した。さらに、鉱山周辺に沈積した鉱滓による土壌の Pb 汚染の傾向は、鉱山周辺の表土をサンプリングし、分析して得られた Pb 含有量と一致した。これ らの結果は、土壌の Pb 汚染が主に集積場からの微細な鉱滓の飛散により生じていることを示唆し ている。

第 3 章では、第 2 章の結果をもとにカブウェ地域の気象要因が重金属汚染のメカニズムに及ぼ す影響を評価した。カブウェの天候は年間をとおして穏やかであるが、雨季と乾季では日射量、湿 度、気温に大きな差があった。風速と日射量の相関は反比例しており、シミュレーションによって 算出された飛散量および沈積量に影響を及ぼした。強風は、煙源からより近い距離にある表土への Pb を含む鉱滓の飛散量に大きな影響を与えた。しかし、強風と弱風は、煙源から一定以上の距離 にある表土への Pb を含む鉱滓の飛散量には影響を与えなかった。風向は、Pb を含む鉱滓の飛散量 と沈積する地点に大きな影響を与えた。これらの結果は、風速や風向だけでなく、複雑に関係する 気象要因が Pb を含む鉱滓の飛散とそれによる土壌汚染に影響を与えていることを示唆している。

第 4 章では、年間をとおして鉱山内に見られる Zn リーチング残渣の集積場における土壌水分量 の状況や Zn を含む鉱滓の飛散への影響を評価するため、Pb を含む Zn リーチング残渣の飛散シ ミュレーションを行った。シミュレーションには、2019 年に収集したカブウェの気象条件のもとで 改良型正規化差分水指数 (modified normalized difference water index、MNDWI) を用いてリーチン グ残渣からの飛散量を分析した。

MNDWI には 2019 年に観測された欧州の光学衛星 (Sentinel-2) データを用いた。この指数は、煙源の土壌水分量を評価し、リーチング残渣飛散量を推定するため に必要なパラメータのひとつである。冠水は、風を媒体とするリーチング残渣飛散にとって効果的な阻害因子である。風速と風向は、MNDWI が負の値を示したとき重金属飛散量に大きな影響を与 えた。Pb や Zn の飛散の要因となりうる環境条件を評価することは、リーチング残渣飛散に対する 効果的な対策と土壌汚染の修復を提案する上で重要である。

第 5 章では、本研究の結果を要約するとともに、結果の活用法を提案した。

Table of Contents

Chapter 1. General introduction

1.1. Background

Heavy metals and metalloids from mining and smelting activities have huge impacts on environmental pollution [1, 2]. Environmental as well as human health issues are increased by heavy metal contaminations from such activities [3]. The impacts of the pollution appear for the workers of mine companies and people living around the mines through incidental dust ingestion and inhalation [4]. In particular, soil pollution by heavy metals from mine areas in arid countries is one of the serious issues to be solved.

Mining is the key industry in Zambia. Mineral resources, such as lead (Pb), zinc (Zn), cobalt (Co) and copper (Cu) had been mined and smelted for over 90 years between 1902 and 1994 in Kabwe, Zambia [5]. Unrefined mining residues have been dumped at the mine like a hill, and they have been exposed to the environment until today. For this reason, Kabwe was ranked as one of the worst polluted areas in the world [6]. The dumping site in Kabwe is thought to be the source of contamination, and the Pb-bearing soils are dispersed by winds around the mine. Thus, the heavy metals contained in the residues directly induce environmental and health problems. Nakayama et al. [7] indicated that soil samples from roadsides in Kabwe had higher concentrations of Pb than benchmark values. Results of spectral measurements and satellite data around the dumping site indicated high Pb contents (>1000 mg/kg as total) in the soils within 2 km from the site [8]. The mean blood Pb levels of the population in Kabwe were estimated at 11.9 μg/dL (11.6–12.1 μg/dL) by blood sampling from volunteers with backgrounds with geographic, demographic, and socioeconomic information. Moreover, Pb contamination has influenced children's health: about 50 % of children took in an intolerable daily intake [9]. For mitigation and remediation of this environmental issue, immobilization techniques by dolomite, calcined dolomite, and magnesium oxide were performed [10], and concurrent dissolution and cementation methods were proposed [11]. Although Pb contamination and its impacts on the environment and human health have been unveiled and mitigated by multilateral approaches in Kabwe, the mechanisms of heavy metal dispersion from the mine are not quantitatively evaluated.

Evaluation of the causes of heavy metal contamination, including Pb and Zn from the dumping site is an indicator for countermeasure of environmental and human health maintenance. In this study, the mechanisms of how Pb- and Zn-bearing mine soils dispersed and deposited from the dumping site are clarified with the year 2019 weather data and three simulation models tailored wind speeds in Kabwe District.

In this chapter, the background, issues, the purpose and the site of the study are summarized.

1.2. Conditions of heavy mental contamination in Kabwe

Kříbek et al. [12] had samples and analyzed the soil contamination at the same area of this study and clarified the conditions of Pb-Zn-bearing soil contaminations and impacts on human health (Figure 1-1). They collected soils from 0 to 3 cm depth and 70 to 90 cm depth for assessment of the extent and intensity of the anthropogenic contamination. In the area at the downwind (northwest direction) from the dumping site, the amounts of Pb and Zn contents in topsoil were higher than the Canadian land where is permitted for ecological limits used only. Kříbek et al. concluded their results agreed with the contamination caused by human activities. High amounts of Pb-bearing soil contaminations at northwest side from the dumping site were detected by sampling soils and geospatial analysis by Wen as shown in Figure 1-2 [13].

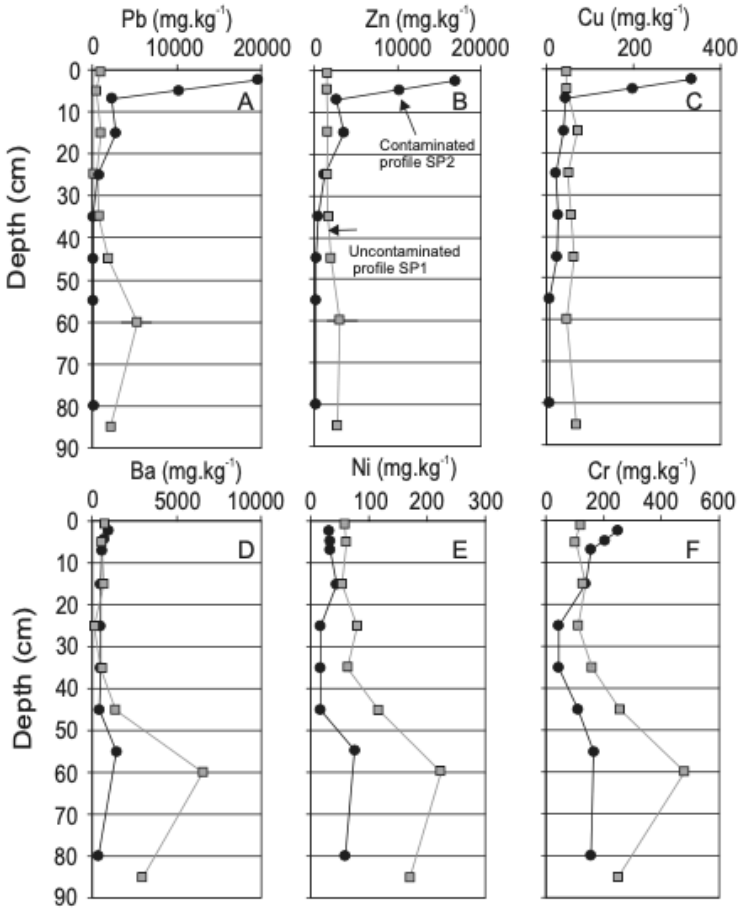

Figure 1- 1. Distribution of Pb (A), Zn (B), Cu (C), Ba (D), Ni (E) and Cr (F) in an uncontaminated soil profile SP-1 and contaminated profile SP-2. FP-XRF data by Kříbek et al. [12]. Charts indicated that amounts of Pb- and Zn-bearing soils at the top were extremely higher than other minerals.

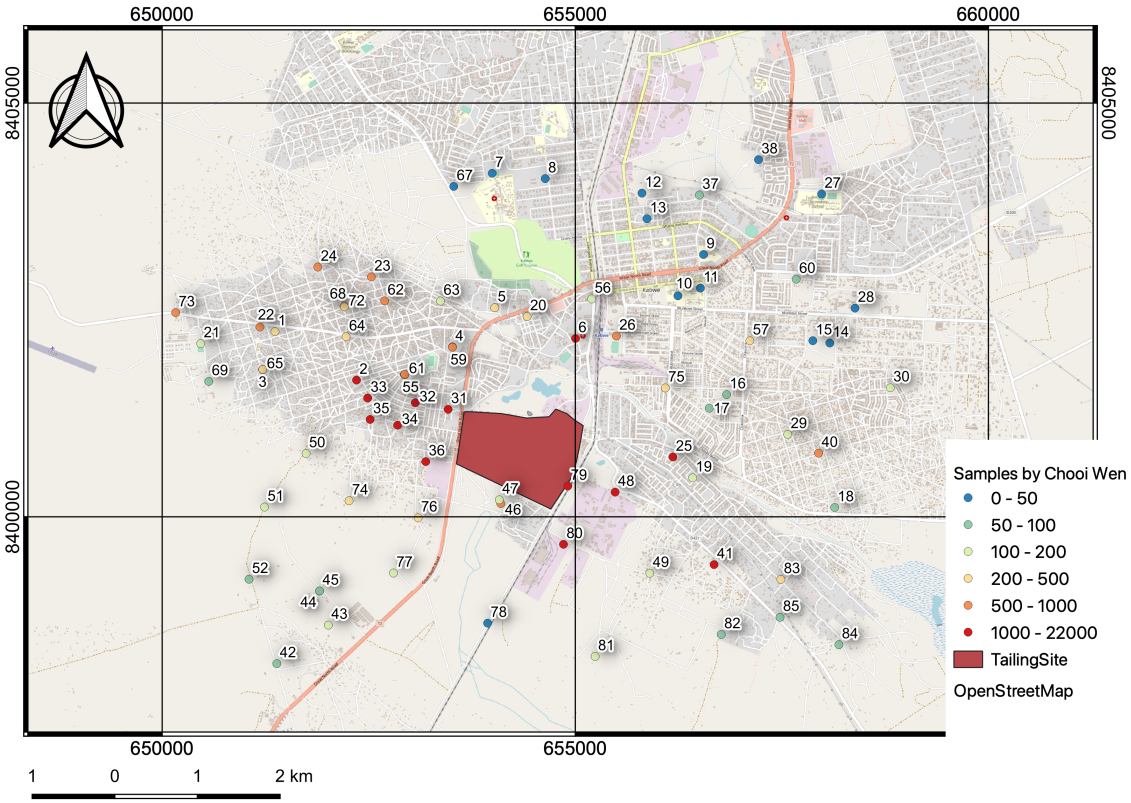

Figure 1- 2. Pb contents of soils by Wen, L. C. [13]. The author mapped Wen's results by QGIS. The results indicated that high amounts of Pb-bearing soils were collected at north-west to west sites widely.

Heavy metal contaminations in Kabwe affect children seriously. Yabe et al. measured Pb excretion levels in children in Kabwe, and they concluded that children near Pb-Zn mine are at serious risks of Pb poisoning because fecal and urine Pb levels very high as 2,252 mg/kg and 2,914 μg/L respectively [14]. Toyomaki et al. took breastmilk and blood samples from 418 pairs of infants and their mothers for measuring the blood lead levels (BLL). The highest BLLs in infants and their mothers were 93.4 μg/dL and 82.6 μg/dL, respectively. They also indicated Pb isotope ratios in infants' feces were similar to those in Pb-bearing soils [15].

From the above literal research results, contaminations of Pb- and Zn-bearing soils expanded from the mine dumping site are obvious, and human health of people especially infants and children are threatened by the heavy metal poisoning caused by mining activities in Kabwe. Although damages and effects of heavy metal contaminations from the mine area have been studied and discussed, the fundamental mechanisms of Pb- and Zn-bearing mine residue dispersions, which are causes of contaminations, have not been identified. Making clear the mechanisms of heavy metal contamination in

Kabwe is one of the indicators for remediation methods of heavy metal dispersion from the mine area and maintaining children's health as a future result in Kabwe.

1.3. Purpose of the study

The purpose of this study is to understand mechanisms of Pb- and Zn-bearing mine residue dispersion and to quantify Pb contamination of soils in Kabwe by simulating Pb dispersion with local weather data of the year 2019, and then comparing the simulated results with measured Pb content in soils. Moreover, by analyses on local weather data of the year 2019 and terrain features of Kabwe, the local mechanisms of heavy metal dispersion are clearly understood. Lead and Zn were selected as target toxic elements for the simulation because Pb and Zn seriously affect the health of children in Kabwe.

1.4. Study site

According to the Provincial Administration, Kabwe is the capital city of the Central Province, the Republic of Zambia. It is located about 139 km north from Lusaka, the capital city of Zambia (Figure 1-3). Kabwe was named after the local name, "Kabwe Ka Mukuba" meaning place of smelting [16].

Mine in Kabwe was one of the oldest mines in Zamba, and it was closed in 1994. About 6.4 million tons of historical tailings have been remained in the south side of Downton Kabwe [17]. 351,386 tons of Pb and 356,843 tons of Zn were estimated to be recovered from the tailing, and the operation has been started in 2019 [18].

In this study, the dumping site and its surrounding area especially northwest side (downwind direction) from the dumping site were selected as the study site. The dumping site as the source area was extracted and calculated geographical features by satellite datasets including Sentinel-2, Shuttle Radar Topography Model (SRTM) and PLASAR digital elevation model (DEM) for simulating Pb- and Zn-bearing soil dispersions to Kabwe area. The simulated results were compared with the results of Pb content in surrounding surface soils.

(a)

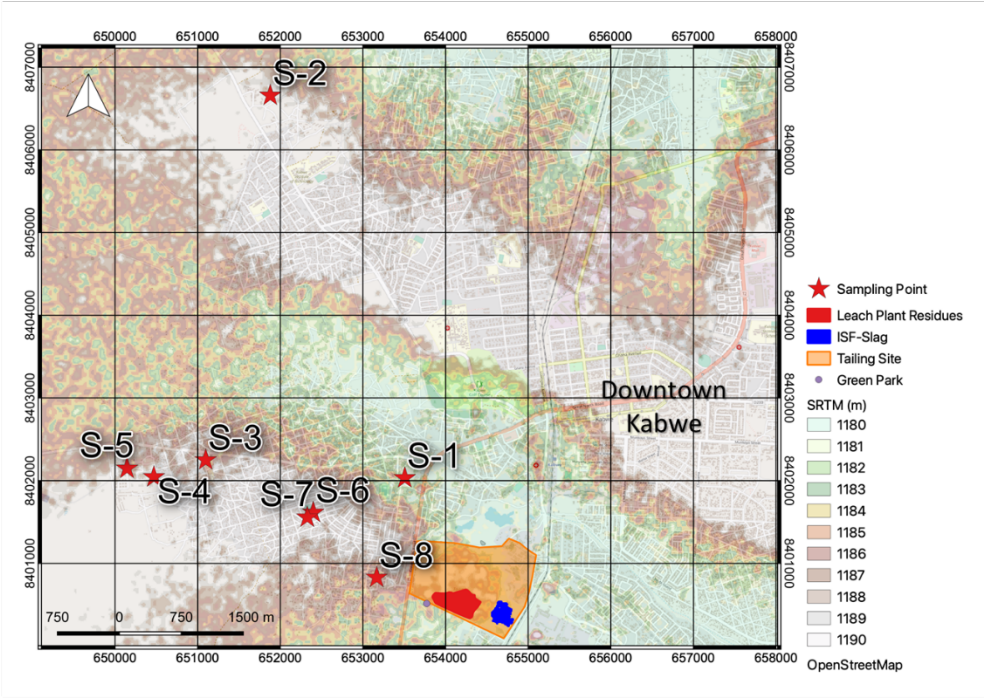

(b)

Figure 1- 3. Study site: (a) territory of Zambia and location of Kabwe and (b) locations of dumping sites (source areas) and playgrounds (sampling points; S-1 - S-8).

1.5. Structure of this thesis

This study consists of five chapters. The content of each chapter is shown below.

In Chapter 1, general introduction including the background, purpose and contents of this study is described.

In Chapter 2, establishment of Pb-bearing soil dispersion models in Kabwe, dispersion simulation between ISF-slag named Black Mountain as the source area and eight playgrounds as target and sampling points of Pb contamination were described and evaluated with local weather data of the year 2019.

In Chapter 3, weather parametric analysis on Pb-bearing soil dispersion in Kabwe, and the dispersion simulations were performed for evaluating the effects of each weather factor (wind speed, solar radiation, barometric pressure, humidity and air temperature) based on the results of Chapter 2. Moreover, effects of wind directions on the dispersion simulation were performed and evaluated while the other weather factors were fixed as the average values of the rainy and dry seasons of the year 2019.

In Chapter 4, water parametric analysis on Pb- and Zn-bearing soil dispersion in Kabwe, and the dispersions by changes and water condition in soils were evaluated on the Pb-bearing Zn plant leach residue site as a source area. The simulations of dispersion were performed to indicate the correlation between surface water and accumulated amounts from the Pb-bearing Zn plant leach residue site.

In Chapter 5, general conclusion based on the results obtained in this study were summarized.

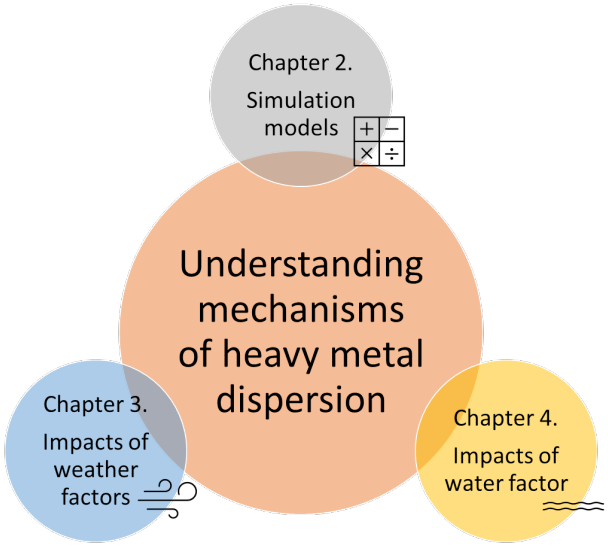

Figure 1- 4. Contents of the thesis: For understanding mechanisms of Pb- and Zn bearing soil dispersion in Kabwe, dispersion models were established in Chapter 2, impacts of local weather factors and water factor on dispersion were analyzed in Chapters 3 and 4, respectively.

References

1. Etter, V. Soil contamination near non-ferrous metal smelters: A review. *Appl. Geochem.* 2016, *64*, 56–74.
2. Nriagu, J.O. A history of global metal pollution. *Science* 1996, *272*, 223.
3. Tchounwou, P.B.; Yedjou, C.G.; Patlolla, A.K.; Sutton, D.J. Heavy Metal Toxicity and the Environment. *Mol. Clin. Environ. Toxicol.* 2012, *101*, 133–164.
4. Ettler, V.; Vítková, M.; Mihaljevicˇ, M.; Šebek, O.; Klementová, M.; Veselovský, F.; Vybíral, P.; Krˇíbek, B. Dust from Zambian smelters: Mineralogy and contaminant bioaccessibility. *Environ. Geochem. Health* 2014, *36*, 919–933.
5. Entwistle, J.A.; Hursthouse, A.S.; Reis, P.A.M.; Stewart, A.G. Metalliferous mine dust: Human health impacts and the potential determinants of disease in mining communities. *Curr. Pollut. Rep.* 2019, *5*, 67–83.
6. Ettler, V.; Sˇteˇpánek, D.; Mihaljevicˇ, M.; Drahota, P.; Jedlicka, R.; Krˇíbek, B.; Vaneˇk, A.; Penížek, V.; Sracek, O.; Nyambe, I. Slag dusts from Kabwe (Zambia): Contaminant mineralogy and oral bioaccessibility. *Chemosphere* 2020, *260*, 127642.
7. Nakayama, S.M.; Ikenaka, Y.; Hamada, K.; Muzandu, K.; Choongo, K.; Teraoka, H.; Mizuno, N.; Ishizuka, M. Metal and metalloid contamination in roadside soil and wild rats around a Pb–Zn mine in Kabwe, Zambia. *Environ. Pollut.* 2011, *159*, 175–181.
8. Uchida, Y.; Banda, K.; Nyambe, I.; Hamamoto, T.; Yoshii, Y.; Munthali, K.; Mwansa, M.; Mukuka, M.; Mutale, M.; Yabe, J.; Toyomaki, H.; Beyene, Y. Y.; Nakayama, S. M. M.; Naruse, N.; Ishizuka, M.; Takahashi, Y. Multidisciplinary field research in Kabwe, Zambia, towards better understanding of lead contamination of the city—A short report from a field survey. *bioRxiv* 2017. Available online: https://www.biorxiv.org/content/10.1101/096164v2.full.pdf (accessed on 28 October 2020).
9. Yamada, D.; Hiwatari, M.; Hangoma, P.; Narita, D.; Mphuka, C.; Chitah, B.; Yabe, J.; Nakayama, S.M.M.; Nakata, H.; Choongo, K.; Ishizuka, M. Assessing the population-wide exposure to lead pollution in Kabwe, Zambia: An econometric estimation based on survey data. *Sci. Rep.* 2020, *10*, 1–11.
10. Tangviroon, P.; Noto, K.; Igarashi, T.; Kawashima, T.; Ito, M.; Sato, T.; Mufalo, W.; Chirwa, M.; Nyambe, I.; Nakata, H.; et al. Immobilization of lead and zinc leached from mining residual materials in Kabwe, Zambia: Possibility of chemical immobilization by dolomite, calcined dolomite, and magnesium oxide. *Minerals* 2020, *10*, 763.
11. Silwamba, M.; Ito, M.; Hiroyoshi, N.; Tabelin, C.B.; Hashizume, R.; Fukushima, T.; Park, I.; Jeon, S.; Igarashi, T.; Sato, T.; et al. Recovery of lead and zinc from zinc

plant leach residues by concurrent dissolution-cementation using zero-valent aluminum in chloride medium. *Metals* 2020, *10*, 531.
12. Kříbek, B.; Nyambe, I.; Majer, V.; Knésl, I.; Mihaljevic, M.; Ettler, V.; Vanek, A.; Penížek, V.; Sracek, O. Soil contamination near the Kabwe Pb-Zn smelter in Zambia: Environmental impacts and remediation measures proposal. *J. Geochem. Explor.* 2018, *197*, 159–173.
13. Wen, L. C. Spatial distribution of heavy metals around the abandoned mine in Kabwe, Zambia. Master's Thesis at Hokkaido University 2018.
14. Yabe, J.; Nakayama, S. M. M.; Ikenaka, Y.; Yohannes, Y. B.; Bortey-Sam, N.; Kabalo, A. N.; Ntapisha, J.; Mizukawa, H.; Umemura, T.; Ishizuka, M. Lead and cadmium excretion in feces and urine of children from polluted townships near a lead-zinc mine in Kabwe, Zambia. *Chemosphere* 2018, *202*, 48-55.
15. Toyomaki, H.; Yabe, J.; Nakayama, S. M. M.; Yohannes, Y. B.; Muzandu, K.; Mufune, T.; Nakata, H.; Ikenaka, Y.; Kuritani, T.; Nakagawa, M.; Choongo, K.; Ishizuka, M. Lead concentrations and isotope ratios in blood, breastmilk and feces: contribution of both lactation and soil/dust exposure to ingants in a lead mining area, Kabwe, Zambia. *Environmental Pollution* 2021, *286*.
16. Provincial Administartion, Centiral Province. A Smart And Value-Centered Public Cervice. Available online: http://www.cen.gov.zm/?page_id=4856 (accessed on 28 November 2021).
17. Mining Technology. Kabwe Mine. Available online: https://www.mining-technology.com/projects/kabwe-mine/ (accessed on 28 November 2021).
18. Jubilee Metals Group. Operations Lead, Zinc & Vanadium. Available online: https://jubileemetalsgroup.com/operations/lead-zinc-vanadium/ (accessed on 28 November 2021).

Chapter 2. Establishment of lead-bearing soil dispersion models in Kabwe

2.1. Introduction

Huge amounts of fine-grained residue materials were processed and stacked through mining activities in Kabwe. The mass of mine waste materials is eroded by winds, and it is a potential of air and soil pollutions [1]. Wind is considered as one of the causes for heavy metal contamination from the mine sites in the world. Lead- and Zn-bearing soils were reported to be dispersed by winds to about 1,500 m away from the mine site and there was not significant difference between metal contents in topsoil and dust samples from the mine site at Kushk Pb-Zn mine, Iran [2]. At Kombat mine, Namibia, Mileusnić et al. revealed high contents of Cu and Pb in tailing site (9,086 mg/kg and 5,589 mg/kg respectively) and agriculture filed (150 mg/kg and 164 mg/kg respectively) in the dry season, and they suggested that winds disperse the tailings predominantly to agricultural fields around the mine area [3]. Tembo et al. collected samples around the Kabwe mine within 20 km and used atomic absorption spectrometry for analyzing soils. They detected 758 mg/kg of Pb and 234 mg/kg of Zn, and they concluded the results were agreed with wind flow patterns in Kabwe [4]. Researchers have suggested that winds are causes of heavy metal dispersion around the mine areas, but the mechanisms of windborne dispersion from the mine areas have fully not been discussed yet.

In this chapter, dispersion of Pb at the dumping site was simulated for reproducing Pb contamination of soil in Kabwe. Local weather data of the year 2019 were collected in situ and used for the simulations. The plume model, the weak puff model, and the no puff model were adopted for calculation of Pb-bearing soil dispersion under different wind conditions.

2.2. Materials and methods

2.2.1. Study site

A dumping site of Pb- and Zn-bearing mine residues in Kabwe (a red polygon on Figure 1-3) was selected as the source of contaminants for simulating Pb-bearing soil dispersion because the wastes are stacked as a small hill, named Black Mountain, and causes fine soil particles to be swirled up by winds [5]. The height of the source was estimated at the same height of the ISF-slag hill, and it was calculated with SRTM with 30 m spatial resolution. Although a single point, such as the location of a chimney in industrial factories, was used for the simulation [6], the source was adopted as a bundle of point sources in this study. The area of the source was estimated as 46,110 m^2. Twelve points were selected as Pb sources in the mine based on the topographical condition. Lead dispersion was calculated and compared with the results of Pb content in surrounding

surface soils. The collected soils were located in the northwest of the dumping site by considering the wind direction.

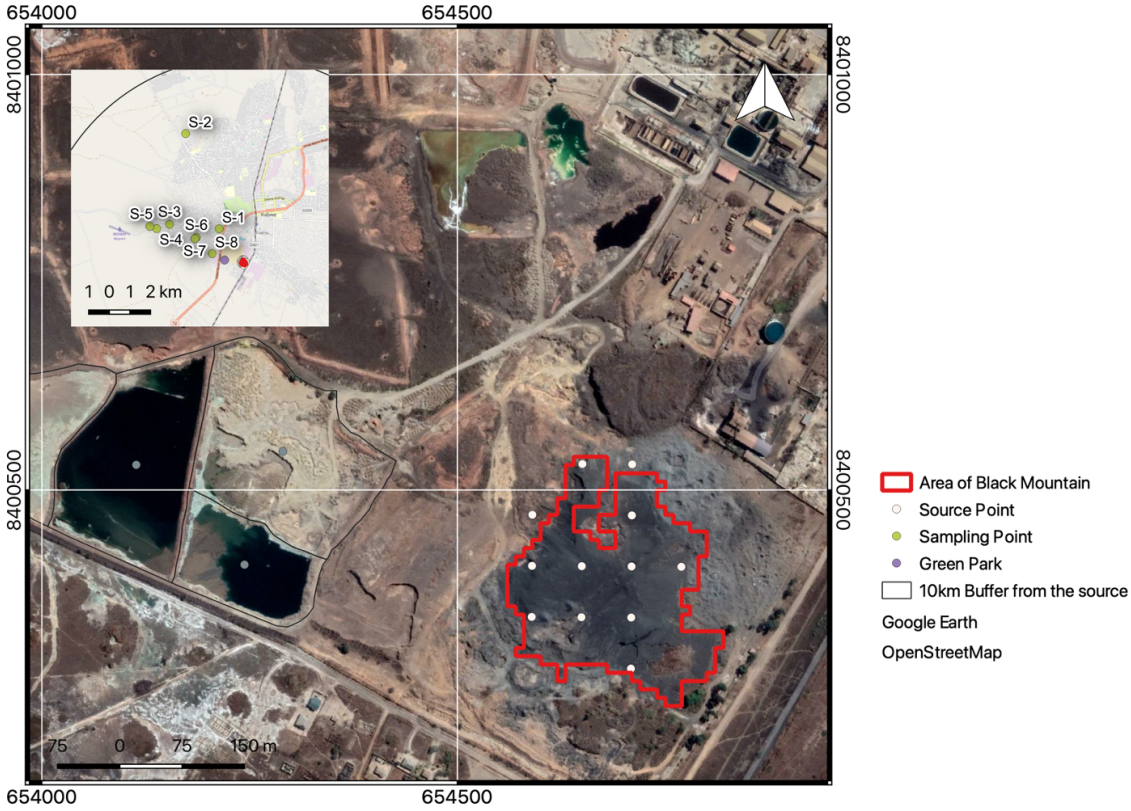

Figure 2- 1. The source area of the simulation and geographical relationships between the source and playgrounds: 12 points were selected as source points for simulating Pb-bearing soil dispersion from the area.

2.2.2. Lead dispersion simulation models

Dispersion of soils and mine residues depends on particle size. Mufalo et al. [7] measured the particle size distribution of collected soils and Zn plant leach residue, and they showed that 50 % of the collected soils had a diameter less than 50 μm. On the other hand, the dumping site that is the source of Pb-bearing soil dispersion simulation is covered by ISF-slags. The slag samples located at Black Mountain were also collected, and the particle size of the slags was measured. The results showed that 6 % of the slag was less than 150 μm. Figure 2-2 shows the particle size distribution of the slag. Sieves with different pore sizes were used for the particles larger than 0.15 mm whereas the particle size less than 0.15 mm was measured by the particle size analyzer based on laser diffraction. Siciliano et al. [8] suggest that slags less than 45 μm have risks of oral bio-accessibility in human beings. The particle size less than 10 μm is regarded as an air

pollution source and the formula of dispersion depends on wind speed [9, 10]. Thus, the target particle sizes of soils were classified into 10, 15, 20, 25, 30, 35, 40, 45, and 50 μm.

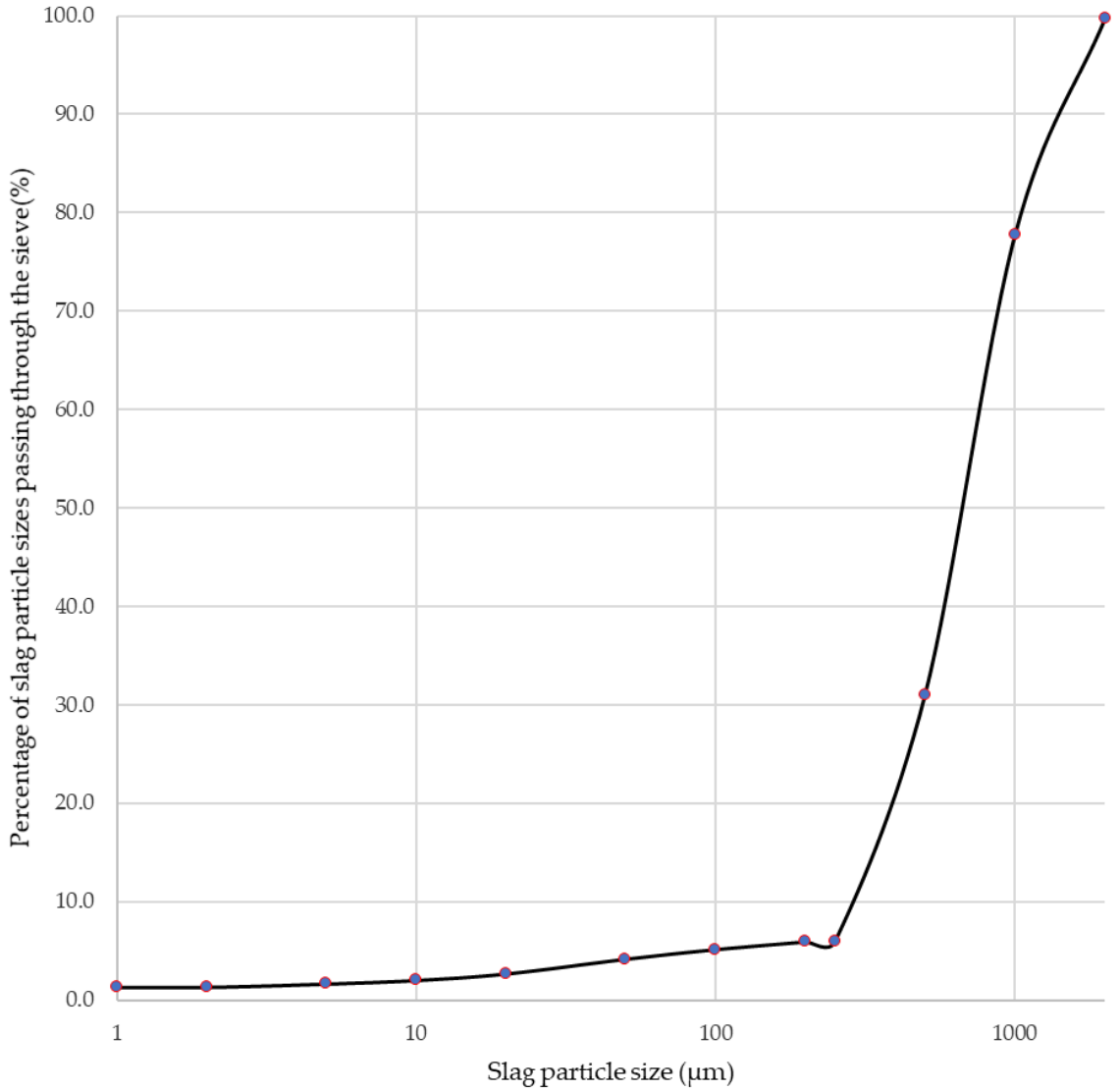

Figure 2- 2. Measured particle-size distribution of the slag sample.

Three models of Pb-bearing soil dispersion and a model of redispersion, depending on wind directions and speeds, were constructed in this study. The plume model was used in the case of wind speed over 1.0 m/s. The weak puff model was used in the case of wind speed lower than 1.0 m/s and higher than 0.4 m/s. The no puff model was used in the case of wind speed lower than 0.4 m/s [11 – 14]. The models are expressed by the following equations.

Plume model:

$$C = \frac{Q}{\sqrt{2\pi}(\pi/8)R\sigma_z u}\left\{exp\left[\frac{(z-He)^2}{2{\sigma_z}^2}\right] + exp\left[\frac{(z+He)^2}{2{\sigma_z}^2}\right]\right\}, \quad \text{(Equation 2-1)}$$

where,

C: Concentration (mg/m^2)

Q: Source strength (estimated at 0.025 m^3/s and 0.0025 m^3/s for the dry and rainy seasons, respectively)

R: Distance from source (= $(x^2 + y^2 + z^2)^{1/2}$)

x: Downwind distance along wind direction (m)

y: Horizontal distance perpendicular to x (m)

z: Elevation at simulating point (m)

σ_z: Diffusion width (m)

u: Wind speed (m/s)

He: Elevation of source (m)

Weak puff model:

$$C = \frac{Q}{\sqrt{2\pi}(\pi/8)\gamma}\left\{\frac{1}{{\eta_-}^2}exp\left[-\frac{u^2(z-He)^2}{2\alpha^2{\eta_-}^2}\right] + \frac{1}{{\eta_+}^2}exp\left[-\frac{u^2(z+He)^2}{2\alpha^2{\eta_+}^2}\right]\right\}, \quad \text{(Equation 2-2)}$$

In this equation

$\eta_-^2 = x^2 + y^2 + (\alpha^2/\gamma^2) \times (z - He)^2$

$\eta_+^2 = x^2 + y^2 + (\alpha^2/\gamma^2) \times (z + He)^2$

where,

α: Dispersivity with respect to horizontal direction

γ: Dispersivity with respect to vertical direction

No puff model:

$$C = \frac{Q}{\sqrt{2\pi}(\pi/8)R\gamma}\left\{\frac{1}{{\eta_-}^2} + \frac{1}{{\eta_+}^2}\right\}, \quad \text{(Equation 2-3)}$$

$R = (x^2 + y^2)^{1/2}$

$\eta_-^2 = x^2 + y^2 + (\alpha^2/\gamma^2) \times (z - He)^2$

$\eta_+^2 = x^2 + y^2 + (\alpha^2/\gamma^2) \times (z + He)^2$

The source strength (Q) is a key parameter to simulate Pb-bearing soil dispersion and redispersion. Here, a total of 1 m^3 of the slag per one second was assumed to be dispersed. However, only finer particles (< 50 μm) are transported to a further distance. Thus, the finer fraction of 2.5 % of the slag was assumed to be dispersed (0.025 m^3/s) as a source strength for the dry season. Rain is another factor to restrain soil dispersion by winds. For the rainy season, the source strength of Pb-bearing soil dispersion by each

model was set at 0.0025 m^3/s, 1/10 of the value of the dry season because the higher water content of the surface restricts the dispersion.

The dispersion of the slag with less than 50 μm was simulated every hour, and the accumulated amount of precipitated slag with Pb was calculated by considering the particle sizes and weather conditions. The amounts of deposition of slag depending on the particle size at each playground were summed up in the rainy and dry seasons in 2019 and throughout the year 2019.

Redispersion is related to particle sizes of soils and slags and wind speed at the deposited locations. Target particle sizes were between 10 μm and 50 μm in this study. So, these particle sizes are similar to the size of cedar pollen (mean diameter: 30 μm). Nakatani and Nakane [15] developed and simulated pollen re-transport behavior. By applying the following model, particles of soils and slags on the ground have five forces: gravity, static friction force, drag force, Saffman lift force, and adhesion force. The particles are able to be re-transported when the drag force is larger than the friction force and Saffman lift force is larger than the gravity plus vertical adhesion forces. Therefore, redispersion at the deposited locations was calculated by Equation 2-4.

Redispersion:

$$R = P_R \times C1 \times \left[F_D - F_f + F_s - g\right], \quad \text{(Equation 2-4)}$$

where,

R: Redispersion (mg)

P_R: Percentage of redispersion

$C1$: Amount of dispersed soils (mg/m^2)

F_D: Drag force ($= \frac{1}{2}\rho_a u^2 C_D \frac{\pi d^2}{4}$)

ρ_a: Fluid density (1.2250 kg/m^3, standard atmospheric density)

u: Wind speed (m/s)

C_D: Drag coefficient (= 0.6, particle was estimated at elliptical pillar)

d: Particle size (μm)

F_f: Friction force ($= \mu \times N$)

μ: Friction coefficient (estimated at 0.52)

N: Normal force (= density of slag (3.45, the average values between 3.3 and 3.6) × volume of particle)

F_S: Saffman lift ($= 6.46 \times \left(\frac{d}{2}\right)^2 u\sqrt{\rho_a \mu}$)

g: Gravity (= density of slag (3.45, the average values between 3.3 and 3.6) × volume of particle)

Value of drag coefficient (C_D) for estimating drag force for the redispersion calculation depends on the shape of the particle. The target soils and slags have various

shapes: sphere, angled cube, cylinder, etc. Here, a spheroid shape with the value of 0.6 between sphere and angled cube was selected.

At the playgrounds, various particle sizes and minerals of soils are mixed, and various conditions, such as human activities and weather, change every moment throughout the year. By referring to the previous studies [16, 17], the friction coefficient (μ) was set at 0.52 with considerations of the environmental conditions under which soils were easily swirled and dispersed Pb-bearing soils were redispersed by winds and flushed by rains after depositing immediately.

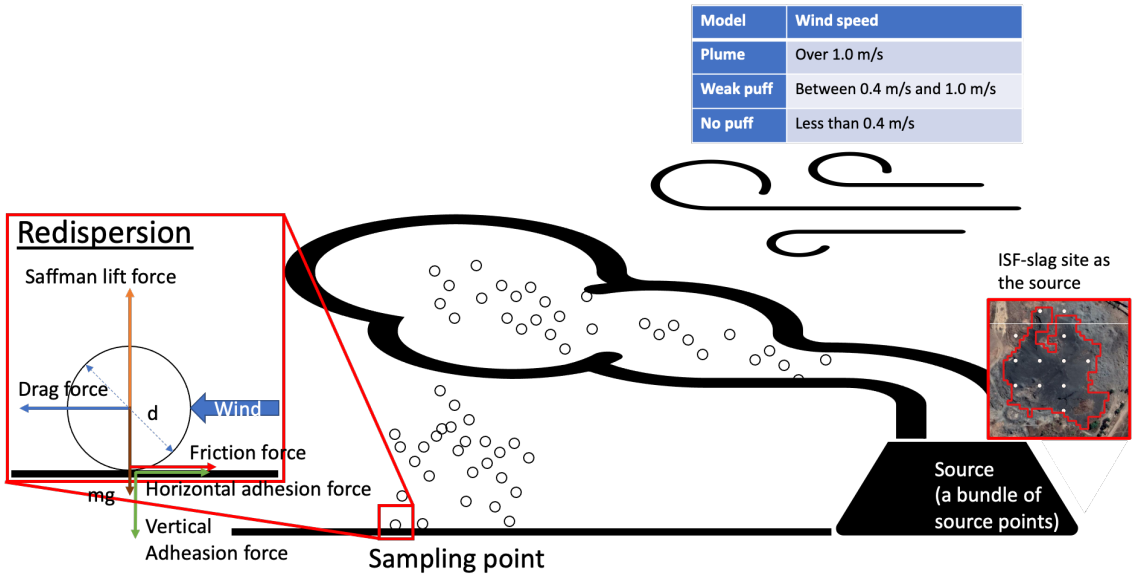

Figure 2- 3. Image of Pb-bearing soil dispersion and redispersion: Pb-bearing soil dispersion was simulated three dispersion models by considering wind speeds. The redispersion model was applied to Pb-bearing soils dispersed on the ground by considering five forces.

2.2.3. Weather data collection

Weather information for the year 2019 was used to simulate Pb-bearing soil dispersion at and around the mine because all required data were collected in situ or in Lusaka. The weather information consists of six items as Pb-bearing soil dispersion parameters: wind direction, wind speed, solar radiation, barometric pressure, humidity, and air temperature [18]. However, due to machine troubles and errors of the data collection system, the data of August 2019 were not collected.

Wind direction and wind speed were collected at Green Park, which is located at the southwest of the mine about 900 m away from the source, and it was prepared for monitoring heavy metals absorbed by plants (Figure 1-3). In addition, a small-sized meteorological instrument named POTEKA (Meisei Electric Co., Ltd., Tokyo, Japan)

collected hourly data. Thus, wind speed and direction data have been monitored at Green Park.

Solar radiation, barometric pressure, humidity, and air temperature data were collected at the test site of the University of Zambia, Lusaka. Although Lusaka, the capital city of Zambia, is about 139 km south from Kabwe, the measured solar radiation, barometric pressure, humidity, and air temperature were collected and applied to the simulation. Thus, the weather data obtained at the two cities were used for simulation.

Values of wind speed and direction were used as parameters of Pb-bearing soil dispersion and redispersion simulation directly. Solar radiation, barometric pressure, humidity, and air temperature were used to determine coefficients of horizontal and vertical dispersivities for the plume, weak puff, and no puff models.

2.2.4. Comparison field survey results

Results of Pb-bearing soil dispersion simulations were compared with results of measured Pb contents by Mufalo et al. [7] (Table 2-1). They collected samples at eight playgrounds within 10 km radius from the dumping site. They took topsoil samples (5 cm depth) by mixing 3 – 4 soils for each sample and analyzing the total contents of Pb in the soils. Their data are appropriate for comparison with the simulated deposition of Pb because the playground is not influenced by change in land use.

Table 2- 1. Pb contents of soil samples (XRF-chemical composition) by Mufalo et al. [3].

Playground	Pb (mg/kg)
S-1	3320
S-2	1080
S-3	1070
S-4	265
S-5	633
S-6	863
S-7	1770
S-8	3170

2.3. Results

2.3.1. Weather data collection

Weather condition sensitively affects Pb-bearing soil dispersion. Winds in Kabwe tended to blow from the east-southeast side (annual frequency was 10.95 %). The frequency of wind from the west was 10.94 %, and from the southeast was 9.78 % throughout the year of 2019. On the other hand, the wind speed was 2.47 m/s from the west whereas 2.19 m/s and 1.50 m/s of winds blew from the east and the south,

respectively. These data are shown in Figure 2-4. The annual average of solar radiation was 0.20 kW/m^2, the annual average of barometric pressure was 874.99 hPa, the annual average of humidity was 58.07 %, and the annual average of air temperature was 21.83 °C.

During the rainy season (January to April and November to December) in Kabwe, the frequent wind directions were from the west (11.79 %), the north (10.45 %), and the east-southeast (7.78 %). Strong winds came from the west (2.45 m/s), the east (1.77 m/s), and the west-southwest (1.59 m/s). The average of solar radiation was 0.22 kW/m^2, the average of barometric pressure was 872.62 hPa, the average of humidity was 68.65%, and the average of air temperature was 23.08 °C.

During the dry season (May to October, August not included) in Kabwe, the frequent wind directions were from the east-southeast (14.71 %), the southeast (14.08 %), and the south-southeast (11.08 %). Strong winds blew from the east (2.72 m/s), the west (2.49 m/s), and the south-southwest (1.85 m/s). The average of solar radiation was 0.19 kW/m^2, the average of barometric pressure was 877.79 hPa, the average of humidity was 45.54 %, and the average of temperature was 20.34 °C.

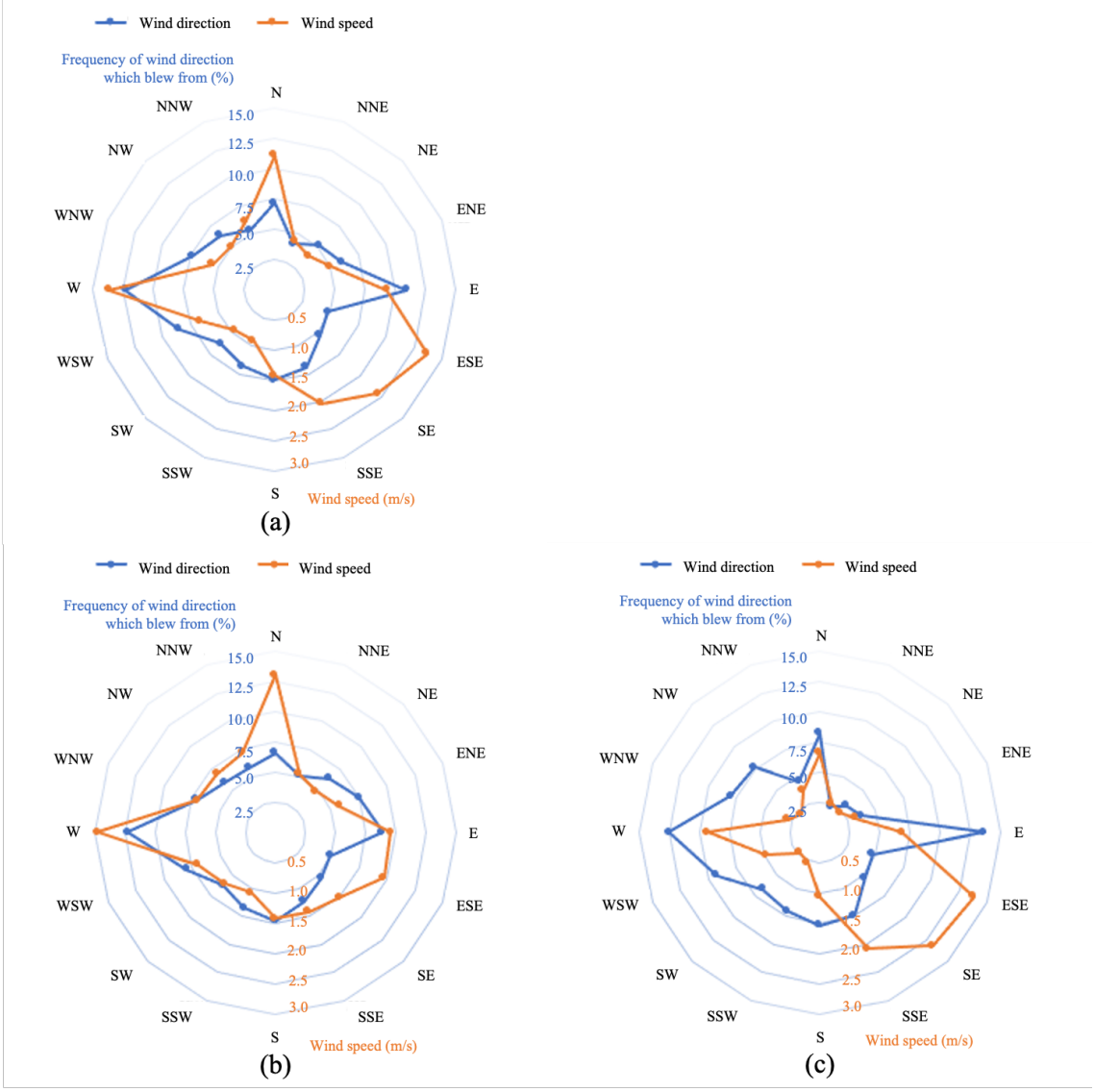

Figure 2- 4. Results of the measured wind conditions in Kabwe in 2019: (a) wind condition throughout the year 2019; (b) wind condition in the rainy season; (c) wind condition in the dry season. Orange plots in these charts show frequencies of wind directions from which wind blew, and the axis was set at 15.0 %, 12.5 %, 10.0 %, 7.5 %, 5.0 %, and 2.5 % from outside to inside, respectively. Blue plots in these charts show wind speeds, and the axis was set at 3.0, 2.5, 2.0, 1.5, 1.0, and 0.5 m/s from outside to inside, respectively.

2.3.2. Lead dispersion simulations

The deposition of Pb-bearing soils at eight playgrounds from the ISF-slag site by dispersion was calculated seasonally; during the rainy season (January to April and November to December), during the dry season (May to October, August not included), and throughout the year (January to December, but August not included). Calculated

seasonal deposition rates at each playground were accumulated. The results for S-2, located 6,904.1 m away from the dumping site (the farthest distance), S-3, located 4,042.2 m (the middle distance), and S-8, located 1,577.4 m (the nearest distance) were compared. The accumulated deposition rates throughout the year by simulation were compared with results of Pb content in soil samples by Mufalo et al. [7].

Figure 2-5 shows the simulated results of the accumulated amount deposited at S-2 located on the north-northwest direction (335.05°) and 6,904.1 m from the source. In the rainy season, the accumulated amount deposited was lower when the winds blew from the east side compared to the winds from the west. The dispersion in the rainy season was not significantly affected by winds from the east even though S-2 is in the north-northwest direction from the source. The total amount deposited by winds from the east and the east-southeast was 0.00014 mg/m^2. The total amount deposited by winds from the northwest, the north-northwest, and the north was 0.00100 mg/m^2. These results indicate that the amount deposited was affected by the lower wind speed from the east-southeast to the south-southeast directions at S-2. In the dry season, the accumulated amount deposited was higher when the winds blew from the east and the south compared to the winds from the west. The total amount deposited by winds from the east-southeast and the southeast was 0.00684 mg/m^2. The total amount deposited by winds from the west was 0.00067 mg/m^2. Dispersion simulations indicate that deposition was affected by the frequency of winds from the east-southeast and the southeast because of low humidity and ignorance of the effects of rain.

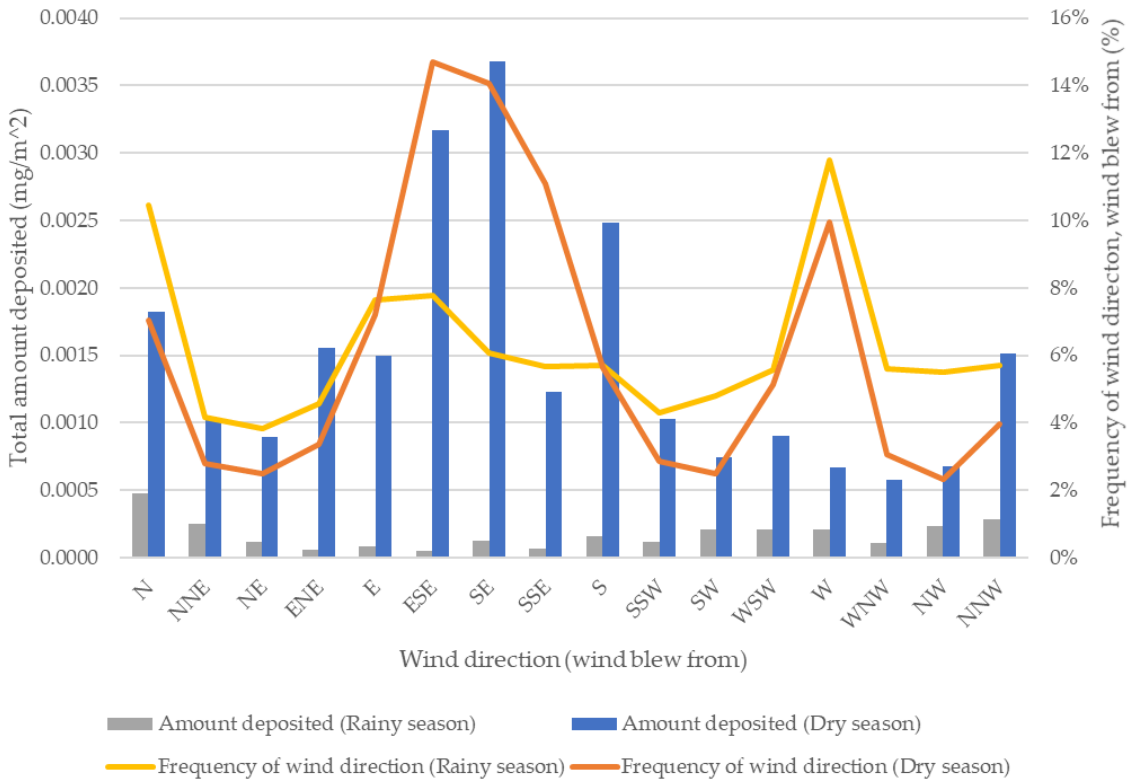

Figure 2- 5. Total amount deposited by the wind directions at S-2: gray and blue bars show total amount deposited by wind directions from which wind blew in the rainy and dry seasons, respectively. Yellow and orange lines show frequencies of wind directions from which wind blew in the rainy and dry seasons, respectively.

Figure 2-6 shows the simulated results of the accumulated amount deposited at S-3 located on the west-northwest direction (296.64°) and 4,042.2 m from the source. In the rainy season, the accumulated amount deposited was lower when the winds blew from the east compared to the winds from the west. The dispersion in the rainy season was not affected by winds from the east even though S-3 is on the north-northwest direction from the source. The total amount deposited by winds from the east and the east-southeast was 0.00034 mg/m^2 whereas the total amount deposited by winds from the west was 0.00066 mg/m^2. The amount deposited was negative (−0.00123 mg/m^2) when the winds blew from the south-southwest. This is due to the net effects of deposition and redispersion by winds from the south-southwest. In the dry season, the accumulated amount deposited was higher when the winds blew from the east and the south compared to the winds from the west. The amount deposited was affected by winds from the east-southeast and the southeast. The total amount deposited by winds from the east-southeast and the southeast was 0.02124 mg/m^2 whereas the total amount deposited by winds from the west was 0.00188 mg/m^2. The results indicate that deposition was affected

by the winds from the east-southeast and the southeast because of low humidity and no rain.

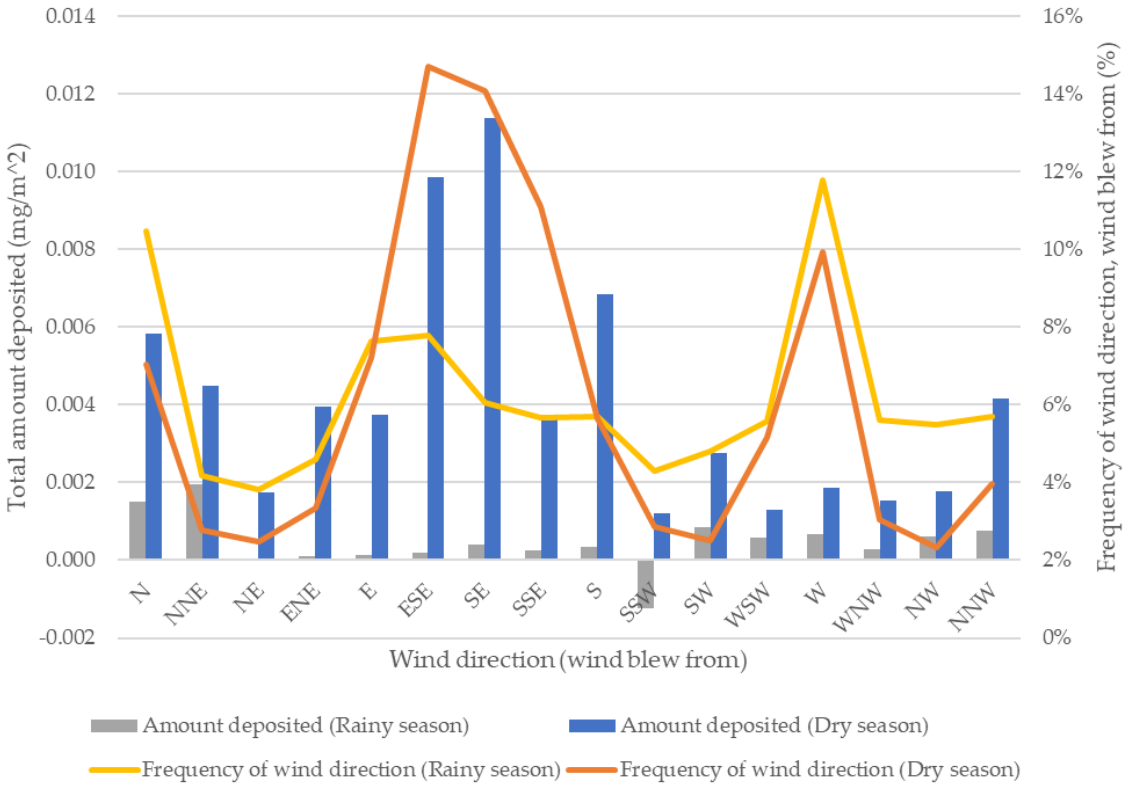

Figure 2- 6. Total amount deposited by wind directions at S-3: gray and blue bars show total amount deposited by wind directions from which wind blew in the rainy and dry seasons, respectively. Yellow and orange lines show frequencies of wind directions from which wind blew in the rainy and dry seasons, respectively.

Figure 2-7 shows the simulated results of the accumulated amount deposited at S-8 located on the west-northwest direction (285.89°) and 1,577.4 m from the source. In the rainy season, the accumulated amount deposited was lower when the winds blew from the east compared to the winds from the west. The results indicate that dispersion in the rainy season was not affected by winds, and that humidity and rain might flush the deposits at the location. The total amount deposited by winds from the east and the east-southeast was 0.00423 mg/m^2. The total amount deposited by winds from the west was 0.00306 mg/m^2. In the dry season, the amount deposited was higher when the winds blew from the east and the south compared to the winds from the west. These results indicate that the amount deposited was affected by the winds from the east-northeast and the south because of low humidity and almost no rain. The total amount deposited by winds

from the east-southeast and the southeast was 0.16561 mg/m^2. The total amount deposited by winds from the west was 0.01075 mg/m^2.

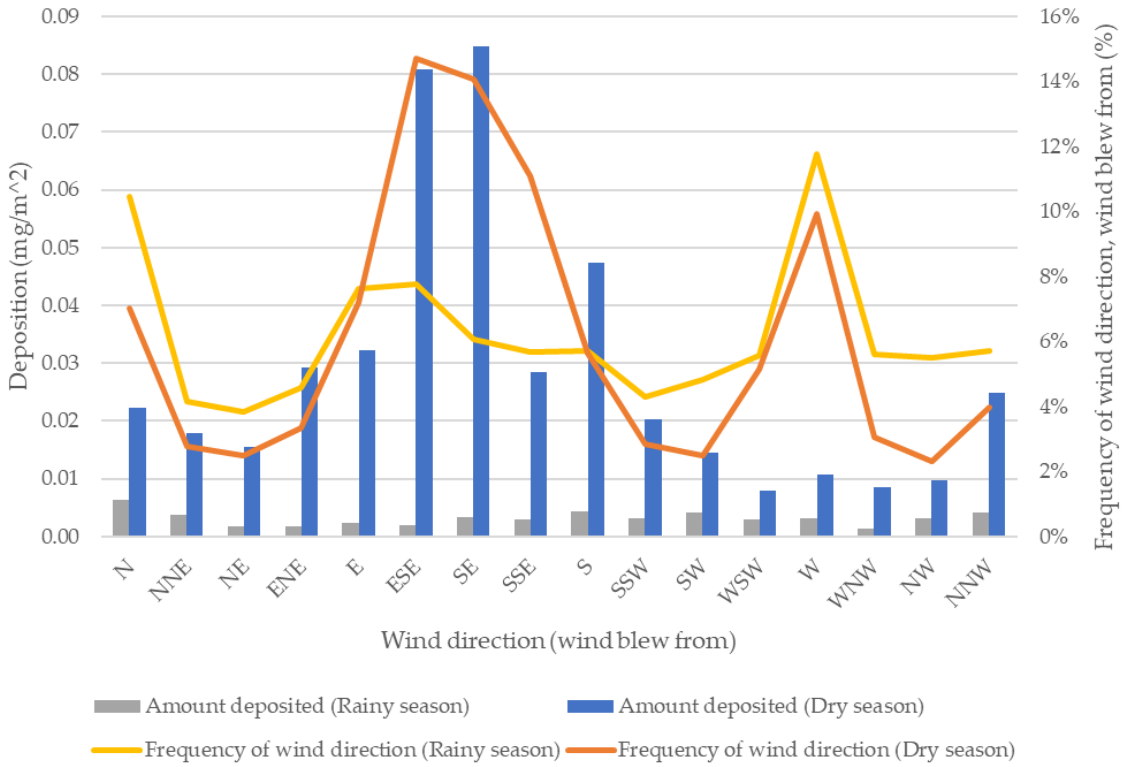

Figure 2- 7. Total amount deposited by wind directions at S-8: gray and blue bars show total amount depos-ited by wind directions from which wind blew in the rainy and dry seasons, respectively. Yellow and orange lines show frequencies of wind directions from which wind blew in the rainy and dry seasons, respectively.

2.4. Discussion

In the rainy season, the amount deposited was affected by higher humidity and rain, and the correlation between winds and the amount deposited was not clearly observed at each playground. On the other hand, in the dry season, the amount deposited at each playground was affected by winds from the east-southeast and the southeast, and winds were found to be a sensitive factor of Pb-bearing soil dispersion from the source.

Simulated results for amounts deposited of Pb-bearing soils were compared with Pb contents in playground soils for their verification. Figure 2-8 shows the relationship between measured Pb content in soil and simulated amount of deposition. The contents of Pb generally increased with the amount deposited. However, when the amount deposited was lower than 0.1 mg/m^2, the Pb content decreased with the amount deposited. This indicates that not only dispersion by wind, but also other factors affect the distribution of Pb.

Figure 2-9 shows the simulated amount of deposition and measured Pb content in soil vs. distance from the source. Both the measured Pb content and the simulated amount of deposition decreased with distance from the source. This indicates that the dispersion model used here can well express Pb-bearing soils dispersion from the ISF-slag site. This means that Pb-bearing soil dispersion is mainly caused by dispersion by winds from the dumping site.

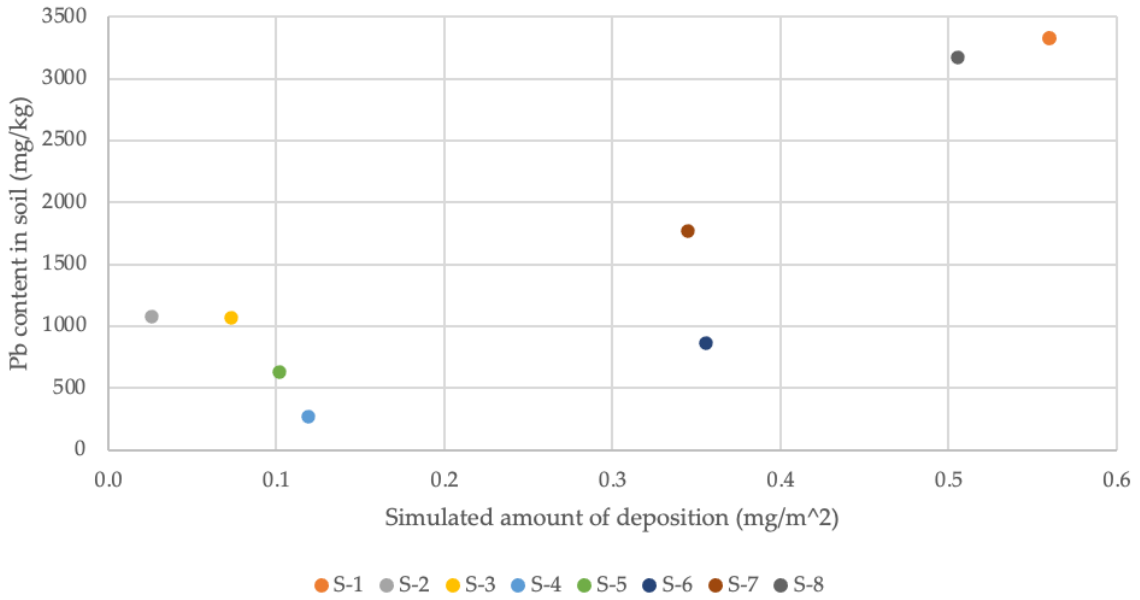

Figure 2- 8. Relationship between measured Pb content in soil and simulated amount of deposition.

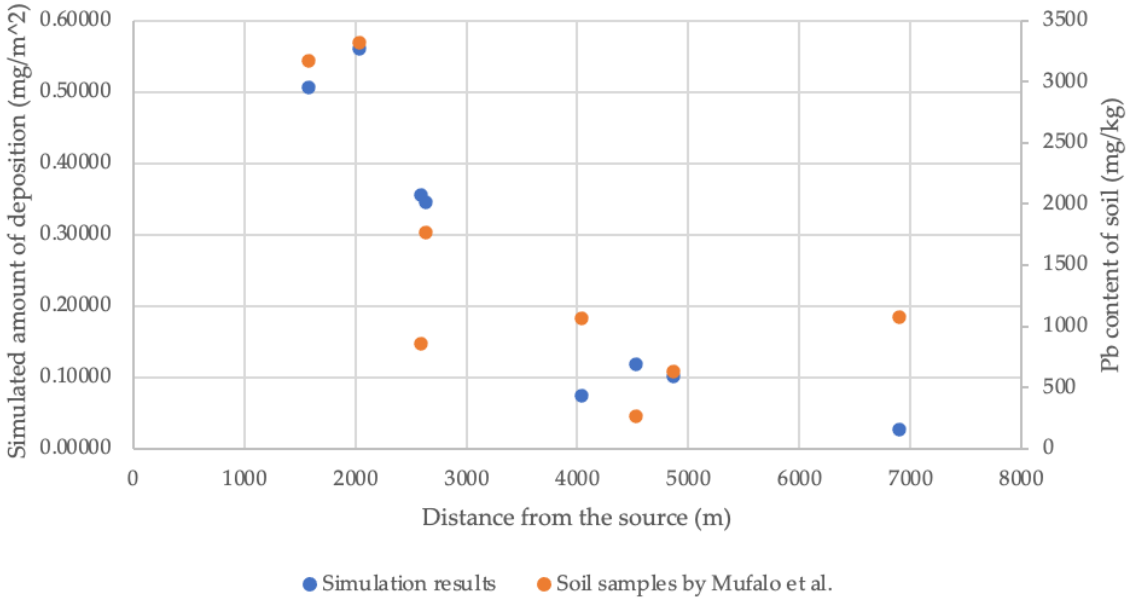

Figure 2- 9. Simulated amount of deposition and Pb content in soil vs. distance from the source.

Figure 2-10 shows the simulated amount of dispersion depending on particle sizes of Pb-bearing soil at S-2, S-3, and S-8 throughout the year 2019. Although the simulated amount of dispersion decreased with distance, the particles are dispersed within a restricted distance whereas the finer particles are dispersed for a longer distance. In addition, the finer particles are easily redistributed because the fraction of finer particles decreased at any location.

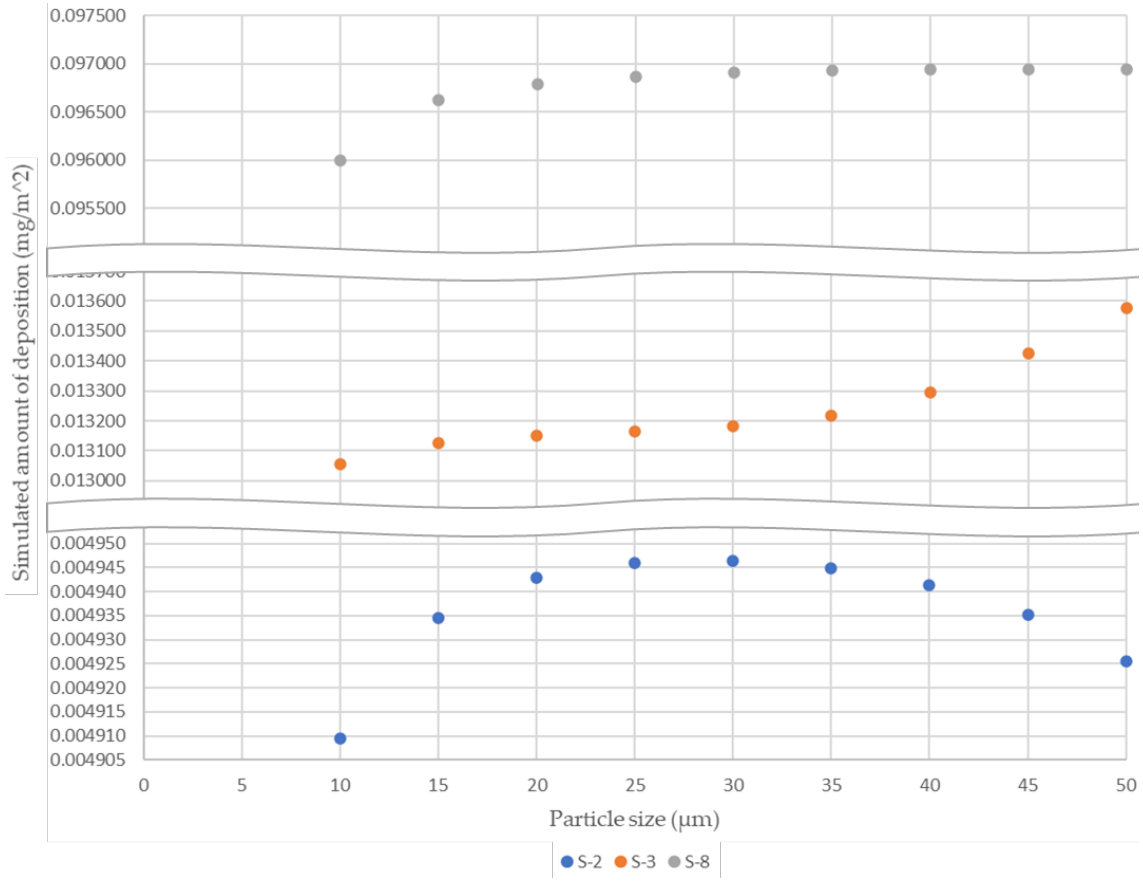

Figure 2- 10. Simulated amount of deposition depending on particle sizes of Pb-bearing soil at S-2, S-3, and S-8.

The dispersion models of fine particles of Pb-bearing soils explained the measured results of Pb contents in soils and qualitatively expressed the dependency of particle size on dispersion. Thus, the obtained results imply that the model used in this study may be applicable to the phenomenon of aerial dispersion of contaminants. However, the applicability of this model should be evaluated by using data of the other year and other sites.

2.5. Conclusion

Pb-bearing soil dispersion simulations using terrain data and local weather data of the year 2019 were conducted and compared with the Pb contents in soils around the dumping site of Kabwe. The following results were found.

1. Wind direction and speed and humidity, including rain, sensitively affected dispersion of soils containing Pb.
2. The simulated amount deposition decreased with distance from the source and agreed with the measured Pb contents of soils.
3. Winds dispersed the smaller sizes of particles farther and dispersed the larger sizes near the source, and easily redispersed the smaller sizes, according to the dispersion simulation, depending on particle sizes.
4. The above results indicate that Pb content in soils is significantly affected by dispersion of mine residues. In other words, Pb contamination of soils is primarily caused by dispersion of mine residues by winds.

Based on the obtained results, effective countermeasures against Pb-bearing soil dispersion and remediation of soil contamination should be proposed by considering Pb-bearing soil dispersion calculations after remediation of the dumping site and surrounding ground surfaces.

References

1. Brotons, J. M.; Díaz, A. R.; Sarría, F. A.; Serrato, F. B. Wind erosion on mining waste in southeast Spain. *Land Degrad. Develop.* 2010, *21*, 196-209.
2. Mokhtari, A. R.; Feiznia, S.; Jafari, M.; Tavili, A. Investigating the role of wind in the dispersion of heavy metals around mines in arid regions (a case study from Kushk Pb-Zn Mine, Bafgh, Iran). *Bulletin of Environmental Contamination and Toxicology*, 2018, *101*, 124-130.
3. Mileusnić, M.; Mapani, B. S.; Kamona, A. F.; Ružičić. S.; Mapaure, I.; Chimwamurombe, P. M. Assessment of agricultural soil contamination by potentially toxic metals dispersed from improperly diposed tailings, Kombat mine, Namibia. *Journal of Geochemical Exploration*, 2014, *144*, 409-420.
4. Tembo, B. D.; Sichilongo, K.; Cernak, J. Distribution of copper, lead, cadmium and zinc concentrations in soils around Kabwe town in Zambia. *Chemosphere*, 2006, *63 (3)*, 497-501.
5. Kataoka, H.; Tabata, Y. *Numerical Prediction Method for Snowdrift Dust Dispersion*; Report of Obayashi Corporation Technical Research Institute: Tokyo, Japan, 2010; Volume 74.
6. Japan Environmental Management Association for Industry; Ministry of Economy, Trade and Industry. Low Rise Industrial Source Dispersion MODEL. 2021. Available online: http://www.jemai.or.jp/tech/meti-lis/detailobj-6117-attachment.pdf (accessed on 28 October 2020).
7. Mufalo, W.; Tangviroon, P.; Igarashi, T.; Ito, M.; Sato, T.; Chirwa, M.; Nyambe, I.; Nakata, H.; Nakayama, S.; Ishizuka, M. Characterization and leaching behavior of playground soils in Kabwe, Zambia. In Proceedings of the International Symposium on Earth Science and Technology, Fukuoka, Japan, 26–27 November 2020; pp. 154–157.
8. Siciliano, S.D.; James, K.; Zhang, G.; Schafer, A.N.; Peak, J.D. Adhesion and enrichment of metals on human hands from contaminated soil at an Arctic urban brownfield. *Environ. Sci. Technol.* 2009, *43*, 6385–6390.
9. Tada, K.; Hazama, H.; Kobayashi, K.; Okamoto, S. Development and evaluation of a diffusion model for particle matter— Application to Kashima area. *J. Japan Soc. Air Pollut.* 1989, *24*, 64–73.
10. Matsusaka, S.; Masuda, H. Reentrainment phenomena of fine particles. *J. Soc. Powder Technol. Jpn.* 1992, *29*, 530–538.
11. Sherman, C.A. A Mass-consistent model for wind fields over complex terrain. *J. Appl. Meteorol.* 1978, *17*, 312–319.
12. Fukuyama, T.; Izumi, K.; Utiyama, M. Dry deposition of atmospheric aerosols— A browse on recent papers. *J. Aerosol Res.* 2004, *19*, 245–253.

13. Ministry of Economy, Trade and Industry of Japan. Technical Manual of Ministry of Economy, Trade and Industry Low rise Industrial Source dispersion model (METI-LIS) ver. 3.02, March 2012. Available online: https://www.jemai.or.jp/tech/meti-lis/detailobj-6117-attachment.pdf (accessed on 30 May 2019).
14. Luhar, A.K. Analytical puff modelling of light-wind dispersion in stable and unstable conditions. *Atmos. Environ.* 2011, *45*, 357–368.
15. Nakatani, N.; Nakane, I. A study of pollen re-transportation in urban environment by using physical model and numerical simulation. *Jpn. Soc. Comput. Methods Eng.* 2017, *17*, 171215.
16. Fuller, D.D. *Coefficient of Friction*; Columbia University: New York, NY, USA; pp. 2-42–2-48. Available online: https://web.mit. edu/8.13/8.13c/references-fall/aip/aip-handbook-section2d.pdf (accessed on 6 May 2020).
17. Nabeel, M.; Karasev, A.; Jönsson, P.G. Friction forces and mechanical dust generation in an iron ore pellet bed subjected to varied applied loads. *ISIJ Int.* 2017, *57*, 656–664.
18. Klingmuller, K.; Metzger, S.; Abdelkader, M.; Karydis, V.A.; Stenchikkov, G.L.; Pozzer, A.; Lelievbeld, J. Revised mineral dust emission in the atmospheric chemistry-climate model EMAC (MESSy 2.52 DU_Astithal KKDU2017 patch). *Geosci. Model Dev.* 2018, *11*, 989–1008.

Chapter 3. Weather parametric analysis on lead-bearing soil dispersion in Kabwe

3.1. Introduction

In Chapter 2, mechanisms of Pb-bearing soil dispersion and deposition were evaluated with the local weather data of the year 2019. Although wind speeds and wind directions are considered as primary indicators of Pb-bearing soil dispersion, changes of other weather conditions: solar radiation, barometric pressure, humidity and air temperature are also factors affecting on wind conditions and Pb-bearing soil dispersion as results.

According to the previous studies, winds and water have been discussed and mentioned as causes of heavy metal contaminations [1 - 5]. Punia suggested that climate factors such as temperature, wind and precipitation affect the dispersal and mobility of heavy metal in the mine area [6]. Solar radiation was used as the factor for determination of dispersivity with respect to horizontal and vertical directions in dispersion models, and barometric pressure and humidity were used for determination of source strength [1, 7 – 10]. Although weather factors were referred for simulating heavy metal dispersion, impacts of these factors, which were collected at the local were not discussed enough.

In this chapter, correlations between wind speed and other weather factors were analyzed. Also, for evaluating the sensitivity of each weather factor in Kabwe, Pb-bearing soil dispersion simulation was conducted with average, top 10 % and bottom 10 % values of weather conditions by using the same simulation models as in Chapter 2.

3.2. Materials and methods

3.2.1. Study site

Twelve source points at ISF-slag site named Black Mountain and eight playgrounds as target and sampling points where were used in Chapter 2 were also used in this chapter for comparing and analyzing the sensitivity of the local weather factors of the year 2019. As the source was mentioned in Chapter 2, it was adopted as a bundle of source points for considering Pb-bearing soil dispersion occurs from ISF-slag site (an area). The locations of the source points and playgrounds were shown Figure 1-3 and Figure 2-1.

3.2.2. Weather data collection and analysis

Local weather data of Kabwe in the year 2019, which were collected and used in Chapter 2 were also used for this chapter. All weather data were collected hourly at Green Park, Kabwe and the test site at the University of Zambia, Lusaka throughout the year 2019. Due to machine troubles and errors of the data collection system, the data of August 2019 were not collected but not used in this chapter, either. Collected weather data were

consisted of six factors: wind speed, wind direction, solar radiation, barometric pressure, humidity, and air temperature.

The weather data were categorized in two seasons: the rainy and dry seasons for analyzing seasonal differences on Pb-bearing soil dispersions. In this study, the rainy season of 2019 was set between January and April and between November and December; and the dry season of 2019 was between May and October, but August was not included.

For the rainy and dry seasons, correlations between wind speed and other weather factors were analyzed. Also, the seasonal differences were compared for estimating which and how weather factors affected on wind speed mostly: wind speed vs. solar radiation; wind speed vs. barometric pressure; wind speed vs. humidity; and wind speed vs. air temperature.

Moreover, average, top 10 % and bottom 10 % values of each weather factor of each season were calculated and prepared for Pb-bearing soil dispersion simulations. Eleven weather conditions in each season were prepared as listed in Table 3-1.

Table 3- 1. Weather condition for simulations of Pb-bearing soil dispersion: Average, top 10 % and bottom 10 % values of each weather parameter of each season were calculated and used for estimating impacts on Pb-bearing soil dispersion in Kabwe.

#	Wind speed	Solar radiation	Barometric pressure	Humidity	Air temperature	Note
1	Average	Average	Average	Average	Average	Average
2	Top 10 %	Average	Average	Average	Average	High wind speed
3	Bottom 10 %	Average	Average	Average	Average	Low wind speed
4	Average	Top 10 %	Average	Average	Average	High solar radiation
5	Average	Bottom 10 %	Average	Average	Average	Low solar radiation
6	Average	Average	Top 10 %	Average	Average	High barometric pressure
7	Average	Average	Bottom 10 %	Average	Average	Low barometric pressure
8	Average	Average	Average	Top 10 %	Average	High humidity
9	Average	Average	Average	Bottom 10 %	Average	Low humidity
10	Average	Average	Average	Average	Top 10 %	High air temperature
11	Average	Average	Average	Average	Bottom 10 %	Low air temperature

3.2.3. Simulation models for lead dispersion

Three models of Pb-bearing soil dispersion which were constructed in Chapter 2 were also used in this chapter. The plume model was prepared when the wind speed condition was over 1.0 m/s; the weak puff model was prepared when the wind speed was between 0.4 m/s and 1.0 m/s; and the no puff model was prepared when the wind speed was less than 0.4 m/s.

Wind directions had impacts on the amounts of dispersions and depositions at playgrounds. For simplifying of weather factor analyses on Pb-bearing soil deposition, the wind direction was fixed as from southeast to northwest in this chapter. Winds from southeast was made clear as the largest impact on dispersion to the playgrounds where were located northwest side from the source area by the study in Chapter 2.

Simulations of Pb-bearing soil dispersion and deposition were performed based on the conditions in Table 3-1.

3.3. Results

3.3.1. Weather data analyses

In 2019, annual weather conditions in Kabwe were calm. 8,016 of datasets were collected during 2019, and 7,806 weather conditions were with wind speed less than 5.0 m/s. Annual average of solar radiation was 2.04 kW/m^2, annual average of barometric pressure was 874.96 hPa, annual average of humidity was 58.07 % and annual average of air temperature was 21.83 ℃ as listed in Table 3-2.

Table 3- 2. Annual Average, top 10 % and bottom 10 % values of weather conditions in Kabwe.

Value	Wind speed	Solar radiation	Barometric pressure	Humidity	Air temperature
Average	1.44 m/s	2.04 kW/m^2	874.96 hPa	58.07 %	21.83 ℃
Top 10 %	3.10 m/s	7.11 kW/m^2	880.10 hPa	89.30 %	28.70 ℃
Bottom 10 %	0.20 m/s	0.00 kW/m^2	872.62 hPa	26.70 %	15.10 ℃

In the rainy season of 2019, average values of solar radiation (2.17 kW/m^2), humidity (68.65 %), and air temperature (23.08 ℃) were higher than the annual average indicated the seasonal features as shown in Table 3-3. The average (1.43 m/s), top 10 % (3.10 m/s) and bottom 10% (0.30 m/s) values of wind speeds were almost similar to the annual. The average values of barometric pressure (872.62 hPa) were lower than the annual.

In the dry season of 2019, average values of solar radiation (1.88kW/m^2), humidity (45.55 %), and air temperature (20.34 ℃) were lower than annual indicated the seasonal features as shown in Table 3-4. The average (1.44 m/s), top 10 % (3.10 m/s) and bottom 10% (0.20 m/s) values of wind speed were almost similar to the annual. The average values of barometric pressure (877.79 hPa) were higher than the annual.

There were no significant differences of wind speeds between the rainy and the dry seasons. Values of solar radiation and air temperature of the rainy season were relatively higher than the dry season because Kabwe located on the south hemisphere of the Earth was in summer between January and April and between November and December.

Table 3- 3. Average, top 10 % and bottom 10 % values of weather conditions in rainy season.

Value	Wind speed	Solar radiation	Barometric pressure	Humidity	Air temperature
Average	1.43 m/s	2.17 kW/m²	872.62 hPa	68.65 %	23.08 ℃
Top 10 %	3.10 m/s	7.73 kW/m²	877.20 hPa	93.60 %	28.88 ℃
Bottom 10 %	0.30 m/s	0.00 kW/m²	872.00 hPa	40.37 %	18.70 ℃

Table 3- 4. Average, top 10 % and bottom 10 % values of weather conditions in dry season.

Value	Wind speed	Solar radiation	Barometric pressure	Humidity	Air temperature
Average	1.44 m/s	1.88 kW/m²	877.79 hPa	45.55 %	20.34 ℃
Top 10 %	3.10 m/s	6.51 kW/m²	881.40 hPa	73.60 %	28.42 ℃
Bottom 10 %	0.20 m/s	0.00 kW/m²	873.55 hPa	19.76 %	12.50 ℃

Correlation between wind speed and solar radiation in both rainy and dry seasons were analyzed and compared. In both rainy and dry seasons, solar radiation was inversely proportional to wind speed as shown in Figure 3-1. The scatter pattern in the rainy season showed wider than the dry season.

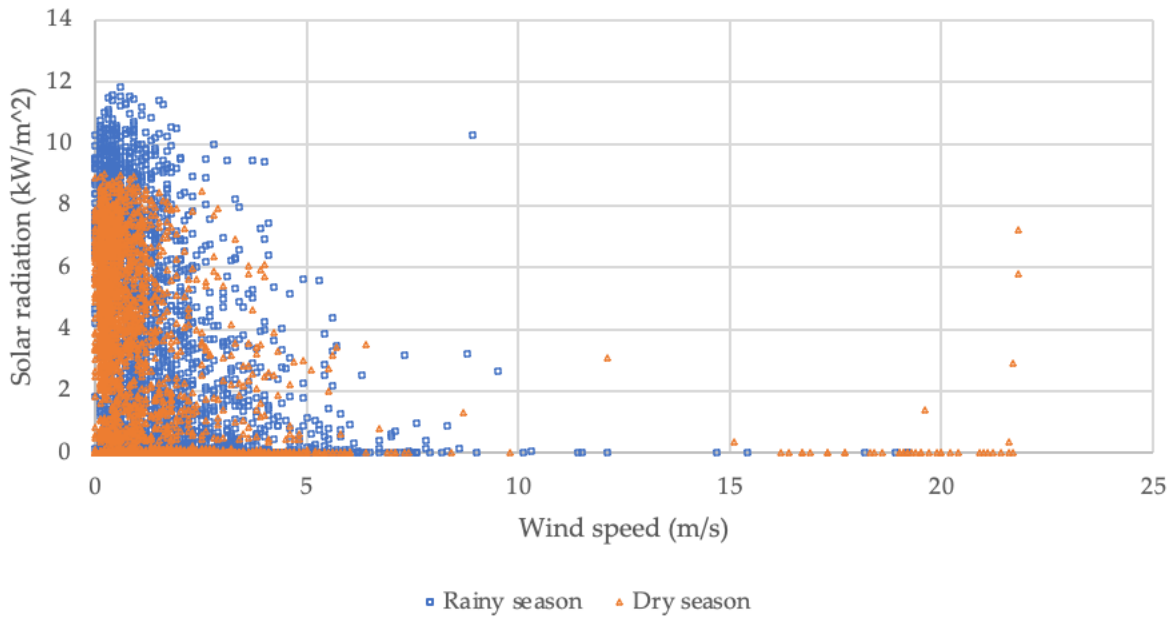

Figure 3- 1. Correlation between wind speed and solar radiation.

Correlation between wind speed and barometric pressure in both rainy and dry seasons were analyzed and compared as shown in Figure 3-2. Although significant correlations were not observed, wind speed had a trend to be high when barometric pressure was also high in the dry season.

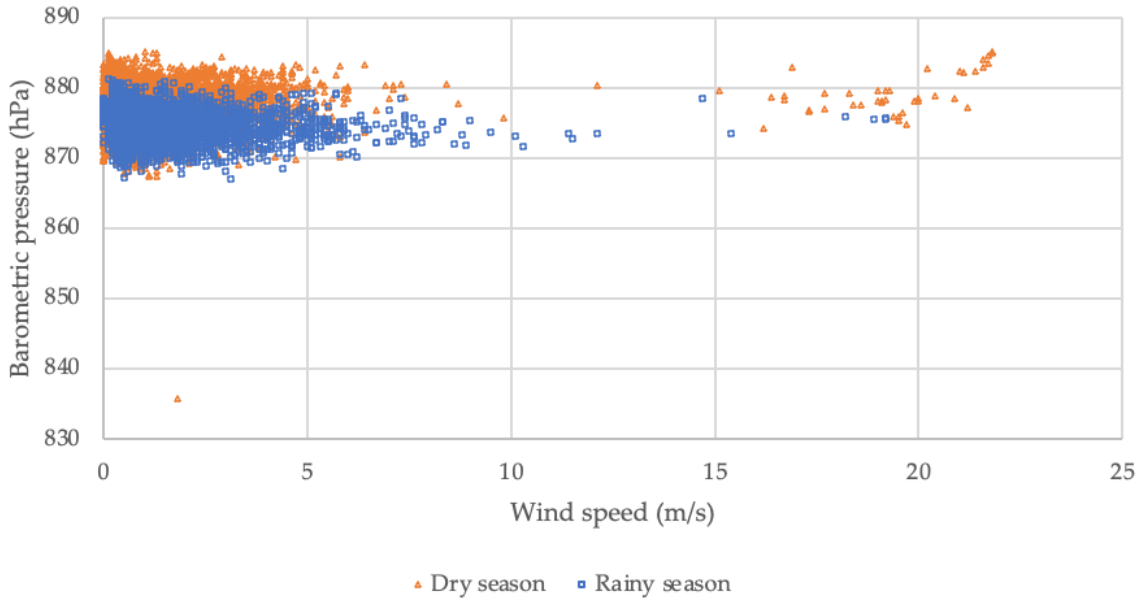

Figure 3- 2. Correlation between wind speed and barometric pressure.

Correlation between wind speed and humidity in both rainy and dry seasons were analyzed and compared as shown in Figure 3-3. Significant correlations were not identified in both rainy and dry seasons. However, the seasonal differences of humidity's value widths were shown significantly detected.

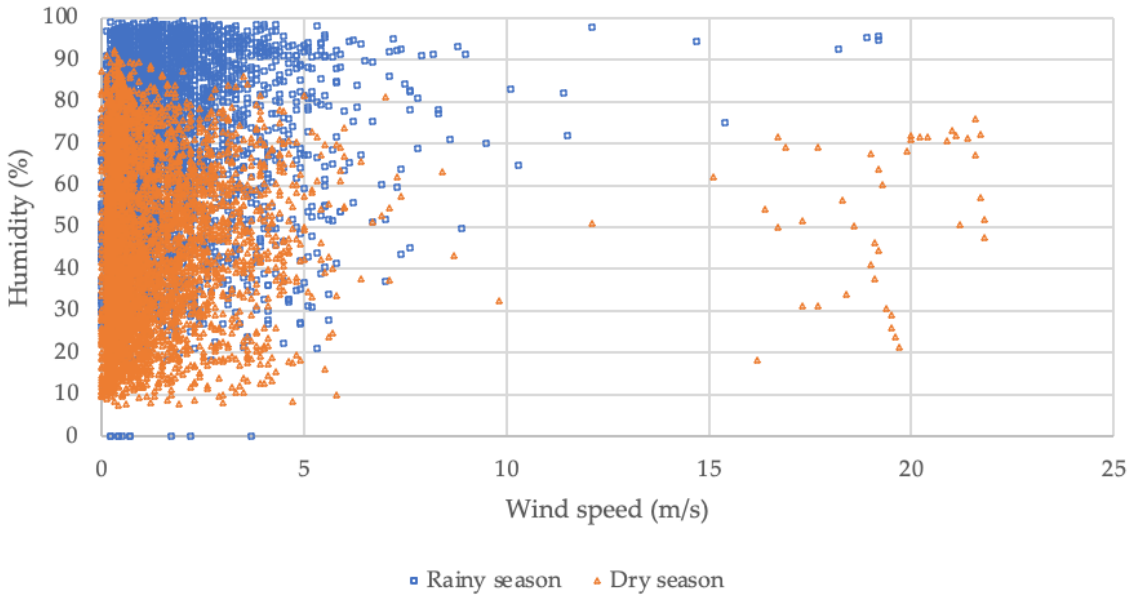

Figure 3- 3. Correlation between wind speed and humidity.

Correlation between wind speed and air temperature in both rainy and dry seasons were analyzed and compared in Figure 3-4. Significant correlations were not identified in both rainy and dry seasons. Wind speed had a trend to be lower when air temperature was high in the dry season.

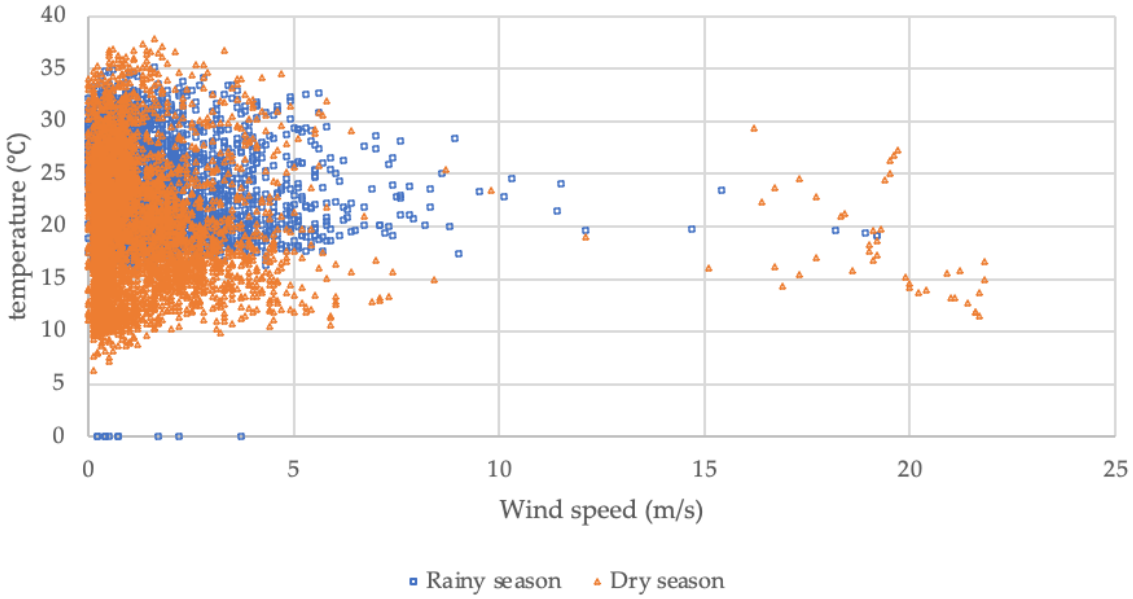

Figure 3- 4. Correlation between wind speed and temperature.

Weather conditions in both rainy and dry seasons for investigating impacts of weather factors on Pb-bearing soil dispersion were prepared (Table 3-5 and Table 3-6).

Table 3- 5. Weather conditions for simulation of Pb-bearing soil dispersion in the rainy season.

#	Wind speed	Solar radiation	Barometric pressure	Humidity	Air temperature	Note
1	1.43 m/s	2.17 kW/m²	872.62 hPa	68.65 %	23.08 ℃	Average
2	3.10 m/s	2.17 kW/m²	872.62 hPa	68.65 %	23.08 ℃	High wind speed
3	0.30 m/s	2.17 kW/m²	872.62 hPa	68.65 %	23.08 ℃	Low wind speed
4	1.43 m/s	7.73 kW/m²	872.62 hPa	68.65 %	23.08 ℃	High solar radiation
5	1.43 m/s	0.00 kW/m²	872.62 hPa	68.65 %	23.08 ℃	Low solar radiation
6	1.43 m/s	2.17 kW/m²	877.20 hPa	68.65 %	23.08 ℃	High barometric pressure
7	1.43 m/s	2.17 kW/m²	872.00 hPa	68.65 %	23.08 ℃	Low barometric pressure
8	1.43 m/s	2.17 kW/m²	872.62 hPa	93.60 %	23.08 ℃	High humidity
9	1.43 m/s	2.17 kW/m²	872.62 hPa	40.37 %	23.08 ℃	Low humidity
10	1.43 m/s	2.17 kW/m²	872.62 hPa	68.65 %	28.88 ℃	High air temperature
11	1.43 m/s	2.17 kW/m²	872.62 hPa	68.65 %	18.70 ℃	Low air temperature

Table 3- 6. Weather conditions for simulation of Pb-bearing soil dispersion in the dry season.

#	Wind speed	Solar radiation	Barometric pressure	Humidity	Air temperature	Note
1	1.44 m/s	1.88 kW/m²	877.79 hPa	45.55 %	20.34 ℃	Average
2	3.10 m/s	1.88 kW/m²	877.79 hPa	45.55 %	20.34 ℃	High wind speed
3	0.20 m/s	1.88 kW/m²	877.79 hPa	45.55 %	20.34 ℃	Low wind speed
4	1.44 m/s	6.51 kW/m²	877.79 hPa	45.55 %	20.34 ℃	High solar radiation
5	1.44 m/s	0.00 kW/m²	877.79 hPa	45.55 %	20.34 ℃	Low solar radiation
6	1.44 m/s	1.88 kW/m²	881.40 hPa	45.55 %	20.34 ℃	High barometric pressure
7	1.44 m/s	1.88 kW/m²	873.55 hPa	45.55 %	20.34 ℃	Low barometric pressure
8	1.44 m/s	1.88 kW/m²	877.79 hPa	73.60 %	20.34 ℃	High humidity
9	1.44 m/s	1.88 kW/m²	877.79 hPa	19.76 %	20.34 ℃	Low humidity
10	1.44 m/s	1.88 kW/m²	877.79 hPa	45.55 %	28.42 ℃	High air temperature
11	1.44 m/s	1.88 kW/m²	877.79 hPa	45.55 %	12.50 ℃	Low air temperature

3.3.2. Impacts of weather factors on dispersion

Pb-bearing soil dispersion to eight playgrounds from the ISF-slag site by local weather factors was calculated seasonally; during the rainy season (January to April and November to December) and during the dry season (May to October, August not included). Calculated seasonal deposition rates at each playground were accumulated. The results for S-2, located 6,904.1 m away from the dumping site (the farthest distance), S-3, located 4,042.2 m (the middle distance), and S-8, located 1,577.4 m (the nearest distance) were compared as listed in Tables 3-5 and 3-6.

At S-2 and S-3 in the rainy and dry seasons, the accumulated amounts deposited patterns were shown as similar (Figures 3-5 3-6, 3-7 and 3-8): the accumulated amounts deposited were significantly lower with high wind speed, low wind speed and low solar radiation conditions.

At S-2 in the rainy season, the accumulated amount deposited was 0.000017 mg/m^2 under high wind speed condition, it was 0.00002 mg/m^2 under low wind speed, and it was 0.00009 mg/m^2 under low solar radiation (Figure 3-5). The result under the high wind speed condition indicates that Pb-bearing soils were dispersed to S-2, but also most of them were redispersed by strong winds and flushed by rain falls from S-2. The result under the low wind speed condition indicates that Pb-bearing soils were difficult to be dispersed to S-2 because Pb-bearing soils were not forced to be dispersed by winds and wet by rain falls and humidity. There was an inversely proportional relationship between wind speed and solar radiation. With the correlation between wind speed and solar radiation, the result of under the low solar radiation indicates that strong winds blew, and Pb-bearing soils were redispersed at S-2 as well as under the high wind speed condition.

At S-2 in the dry season, the accumulated amount deposited was 0.01299 mg/m^2 under high wind speed condition, it was 0.00171 mg/m^2 under low wind speed, and it was 0.00692 mg/m^2 under low solar radiation (Figure 3-6). The result under the high wind speed condition indicates that Pb-bearing soils were dispersed to S-2, but also most of them were redispersed by strong winds at S-2. The result under the low wind speed condition indicates that Pb-bearing soils were difficult to be dispersed to S-2. There was an inversely proportional relationship between wind speed and solar radiation. With the correlation between wind speed and solar radiation, the result of under the low solar radiation indicates strong winds blew, and Pb-bearing soils were redispersed at S-2 as well as under the high wind speed condition.

At S-3 in the rainy season, the accumulated amount deposited was 0.00043 mg/m^2 under high wind speed condition, it was 0.00006 mg/m^2 under low wind speed, and it was 0.00018 mg/m^2 under low solar radiation (Figure 3-7). The result under the high wind speed condition indicates that Pb-bearing soils were dispersed to S-3, but also most of them were redispersed by strong winds and flushed by rain falls from S-3. The result under the low wind speed condition indicates that Pb-bearing soils were difficult to be dispersed to S-3 because Pb-bearing soils were not forced to be dispersed by winds and wet by rain falls and humidity. There was an inversely proportional relationship between wind speed and solar radiation. With the correlation between wind speed and solar radiation, the result of under the low solar radiation indicates that strong winds blew, and Pb-bearing soils were redispersed at S-3 as well as under the high wind speed condition.

At S-3 in the dry season, the accumulated amount deposited was 0.03704 mg/m^2 under high wind speed condition, it was 0.00479 mg/m^2 under low wind speed, and it

was 0.01534 mg/m^2 under low solar radiation as shown in Figure 3-8. The result under the high wind speed condition indicates that Pb-bearing soils were dispersed to S-3, but also most of them were redispersed by strong winds at S-3. The result under the low wind speed condition indicates that Pb-bearing soils were difficult to be dispersed to S-3. There was an inversely proportional relationship between wind speed and solar radiation. With the correlation between wind speed and solar radiation, the result of under the low solar radiation indicates that strong winds blew, and Pb-bearing soils were redispersed at S-3 as well as under the high wind speed condition.

At S-8 in the rainy and dry season, the accumulated amounts deposited patterns were shown as similar (Figures 3-9 and 3-10): the accumulated amounts deposited were significantly higher when high wind speed and low solar radiation conditions.

At S-8 in the rainy season, the accumulated amount deposited was 0.00315 mg/m^2 under high wind speed condition, and it was 0.00106 mg/m^2 under low solar radiation as shown in Figure 3-9. The result under the high wind speed condition indicates that huge amount of Pb-bearing soils were dispersed to S-8 by winds rather than to other playgrounds located farther from the source. There was an inversely proportional relationship between wind speed and solar radiation. With the correlation between wind speed and solar radiation, the result of under the low solar radiation indicates that strong winds blew, and Pb-bearing soils were redispersed at S-8 as well as under the high wind speed condition.

At S-8 in the dry season, the accumulated amount deposited was 0.26669 mg/m^2 under high wind speed condition, and it was 0.08978 mg/m^2 under low solar radiation as shown in Figure 3-10. The result under the high wind speed condition indicates that huge amount of Pb-bearing soils were dispersed to S-8 by winds at one time and deposited than redispersed there. There was an inversely proportional relationship between wind speed and solar radiation. With the correlation between wind speed and solar radiation, the result of under the low solar radiation indicates that strong winds blew, and Pb-bearing soils were redispersed at S-8 as well as under the high wind speed condition.

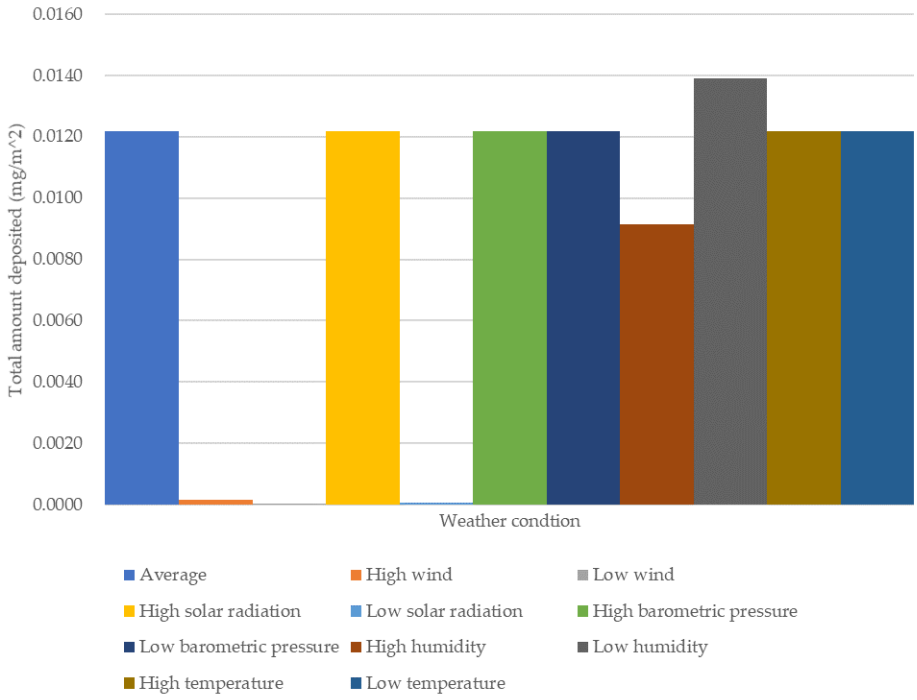

Figure 3- 5. Accumulated amounts deposited at S-2 by average and different weather conditions of the rainy season.

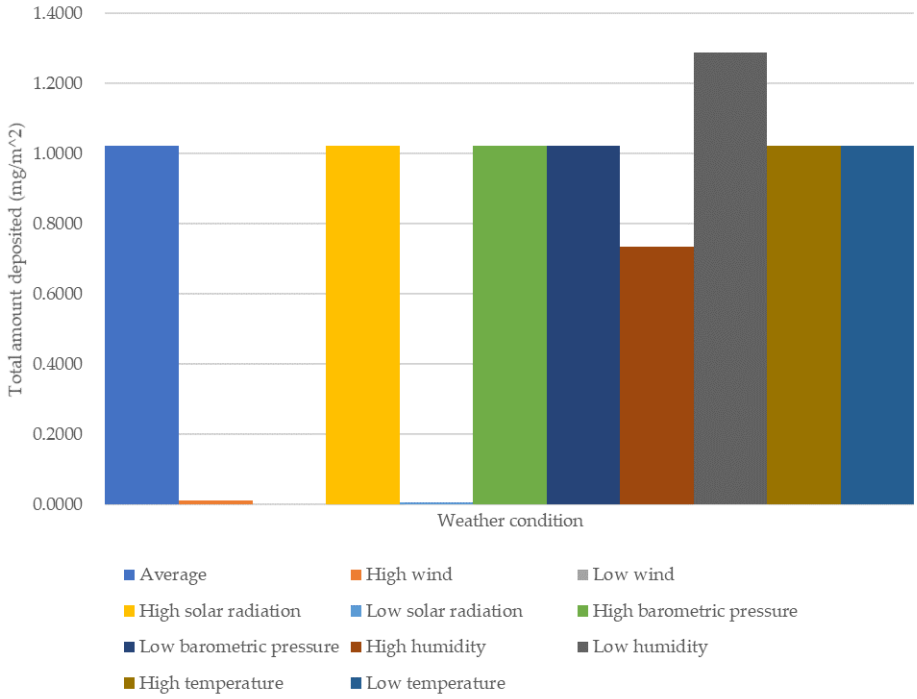

Figure 3- 6. Accumulated amounts deposited at S-2 by average and different weather conditions of the dry season.

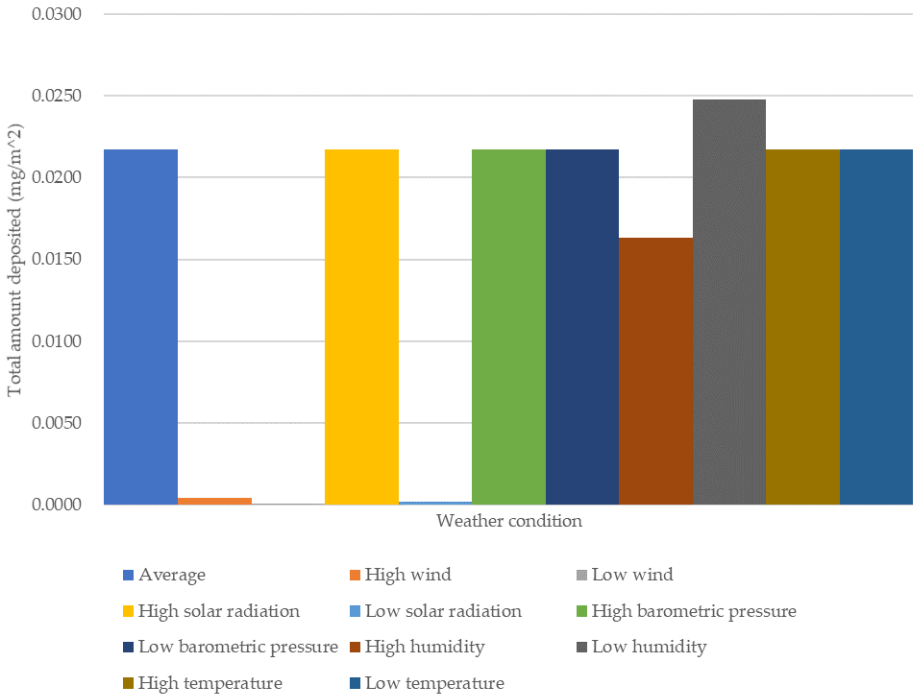

Figure 3- 7. Accumulated amounts deposited at S-3 by average and different weather conditions of the rainy season.

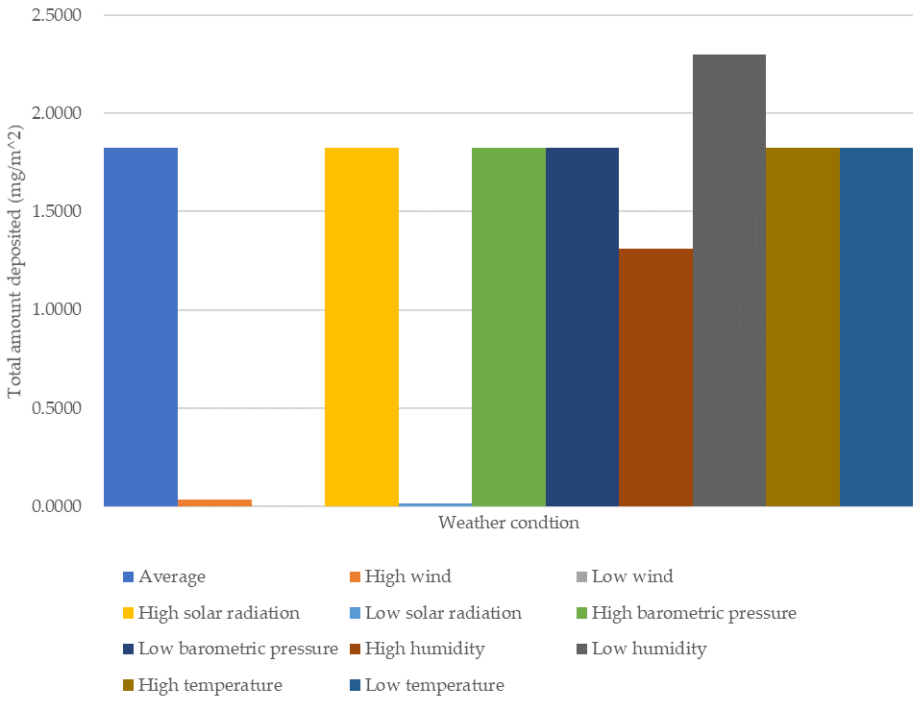

Figure 3- 8. Accumulated amounts deposited at S-3 by average and different weather conditions of the dry season.

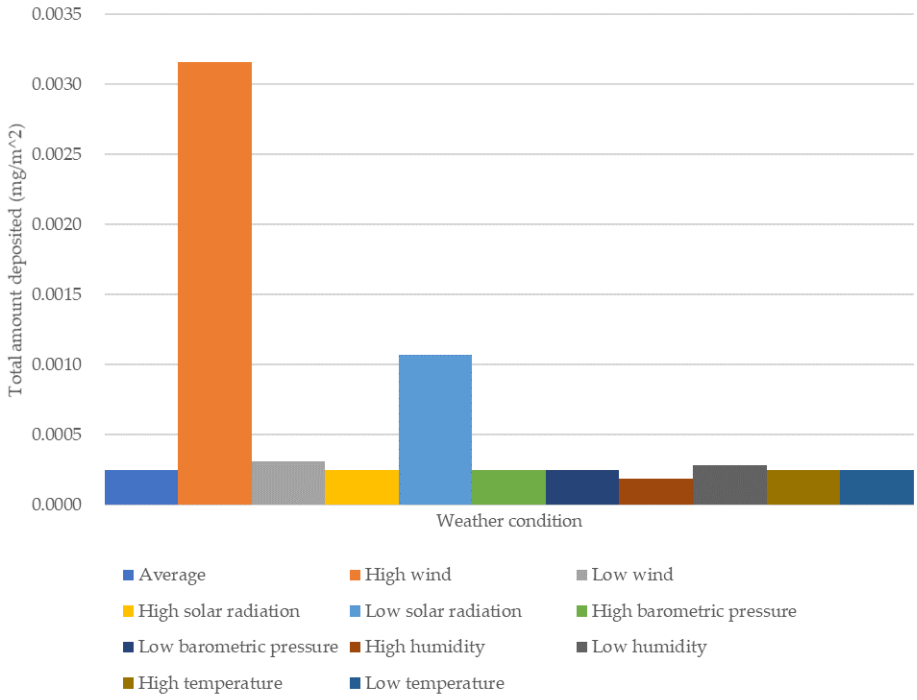

Figure 3- 9. Accumulated amount deposited depended at S-8 by average and different weather conditions of the rainy season.

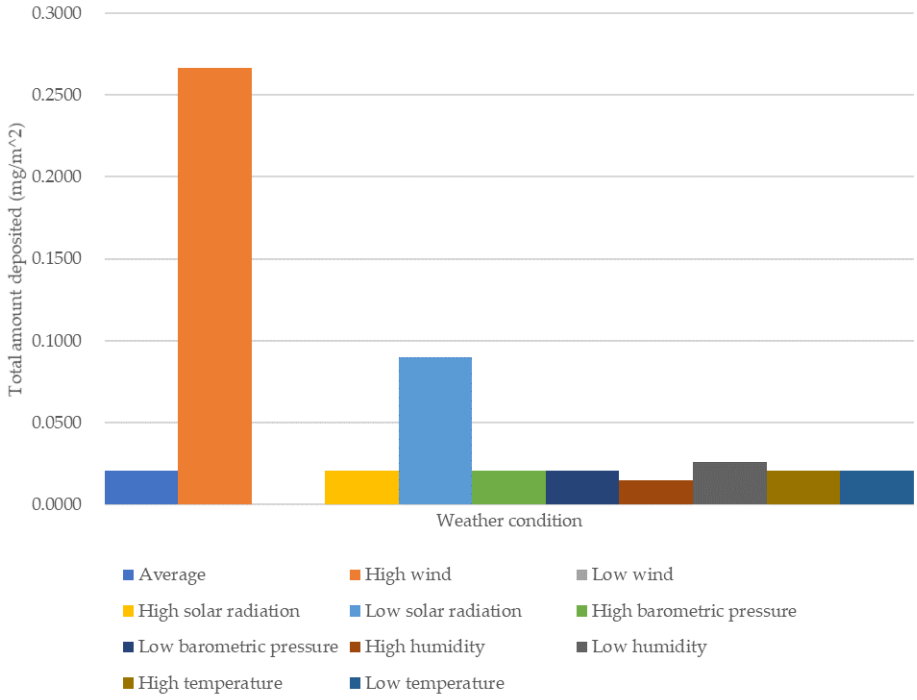

Figure 3- 10. Accumulated amounts deposited at S-8 by average and different weather conditions of the dry season.

Patterns of accumulated amounts deposited with particle sizes at S-2, S-3 and S-8 in the rainy and dry seasons were analyzed.

Figure 3-11 and Figure 3-12 show that the accumulated amounts deposited were depended on particle sizes at S-2, S-3 and S-8 under the average weather condition of the rainy and dry seasons, respectively. In both rainy and dry seasons, each particle size of soils was dispersed to sampling points located certain distances when the average weather conditions with average speed of the wind from the southeast were set for the simulation. The results did not agree with the results in Chapter 2 (Figure 2-10). The results indicate that Pb-bearing soils were dispersed easily through receiving certain force by average speed of wind blowing from one direction continuously. However, the winds blow variously under the actual weather environment, and Pb-bearing soils do not receive certain force from one direction continuously, and they are dispersed and deposited at sampling points near to the source.

Accumulated amounts deposited were increased with larger particle sizes of Pb-bearing soils at S-2 in the rainy season. The result indicates that smaller particle sizes of Pb-bearing soils were difficult to deposited at S-2 because they were redispersed by winds and flushed by rains easier than larger sizes (Figure 3-11).

Accumulated amounts deposited were decreased with particle sizes of Pb-bearing soils at S-3 in the rainy season. The result indicates that larger sizes of Pb-bearing soils were difficult to be dispersed to S-3 due to the high humidity and rain falls than finer sizes although finer particle sizes of Pb-bearing soil had abilities to be redispersed by and rain falls at S-3 (Figure 3-11).

Accumulated amounts deposited were increased with larger particle sizes of Pb-bearing soils at S-8 in the rainy season. The result indicates that finer particle sizes of Pb-bearing soils were difficult to be deposited at S-8 because they were redispersed by winds and flushed by rains easier than larger sizes although huge amount of Pb-bearing soils were dispersed to S-8. The results showed that high speed wind and low solar radiation conditions affected on swirling up fine particles of Pb-bearing soils from the source, and most of the large particle sizes of Pb-bearing soils were dispersed and deposited at S-8 (Figure 3-11).

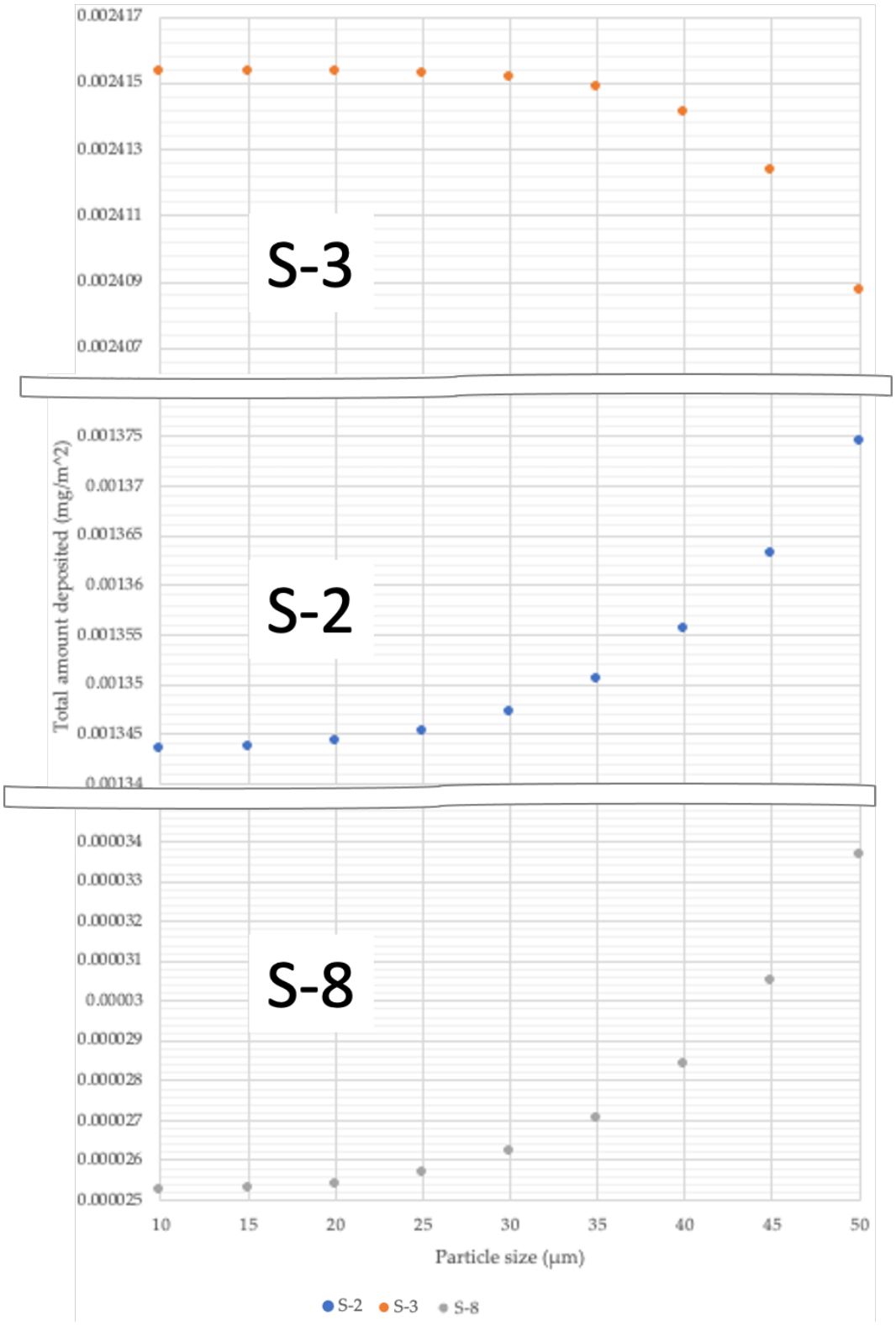

Figure 3- 11. Accumulated amounts deposited depending on particle sizes of Pb-bearing soils at S-2, S-3 and S-8 in the rainy season.

Accumulated amounts deposited were depended on particle sizes at S-2 under the average weather condition of the dry season. The amounts were increased with larger particle sizes of Pb-bearing soils. The result indicates that smaller particle sizes of Pb-bearing soils were difficult to be deposited at S-2 because they were redispersed by winds easier than larger sizes (Figure 3-12).

Accumulated amounts deposited depended on particle sizes at S-3 under the average weather condition of the dry season. The amounts were decreased with larger particle sizes of Pb-bearing soils. The result indicates that finer particle sizes of Pb-bearing soils were easier to be dispersed than larger particle sizes at S-3 under the dry condition (Figure 3-12).

Accumulated amounts deposited were depended on particle sizes at S-8 under the average weather condition of the dry season. The amounts were increased with larger particle sizes of Pb-bearing soils. The result indicates that finer particle sizes of Pb-bearing soils were difficult to be deposited at S-8 because they were dispersed farther and redispersed by winds easier than larger sizes although huge amounts of Pb-bearing soils were dispersed to S-8. The results showed that high speed wind and low solar radiation conditions affected on swirling up fine particles of Pb-bearing soils from the source, and most of the large particle sizes of Pb-bearing soils were dispersed and deposited at S-8 (Figure 3-12).

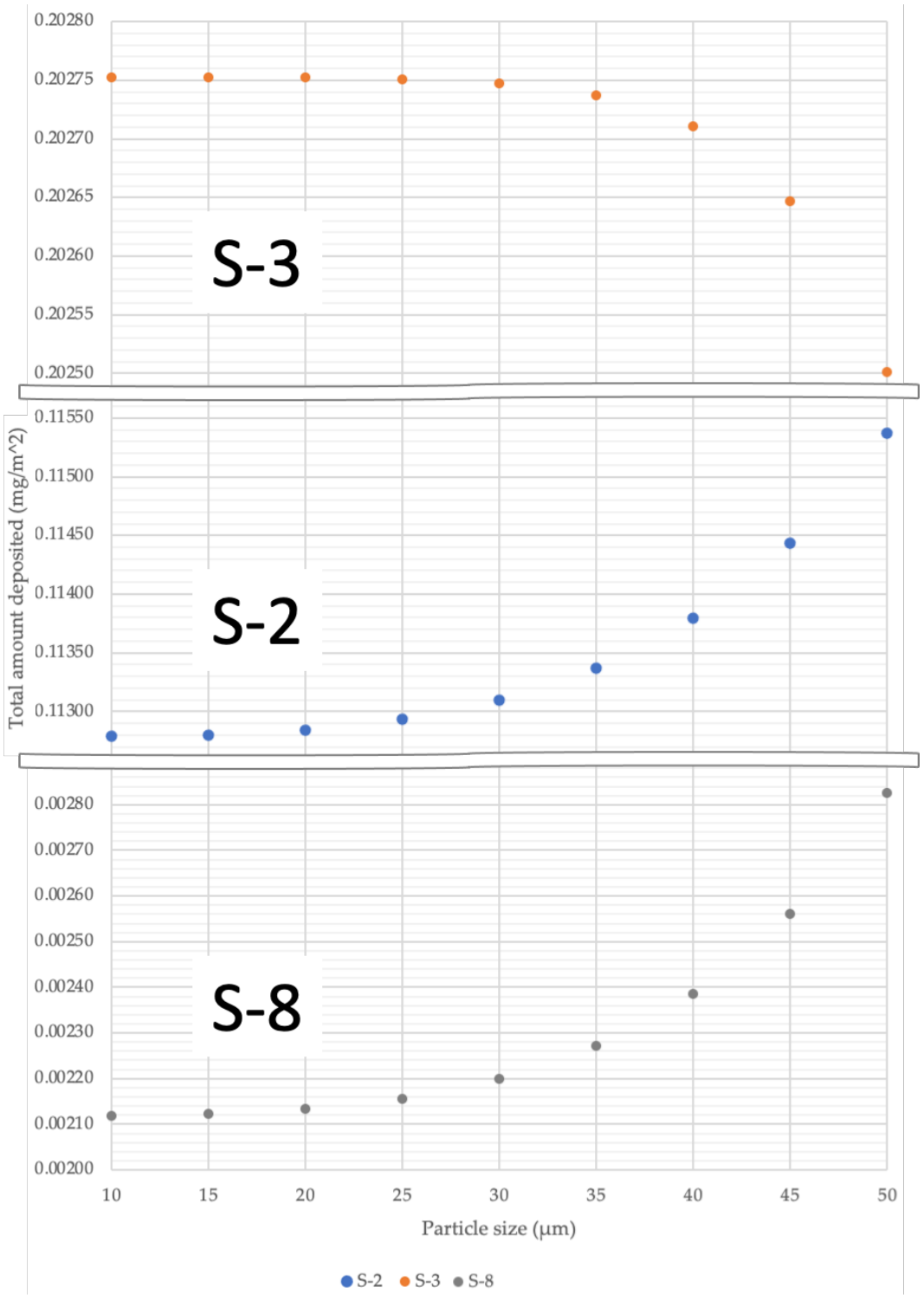

Figure 3- 12. Accumulated amounts deposited depending on particle sizes of Pb-bearing soils at S-2, S-3 and S-8 in the dry season.

3.4. Discussion

Local weather data in Kabwe in the year 2019 were analyzed and characterized the differences between the rainy and dry seasons. Wind speeds in both seasons did not have any significant differences, but solar radiation, barometric pressure, humidity, and air temperature had seasonal differences. These weather parametric differences affected on the accumulated amount deposited at playgrounds beside wind speed.

Correlations between wind speed and solar radiation in both rainy and dry seasons showed the inversely proportional. These relationships were appeared in the sensitivity of the accumulated amounts deposited at S-2, S-3 and S-8 in both rainy and dry seasons significantly.

Both high and low wind speeds did not affect on amount deposited at a certain distance from the source in both rainy and dry seasons. The results indicates that high wind speed has abilities to disperse and redisperse huge amount Pb-bearing soils to and from playgrounds at the moment. On the other hand, low wind speed did not have abilities to disperse and redisperse huge amount of Pb-bearing soils. Moreover, solar radiation was inversely proportional to wind speed, and low solar radiation led to high-wind-speed-like conditions, and it did not affect on Pb-bearing soils dispersion from the source to playgrounds at certain distances in Kabwe.

Impacts of wind directions were indicated in Chapter 2. Figure 3-13 to Figure 3-16 show the heatmaps of impacts of wind directions on the sampling points in the dry season when the accumulated amount deposited at each playground was higher than the rainy season. When wind directions were changed, but other weather factors were fixed as their average values in the dry season (Table 3-6).

Lead-bearing soil dispersion to the sampling points were indicated to be most affected by winds blew from the southeast in Chapter 2. Winds from the southeast had impacts on S-1, S-3, S-6 and S-7 located near the source mainly (Figure 3-13). The accumulated amount deposited at S-1 was 12.6 $\mu g/m^2$, and it was the highest amount among the sampling points.

Lead-bearing soil dispersion to the sampling points were also affected by winds from the east (Figure 3-14). Winds from the east had impacts on S-1, S-3, S-6 and S-7 located near the source mainly. The accumulated amount deposited at S-1 was 8.6 $\mu g/m^2$, and it was the highest amount among the sampling points.

Lead bearing soil dispersion to the sampling points were not much affected by winds from the west and north sides which the sampling points were upstream of the winds to the source (Figure 3-15 and Figure 3-16). The calculated and accumulated amount deposited at S-1 was -12.6 $\mu g/m^2$, and it was the lowest amount among the sampling points when the winds blew from the west. On the other hand, the calculated and accumulated amount deposited at S-1 was -8.53 $\mu g/m^2$, and it was the lowest amount

among the sampling points when the winds blew from the north. Those negative values are due to the net effects of deposition and redispersion by winds from the west and north.

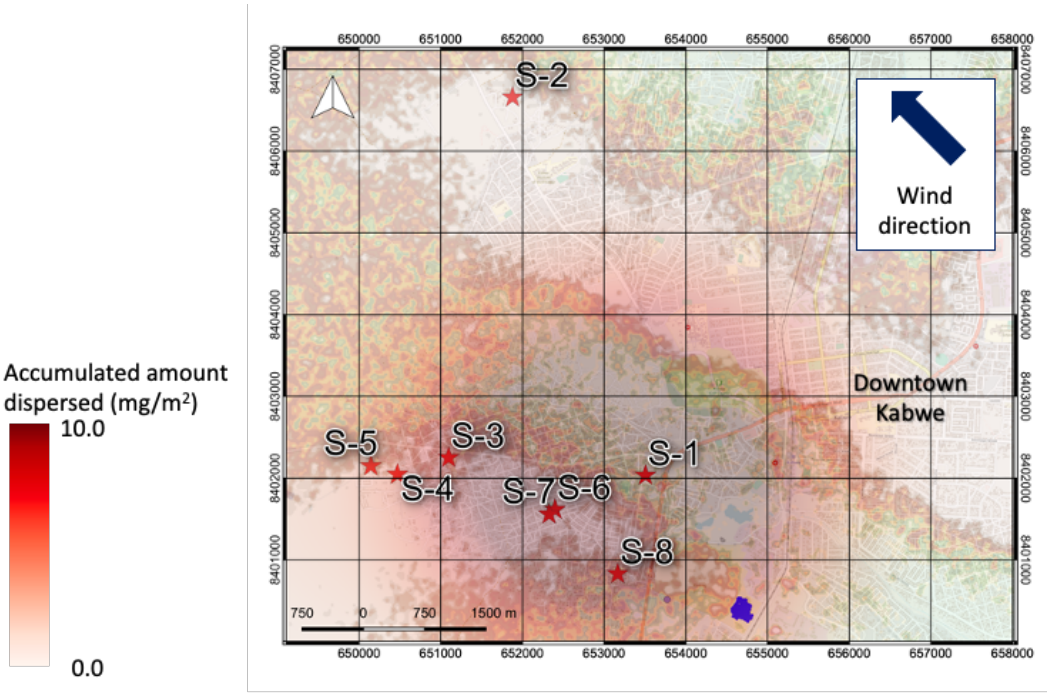

Figure 3- 13. Heatmap of impacts by wind from the southeast.

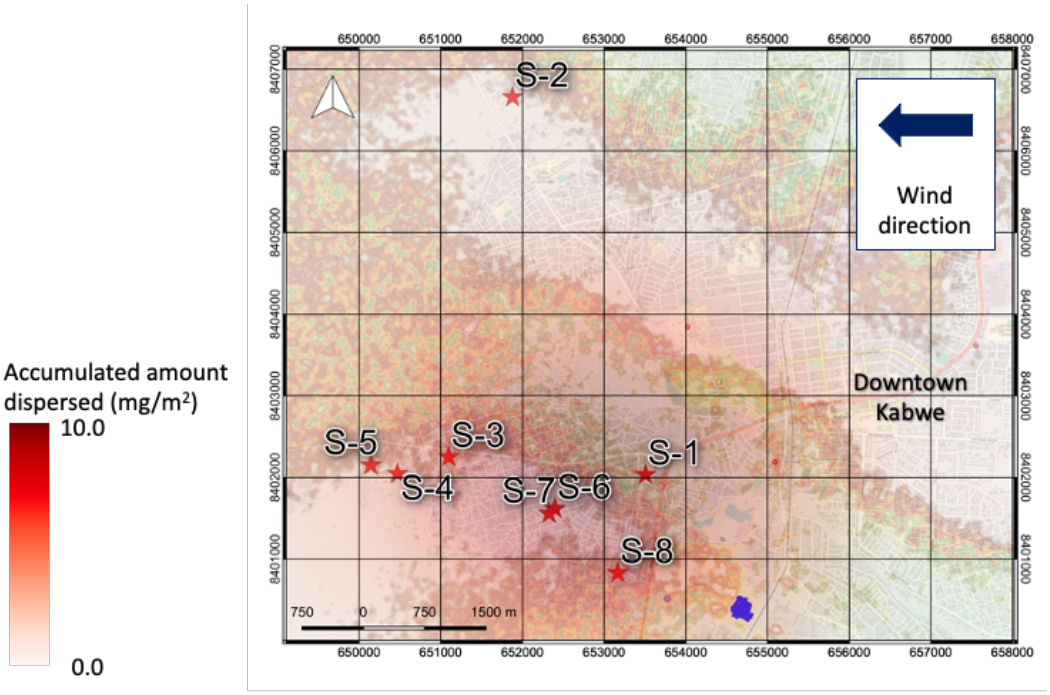

Figure 3- 14. Heatmap of impacts by winds from the east.

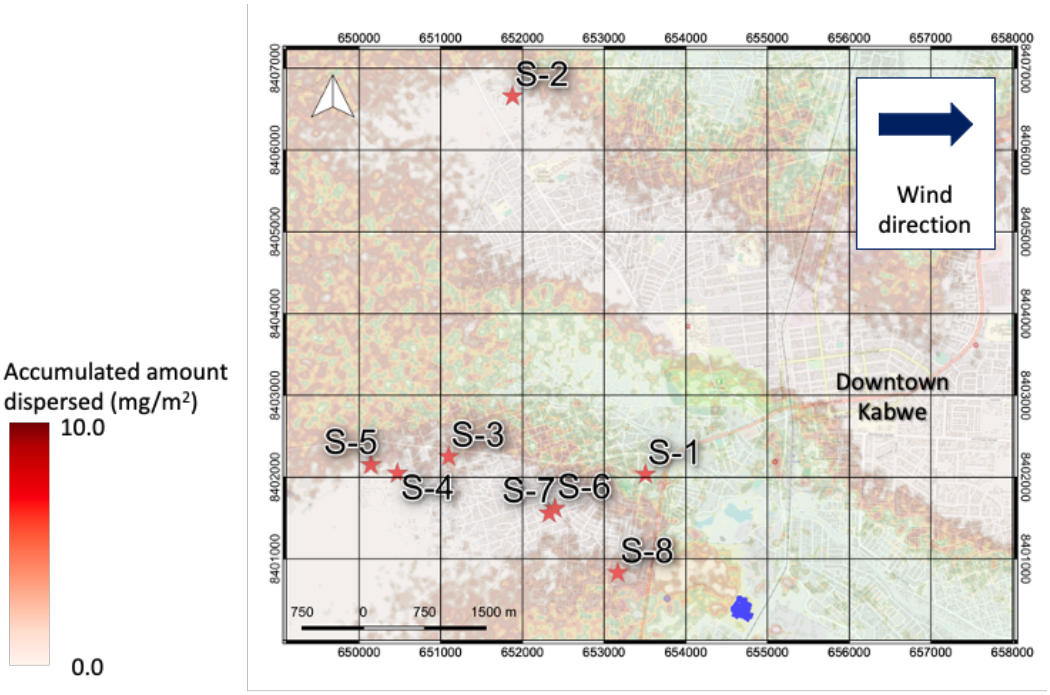

Figure 3- 15. Heatmap of impacts by winds from the west.

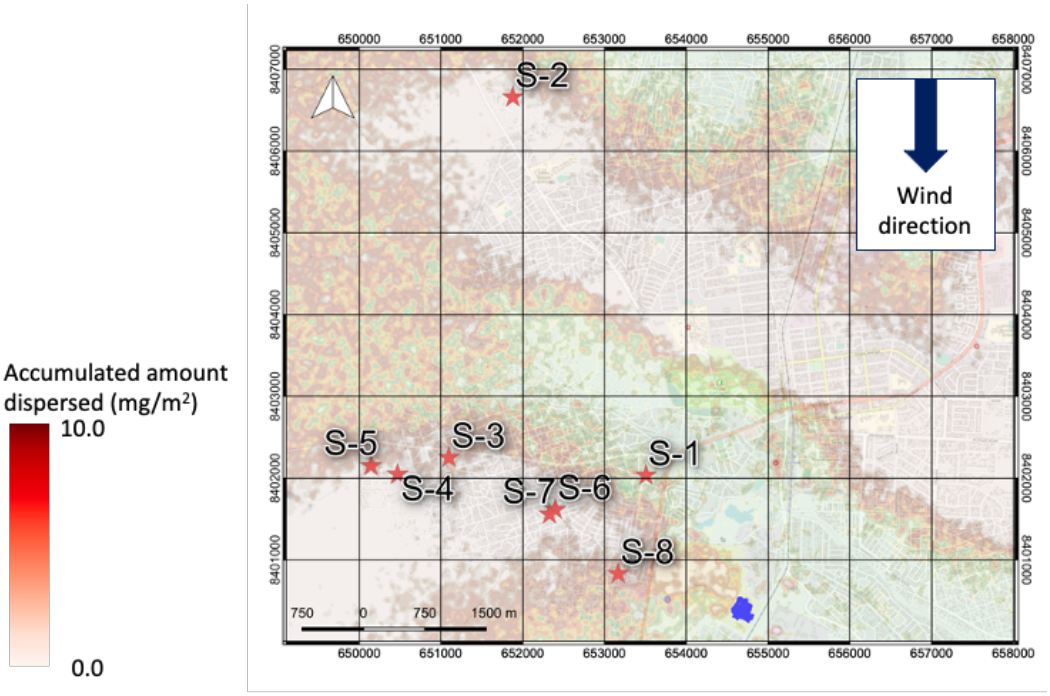

Figure 3- 16. Heatmap of impacts by winds from the north.

3.5. Conclusion

Simulations of Pb-bearing soil dispersion were performed under the average, top 10 % and bottom 10 % values of local weather data in the year 2019 for estimating impacts of weather factors on Pb-bearing soil dispersion from the source. The following results were obtained.

1. Weather in Kabwe was calm through the year, but there were significant differences of solar radiation, barometric pressure, humidity, and air temperature between rainy and dry seasons.
2. Correlation between wind speed and solar radiation was the inversely proportional, and the relationships affected the accumulated amounts deposited by simulations.
3. High and low wind speeds did not affect on the accumulated amounts deposited at certain distances from the source.
4. Wind directions had huge impacts on deposition amounts and areas.

Pb-bearing soil dispersion and deposition were affected by not only wind speeds and directions but also complicated relationships among weather factors. In-depth understanding about relationships between local weather conditions and heavy metal dispersion is of importance for proposing effective countermeasures against Pb-bearing soil dispersion and remediation of soil contamination.

References

1. Nakamura, S.; Igarashi, T.; Uchida, Y.; Ito, M.; Hirose, K.; Sato, T.; Mufalo, W.; Chirwa, M.; Nyambe, I.; Nakata H.; Nakayama, S.; Ishizuka, M. Evaluation of dispersion of lead-bearing mine wastes in Kabwe District, Zambia. *Minerals*, 2021, *11*(8), 901.
2. Brotons, J. M.; Díaz, A. R.; Sarría, F. A.; Serrato, F. B. Wind erosion on mining waste in southeast Spain. *Land Degrad. Develop.* 2010, *21*, 196-209.
3. Mokhtari, A. R.; Feiznia, S.; Jafari, M.; Tavili, A. Investigating the role of wind in the dispersion of heavy metals around mines in arid regions (a case study from Kushk Pb-Zn Mine, Bafgh, Iran). *Bulletin of Environmental Contamination and Toxicology*, 2018; *101*(4).
4. Mileusnić, M.; Mapani, B. S.; Kamona, A. F.; Ružičić. S.; Mapaure, I.; Chimwamurombe, P. M. Assessment of agricultural soil contamination by potentially toxic metals dispersed from improperly diposed tailings, Kombat mine, Namibia. *Journal of Geochemical Exploration*, 2014, *144*, 409-420.
5. Tembo, B. D.; Sichilongo, K.; Cernak, J. Distribution of copper, lead, cadmium and zic concentrations in soils around Kabwe town in Zambia. *Chemosphere*, 2006, *63* (3), 497-501.
6. Punia A. Role of temperature, wind and precipitation in heavy metal contamination at copper mines: A review. *Environmental Science and Pollution Research*, 2021, *28*, 4056 – 4072.
7. Sherman, C.A. A mass-consistent model for wind fields over complex terrain. *J. Appl. Meteorol.* 1978, *17*, 312–319.
8. Fukuyama, T.; Izumi, K.; Utiyama, M. Dry deposition of atmospheric aerosols—A browse on recent papers. *J. Aerosol Res.* 2004, *19*, 245–253.
9. Ministry of Economy, Trade and Industry of Japan. Technical Manual of Ministry of Economy, Trade and Industry Low rise Industrial Source dispersion model (METI-LIS) ver. 3.02, March 2012. Available online: https://www.jemai.or.jp/tech/meti-lis/detailobj-6117-attachment.pdf (accessed on 30 May 2019).
10. Luhar, A.K. Analytical puff modelling of light-wind dispersion in stable and unstable conditions. *Atmos. Environ.* 2011, *45*, 357–368.

Chapter 4. Water parametric analysis on lead- and zinc-bearing soil dispersion in Kabwe

4.1. Introduction

In this chapter, impacts of water conditions of soils at the source on Pb- and Zn-bearing soil dispersion are analyzed and discussed.

In Chapter 3 and the previous studies [1 - 3], the impacts of wind speeds and directions and other weather factors on heavy metal dispersion and deposition were examined. Dispersion and redispersion models have been designed to perform by following local weather factors, and mechanisms of heavy metal contaminations have been simulated and discussed [4, 5]. On the other hand, impacts of water condition of the surface soils of the source on dispersion by winds are not discussed even though the soil dispersion was considered with humidity and barometric pressure.

In this chapter, for estimating impacts of water on dispersion, simulation of Pb- and Zn-bearing soil dispersion were performed by consideration of water conditions on Pb-bearing Zn plant leach residue site through satellite data analyses.

4.2. Materials and methods

4.2.1. Study site

At the Kabwe mine, Pb-bearing Zn plant leach residue site was recognized to have a cycle of the covered and non-covered by water bodies throughout the year 2019 by satellite data observations. In this chapter, Pb-bearing Zn plant leach residue site was suitable for analysis the impacts of water on dispersion and selected as the source site.

The area of the source was extracted by analyzing European optical satellite, named Sentinel-2. Four source points at the source site were selected for this study because the source site was separated four areas by ridges, and different amounts of water bodies were recognized throughout the year 2019. Moreover, the source was adopted as a bundle of source points for considering Pb- and Zn bearing soils would be dispersed from the area although a single point, such as a chimney in an industrial factory, was used for the simulation [6]. The height of the source was estimated at the same height of the source, and it was calculated with Digital Elevation Model by Japanese spaceborne synthetic aperture radar, named PALSAR (PALSAR DEM) with 12.5 m spatial resolution [7]. The location of Pb-bearing Zn plant leach residue site was shown in Figure 4-1.

Eight playgrounds as target and sampling points where were used in Chapters 2 and 3 were also used in this chapter for comparing and analyzing the effects of the local weather factors of the year 2019. Figure 4-1 also shows the locations of the source area and playgrounds.

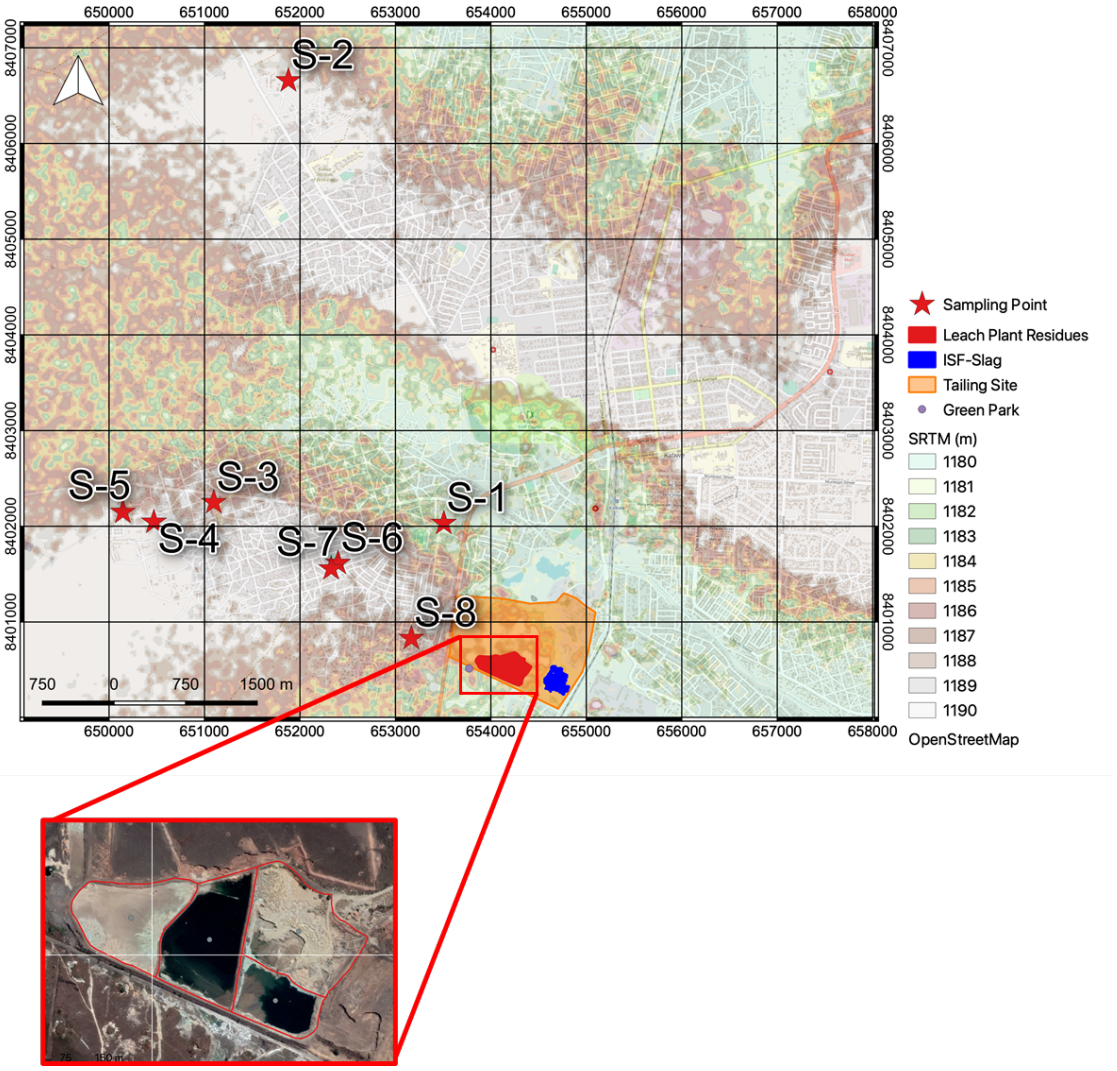

Figure 4- 1. Location of the study site: Pb-bearing Zn plant leach residue site was separated into four areas by ridges, and two of them were covered by water throughout the year 2019: Pb-bearing Zn plant leach residue site was in relatively lower than other dumping and several playgrounds.

4.2.2. Normalized difference water index

Normalized difference water index (NDWI) is a method of estimating open water features by using short wave infrared bands of spectral sensors. The basic idea of NDWI is to use green and near infrared bands of remote sensing which water has strong absorption and low radiation in the range between visible and near infrared wavelengths [8]. Various studies have been conducted with optical satellite data, and NDWI has been improved, and modified normalized difference water index (MNDWI) was developed by its abilities to estimate water information and extract water bodies [9, 10].

For estimating water features of the surface soil on Pb-bearing Zn plant leach residue site by MNDWI, Sentinel-2 datasets were used. Author tried to download various satellite data not only Sentinel-2 series but also Landsat (American) and ASTER (Japanese) for analyzing every month of the year 2019, but some datasets were covered by clouds, and it was difficult to analyze the water conditions on the source site.

European Space Agency (ESA) launched a constellation of spaceborne multispectral sensor satellites named Sentinel-2 A and Sentinel-2 B in 2015 and 2017 respectively under Copernicus Program on behalf of European Committee. The Earth observations by the constellation of satellites are improved through high observation frequency and global coverage [11]. The bands of Sentinel-2 series and equation of MNDWI are shown in Table 4-1 and Equation 4-1.

Table 4- 1. Band specification of Sentinel-2 series.

Band	Spatial resolution (m)	Central wavelength (nm)	Band width (nm)
B1	60	443	20
B2	10	490	65
B3	10	560	35
B4	10	665	30
B5	20	705	15
B6	20	740	15
B7	20	783	20
B8	10	842	115
B8A	20	865	20
B9	60	945	20
B10	60	1375	20
B11	20	1610	20
B12	20	2190	20

$$MNDWI = \frac{B3-B11}{B3+B11}, \quad \text{(Equation 4-1)}$$

The range of MNDVI is from -1.0 (dry) to 1.0 (wet).

4.2.3. Weather data collection

Local weather data in Kabwe in the year 2019, which were collected and used in Chapter 2 were used for this chapter. All weather data were collected hourly at Green Park, Kabwe and the test site at the University of Zambia, Lusaka throughout the year 2019. Due to machine troubles and errors of the data collection system, the data of August 2019 were not collected but not used in this chapter, either. Kabwe local weather data on the dates of satellite data acquisitions were used for the simulation in this chapter.

4.2.4. Simulation models of Lead- and zinc-bearing soil dispersion

Three models of Pb-bearing soil dispersion which were constructed and used in Chapters 2 and 3 were also used in this chapter. The plume model was prepared when wind speed was over 1.0 m/s; the weak puff model was prepared when wind speed was between 0.4 m/s and 1.0 m/s; and the no puff model was prepared when wind speed was less than 0.4 m/s.

The source strength (Q) is a key parameter to simulate Pb- and Zn-bearing soil dispersion. Here, a total of 1 m^3 of soils per one second was assumed to be dispersed. However, only finer particles (< 50 μm) are transported to a further distance. Also, the estimated amounts of Pb and Zn productions from the tailing site were almost same [12]. Thus, the finer fraction of 2.5 % of the soils were assumed to be dispersed (0.0250 m^3/s) as a source strength for the dry soils. In Chapters 2 and 3, humidity and rain falls were factors affecting on the source strength for the simulation. In this chapter, results of MNDWI were used to determine the source strength as shown in Table 4-2. Moreover, Pb-bearing Zn plant leach residue site was assumed to be completely ponded when the MNDWI indicated over 0.8 [13], and the source strength was set as zero. The values of source strength were set by following the study in Chapter 2.

Table 4- 2. Chart between MNDWI and source strength: the source strength is set depending on the value of MNDWI.

MNDWI	Source strength
MNDWI = -1.0	0.0250 m^3/s
-0.1 < MNDWI <= -0.8	0.0230 m^3/s
-0.8 < MNDWI <= -0.6	0.0200 m^3/s
-0.6 < MNDWI <= -0.4	0.0180 m^3/s
-0.4 < MNDWI <= -0.2	0.0150 m^3/s
-0.2 <M NDWI <= 0.0	0.0130 m^3/s
0.0 < MNDWI <= 0.2	0.0100 m^3/s
0.2 < MNDWI <= 0.4	0.0080 m^3/s
0.4 < MNDWI <= 0.6	0.0050 m^3/s
0.6 < MNDWI <= 0.8	0.0025 m^3/s
0.8 < MNDWI <= 1.0	0.0000 m^3/s

4.3. Results

4.3.1. Modified normalized difference water index

The following Sentinel-2 datasets were collected and calculated for water feature estimations on Pb-bearing Zn plant leach residue site (Table 4-3). Level-1C is a product level of Sentinel-2, and the product is composed as ortho-images in Universal Transverse Mercator (UTM)/WGS 84 [14]. The satellite data, which were acquired on 18 August 2019, were not used because the local weather data collection was failed due to machine troubles.

Table 4- 3. List of satellite datasets for NDWI.

#	Observation Date (year-month-day)	Satellite	Product Level	Note
1	2019-03-31	Sentinel-2 B	Level-1C	Rainy season
2	2019-04-30	Sentinel-2 B	Level-1C	Rainy season
3	2019-05-20	Sentinel-2 B	Level-1C	Dry season
4	2019-06-29	Sentinel-2 B	Level-1C	Dry season
5	2019-07-19	Sentinel-2 B	Level-1C	Dry season
6	2019-08-18	Sentinel-2 B	Level-1C	No weather data
7	2019-09-07	Sentinel-2 B	Level-1C	Dry season
8	2019-11-06	Sentinel-2 B	Level-1C	Rainy season
9	2019-12-16	Sentinel-2 B	Level-1C	Rainy season

MNDWI was applied to all satellite datasets listed in Table 4-3. For convenience, Pb-bearing Zn plant leach residue site was divided by ridges and set an area at the southeast side as #1, an area at the northeast as #2, an area at the westmost as #3 and the other as #4.

In the rainy season, water features were clearly estimated on #3 and #4 mainly. The values of MNDWI on areas #1 (average value: -0.078) and #2 (average value: -0.090) were relatively lower than on #3 (average value: 0.373) and #4 (average value: 0.470) throughout the season (Figure 4-2, Table 4-4).

In the dry season, the values of MNDWI were negative and indicated drier than the rainy season (Figure 4-3, Table 4-5). The values of MNDWI on areas #3 (average value: 0.010) and #4 (average value: 0.015) were higher than the values on the same locations on 30 April 2019: -0.110 and -0.230, respectively. The results indicate that Pb-bearing Zn plant leach residue site had possibilities to be affected by rain falls but also leaching activities at the Kabwe mine.

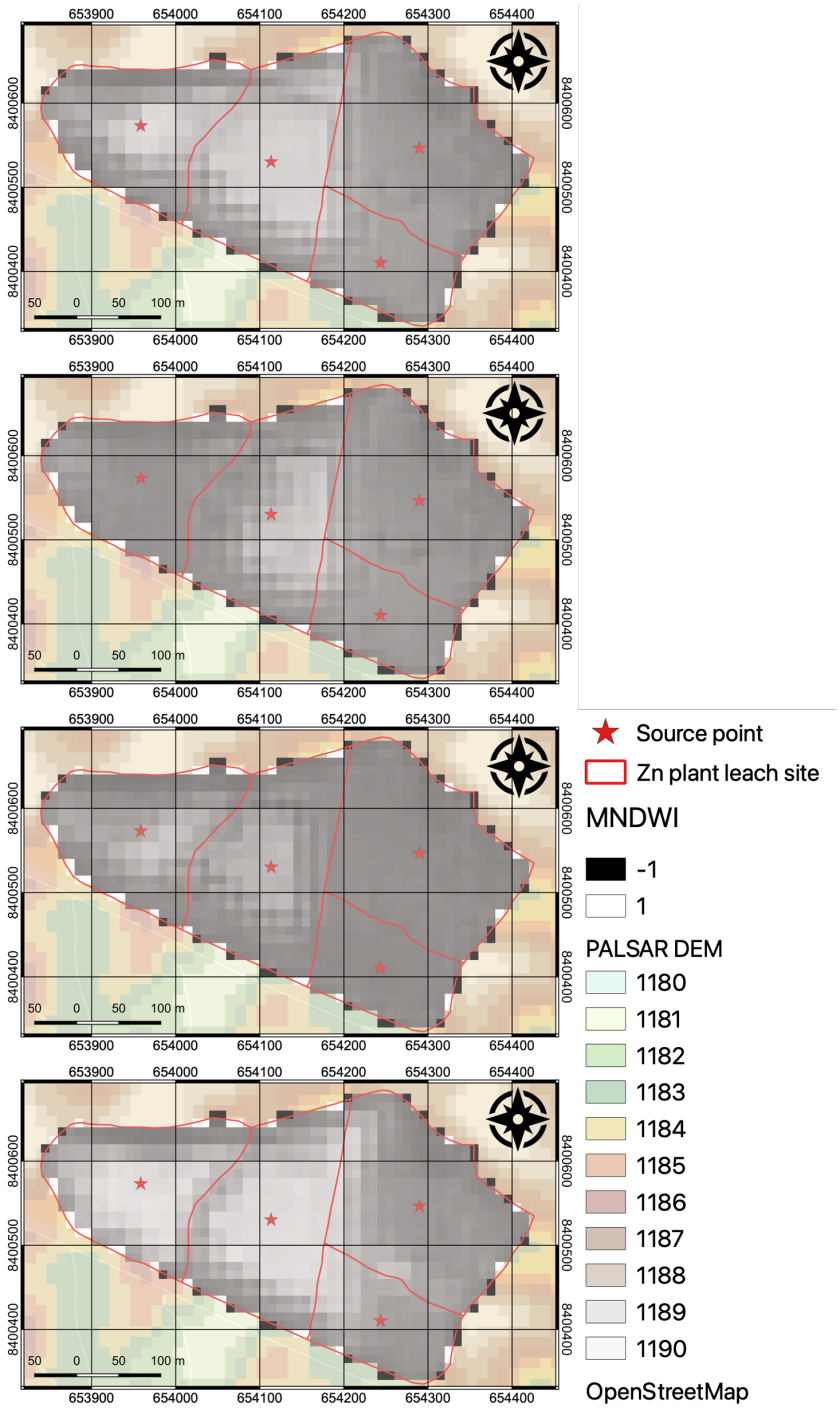

Figure 4- 2. Results of MNDWI in the rainy season: bright pixels indicate water in soils, and dark pixels indicate dry soils. (a) MNDWI results on 31 March 2019; (b) MNDWI results on 30 April 2019; (c) MNDWI results on 6 November 2019; and (d) MNDWI results on 16 December 2019. Water bodies were estimated in #3 and #4 through the rainy season mainly.

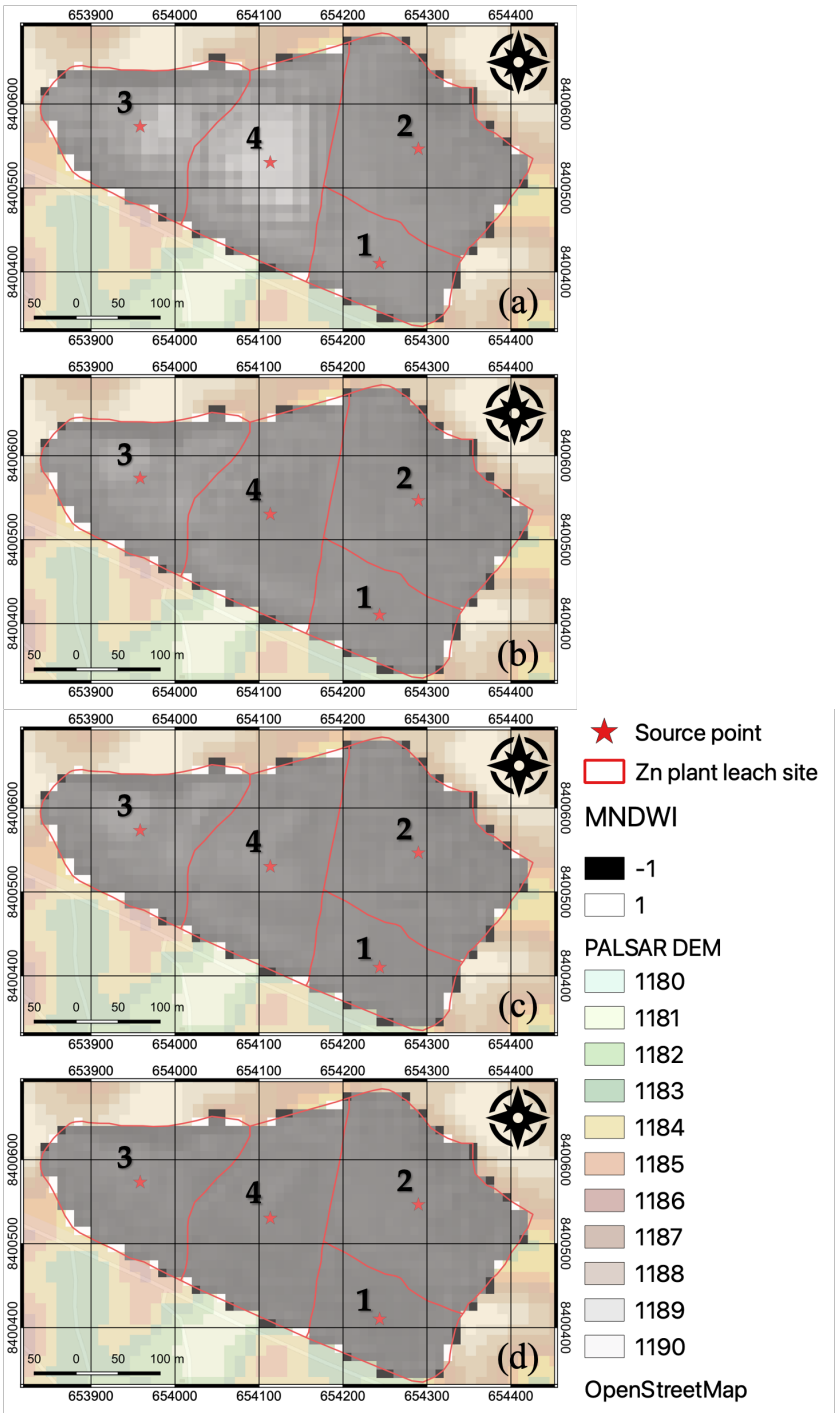

Figure 4- 3. Results of NDWI in the dry season: bright pixels indicate water in soils, and dark pixels indicate dry soils. (a) MNDWI results on 20 May 2019; (b) MNDWI results on 29 June 2019; (c) MNDWI results on 19 July 2019; and (d) MNDWI results on 7 September 2019.

Table 4- 4. Values of MNDWI in the rainy season 2019.

Area	31 Mar. 2019	30 Apr. 2019	06 Nov. 2019	16 Dec. 2019
#1	-0.03	-0.04	-0.24	0.00
#2	-0.05	-0.09	-0.19	-0.03
#3	0.70	-0.11	0.25	0.65
#4	0.49	0.23	0.27	0.65

Table 4- 5. Results of NDWI in the dry season 2019.

Area	20 May. 2019	29 Jun. 2019	19 Jul. 2019	07 Sept. 2019
#1	-0.07	-0.17	-0.20	-0.26
#2	-0.13	-0.17	-0.18	-0.20
#3	0.27	0.01	-0.10	-0.14
#4	0.50	-0.17	-0.07	-0.20

4.3.2. Weather conditions on the dates of Sentinel-2 observations

Wind conditions on 31 March 2019 had typical features of the rainy season in Kabwe: strong winds (0.912 m/s) blew from the west, and winds blew from the west and east frequently (29.1 % and 21.0% from the west and the east, respectively). Wind conditions on 30 April 2019 also had typical features of the rainy season: strong winds (0.594 m/s) blew from west sides frequently (29.1 %). Wind conditions on 6 November 2019 had unique features: strong winds (0.751 m/s) blew from northeast, and winds blew from the west and the east frequently (29.1 % and 45.8 % from the west and the east, respectively). Wind conditions on 16 December 2019 had also a unique feature: strong winds (0.843 m/s) blew from south sides frequently (33.3 %) as wind conditions like in the dry season.

Wind conditions on 20 May 2019 had a unique feature: winds (0.267 m/s) blew from west sides as like in the rainy season. Wind conditions on 29 June 2019 had winds (0.41 m/s) from the southeast and south sides frequently (50.0 %) although weak winds (0.001 m/s) blew from the northwest sides. Wind conditions on 19 July 2019 had a typical feature of the dry season: strong winds (0.625 m/s) blew from the south sides although winds blew from the west sides frequently (37.5 %).

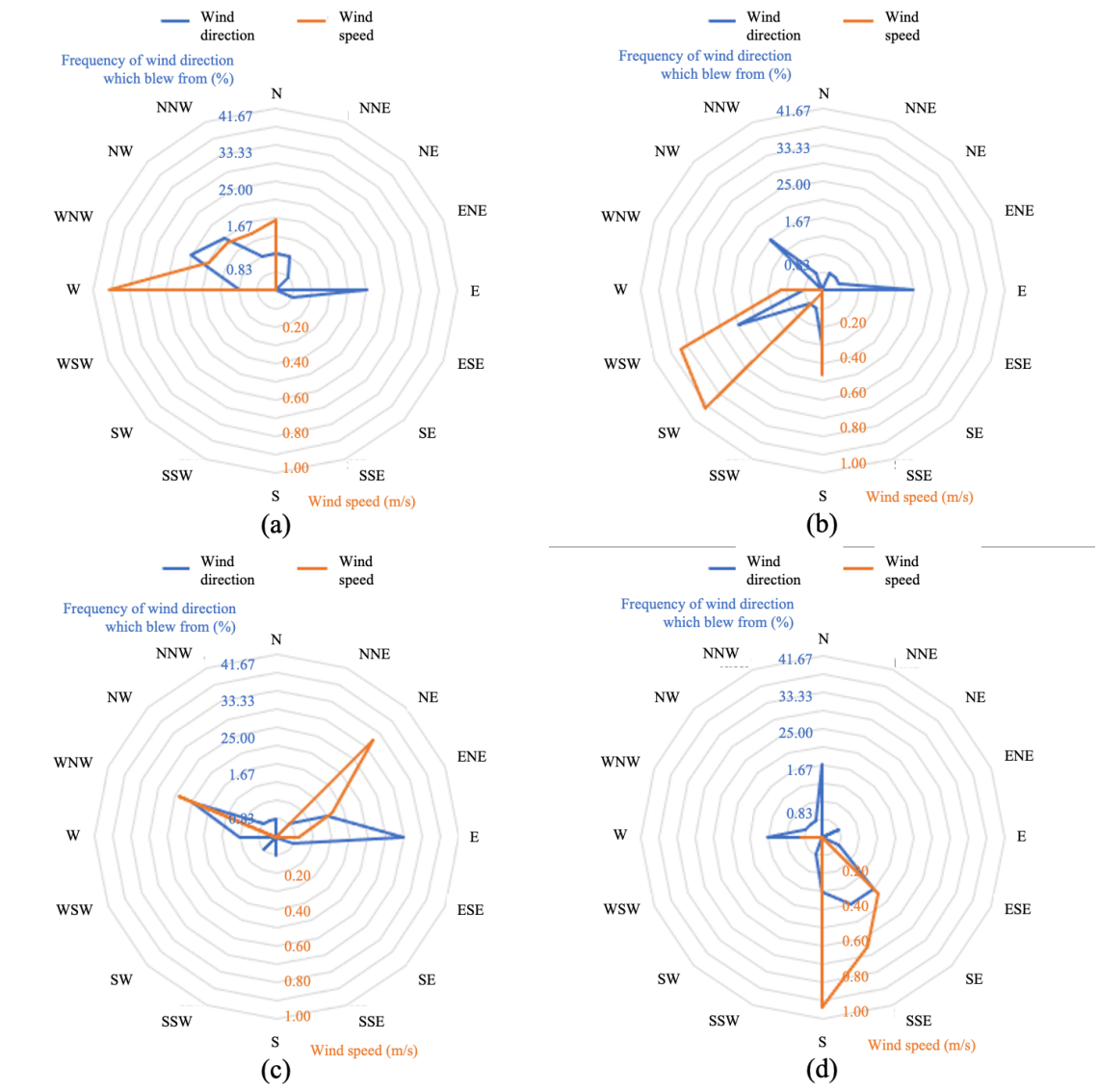

Figure 4- 4. Wind speed and frequency of wind directions on Sentinel-2 observation dates in the rainy season: (a) a chart of 31 March 2019; (b) a chart of 30 April 2019; (c) a chart of 6 November 2019; and (d) a chart of 16 December 2019.

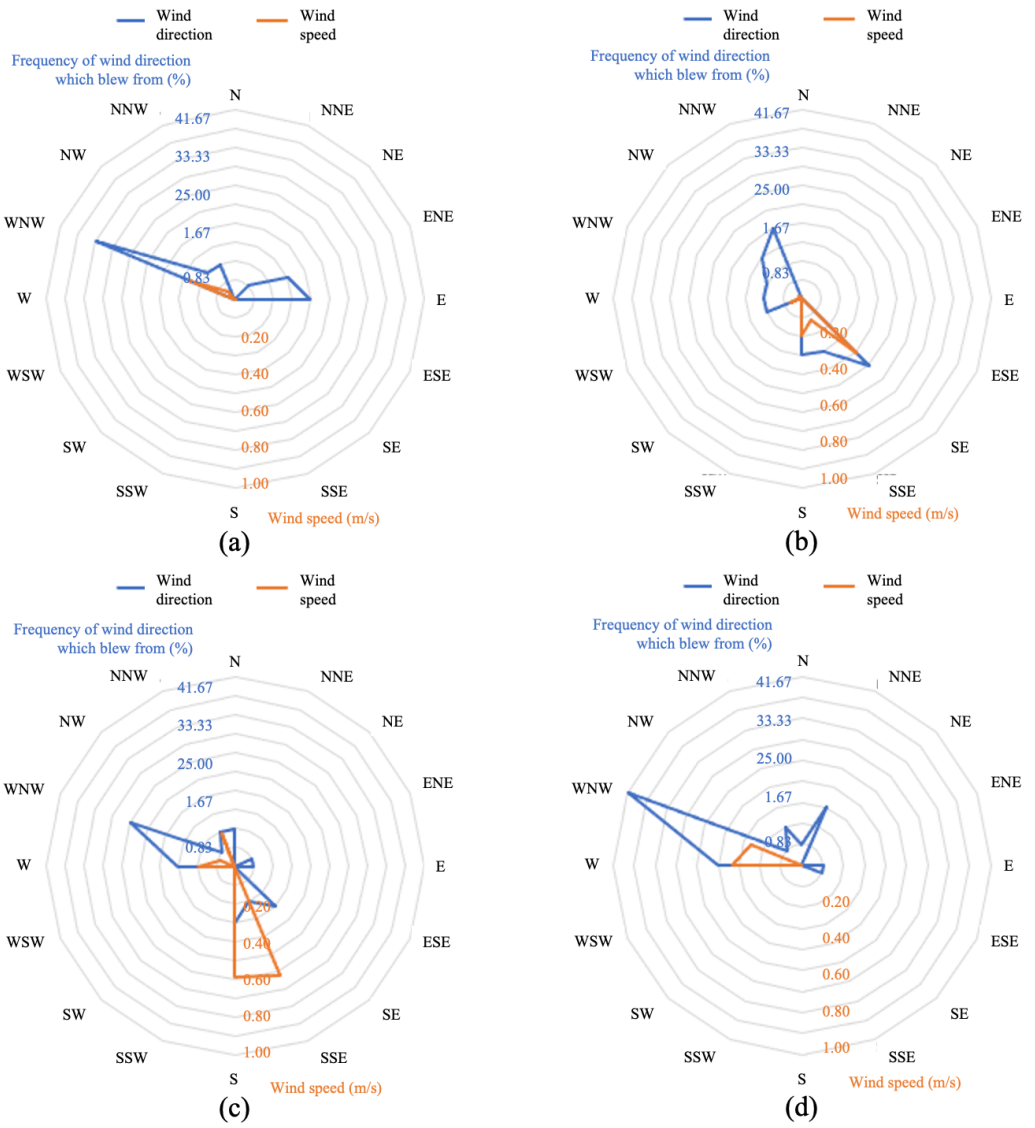

Figure 4- 5. Wind speed and frequency of wind directions on Sentinel-2 observation dates in the rainy season: (a) a chart of 20 May 2019; (b) a chart of 29 June 2019; (c) a chart of 19 July 2019; and (d) a chart of 07 September 2019.

Table 4- 6. Daily average values of weather data on Sentinel-2 observation dates in the rainy season: in practice, 24-hour of weather data per each Sentinel-2 observation date were applied to the simulation of leached Zn soil dispersion.

Date	Wind speed	Solar radiation	Barometric pressure	Humidity	Air temperature
2019/03/31	1.33 m/s	2.82 kW/m^2	875.78 hPa	55.10 %	22.46 ℃
2019/04/30	1.58 m/s	2.53 kW/m^2	878.76 hPa	63.60 %	20.19 ℃
2019/11/06	1.44 m/s	2.23 kW/m^2	874.50 hPa	40.98 %	26.03 ℃
2019/12/16	0.81 m/s	2.82 kW/m^2	874.40 hPa	68.57 %	24.38 ℃

Table 4- 7. Daily average values of weather data on Sentinel-2 observation dates in the dry season: in practice, 24-hour of weather data per each Sentinel-2 observation date were applied to the simulation of leached Zn soil dispersion.

Date	Wind speed	Solar radiation	Barometric pressure	Humidity	Air temperature
2019/05/20	1.12 m/s	1.95 kW/m^2	877.69 hPa	60.74 %	20.21 ℃
2019/06/29	1.29 m/s	1.34 kW/m^2	879.83 hPa	53.11 %	16.00 ℃
2019/07/19	0.96 m/s	1.87 kW/m^2	879.03 hPa	43.95 %	17.07 ℃
2019/09/07	2.41 m/s	1.71 kW/m^2	883.02 hPa	52.33 %	17.85 ℃

4.3.3. Impact of surface water on dispersion

At Pb-bearing Zn plant leach residue site, the accumulated amounts dispersed decreased by following MNDWI by Sentinel-2 were simulated.

Certain amounts of Pb- and Zn-bearing soils were simulated to be dispersed when the values of MNDWI were negative. The total of accumulated amount dispersed was 2.632 mg/m^2 when the values of MNDWI were negative. On the other hand, the total of accumulated amount dispersed was 0.606 mg/m^2 when the values of MNDWI were positive. The correlation between accumulated amount dispersed and the values of MNDWI were indicated as an inversely proportional (Figure 4-6).

The seasonal difference on Pb- and Zn-bearing soil dispersions were compared. Accumulated amounts dispersed in the dry season (2.369 mg/m^2) were relatively higher than the rainy season (0.254 mg/m^2) when the values of MNDWI were negative (Figure 4-7).

In the rainy season, accumulated amounts dispersed were low (0.425 mg/m^2 as total). The results agree with results from Chapters 2 and 3 which indicated that low humidity and wert conditions by rain falls had impacts on Pb- and Zn-bearing soil dispersion.

Results on 19 July and 7 September 2019 showed accumulated amounts dispersed as negative in the dry season. This is due to the net effects of deposition and redispersion by winds and dry conditions. The results indicate that dry condition on the surface of the source is a condition for Pb- and Zn-bearing soils easy to be dispersed and redispersed.

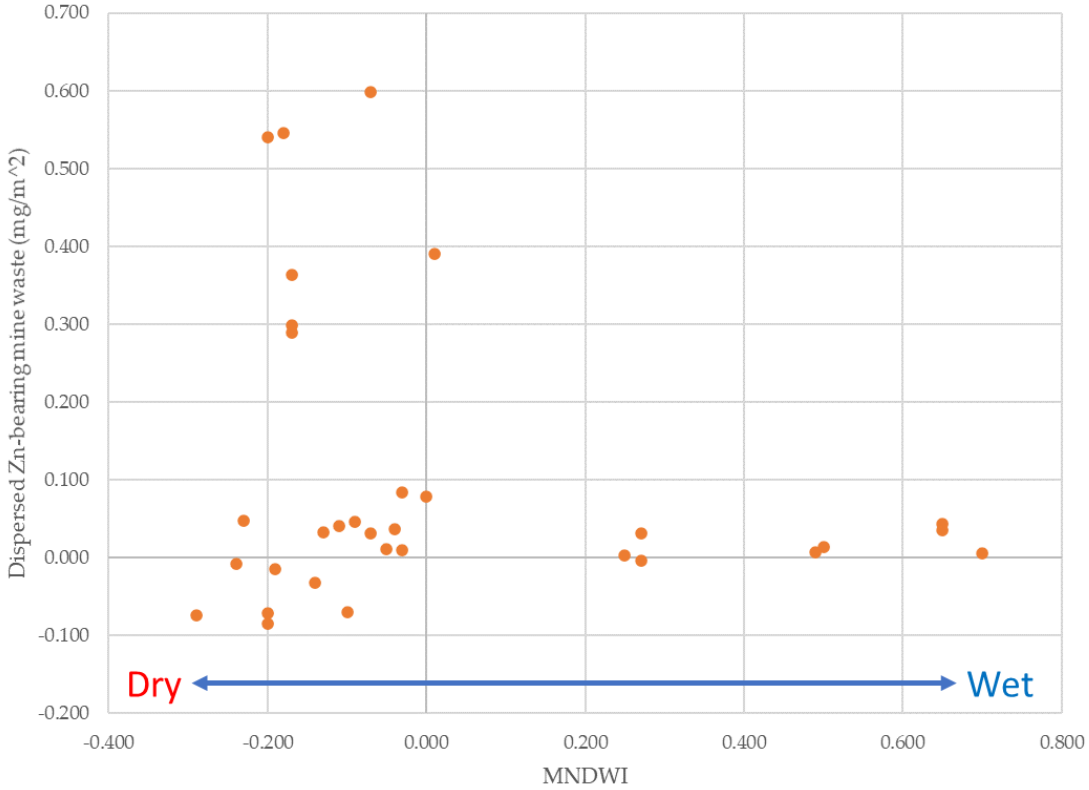

Figure 4- 6. Correlation between accumulated amount dispersed vs. values of MNDWI: Amounts of Pb- and Zn-bearing soil dispersion had a trend to decrease with the value of MNDWI increased to 1.

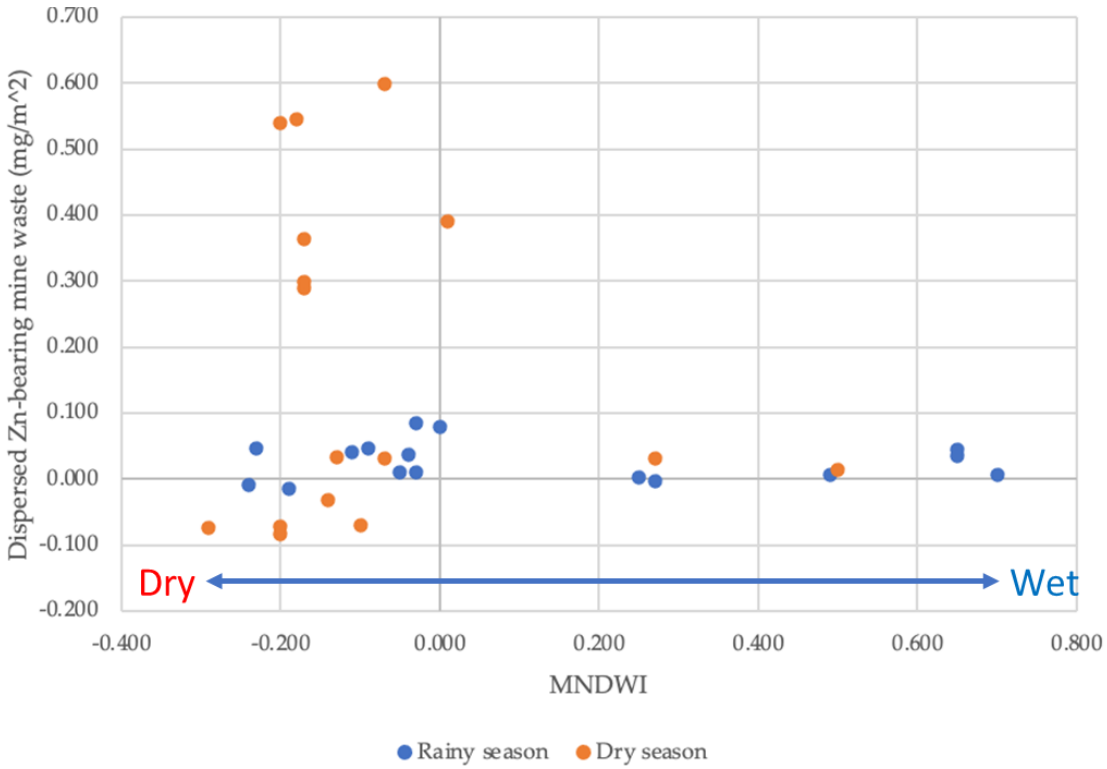

Figure 4- 7. Seasonal correlation between accumulated amount dispersed and MNDWI on Pb-bearing Zn plant leach residue site.

At the area #1, MNDWI indicated drier conditions on every Sentinel-2 observation date in 2019 (Figure 4-8 (a)). On 19 July 2019, accumulated amount dispersed (0.540 mg/m^2) were higher than other dates because the soils were dry but also strong winds blew from south sides of the source was another reason for the high amount of dispersion.

At the area #2, MNDWI indicated dry conditions on every Sentinel-2 observation date in 2019 (Figure 4-8 (b)). On 19 July 2019, accumulated amount dispersed (0.546 mg/m^2) were higher than other dates. It is because the soils were dry but also strong winds blew from south sides of the source was another reason for the high amount of dispersion. Also, accumulated amounts dispersed on 7 September 2019 and 6 November 2019 were negative. These were due to the net effects of deposition and redispersion by winds from west and northeast sides respectively.

At the area #3, MNDWI indicated some water covered the surface of the source through the year 2019 (Figure 4-8 (c)). On 29 June 2019, accumulated amount dispersed (0.390 mg/m^2) was higher than other Sentinel-2 observation dates. Strong and frequent winds blew from southeast side of the source was a reason for the high amount of dispersion. On 19 July 2019 and 7 September 2019, the values of MNDWI indicated drier surface on the source, but the accumulated amounts dispersed were negative: -0.070 mg/m^2 and -0.032 mg/m^2, respectively. These are due to the net effects of deposition and redispersion by winds and dry conditions, but also the results indicate that the surface of

the source had easy-to-disperse and redisperse environments especially on 19 July 2019: dry surface soil condition (-0.100), not-too-strong winds from south-southeast (0.625 m/s).

At the area #4, MNDWI indicated some water on surface soils of Pb-bearing Zn plant leach residue site through the rainy season 2019 (Figure 4-8 (d)). On 19 July 2019, accumulated amount dispersed (0.599 mg/m^2) were higher than other dates. It is because the soils were dry but also strong winds blew from south sides of the source was another reason for the high amount of dispersion.

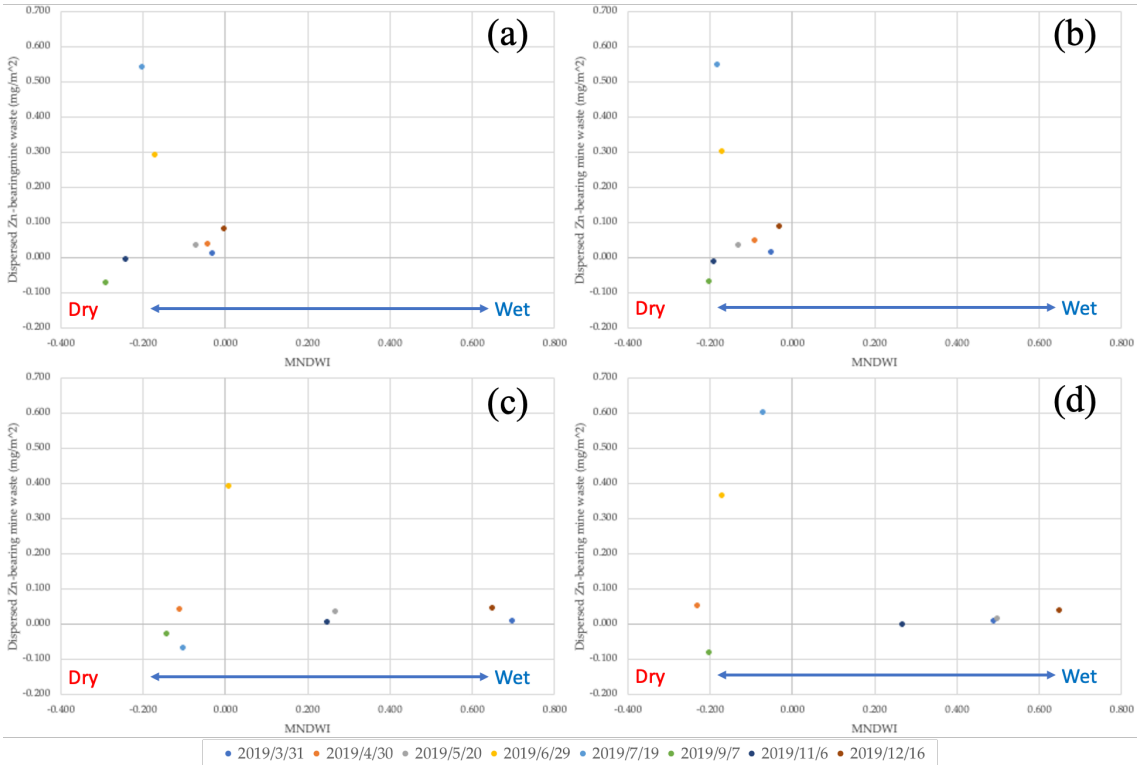

Figure 4- 8. Correlations between MNDWI and accumulated amount dispersed from each area of Pb-bearing Zn plant leach residue site: (a) correlation at area #1; (b) correlation at area #2; (c) correlation at area #3; and (d) correlation at area #4.

4.4. Discussion

Effects of water on the surface soils at Pb-bearing Zn plant leach residue site under the local environment in Kabwe were estimated by simulation of Pb- and Zn-bearing soil dispersion and the values of MNDWI of Sentinel-2 data analysis. However, the impacts of wind conditions affected on Pb- and Zn-bearing soil dispersion although wind speeds were gentle and calm (less than 1.0 m/s) on Sentinel-2 observation dates throughout the year 2019.

Figure 4-9 shows the simulated amounts of deposition in Chapters 2 and 4 and measured Pb content in soil by Mufalo et al [15] vs. distance from the source. Both the

simulated amounts of deposition and measured Pb content decreased with distance from the source. This indicates that the dispersion model used here can well express the Pb- and Zn-bearing soil dispersion from the tailing site. This means that Pb-bearing soil dispersion is mainly caused by dispersion by winds from the dumping site.

The simulated values with consideration of water conditions on the surface by MNDWI were lower than the values in Chapter 2. The results indicate that certain impacts of water to inhibit windborne heavy metal dispersion.

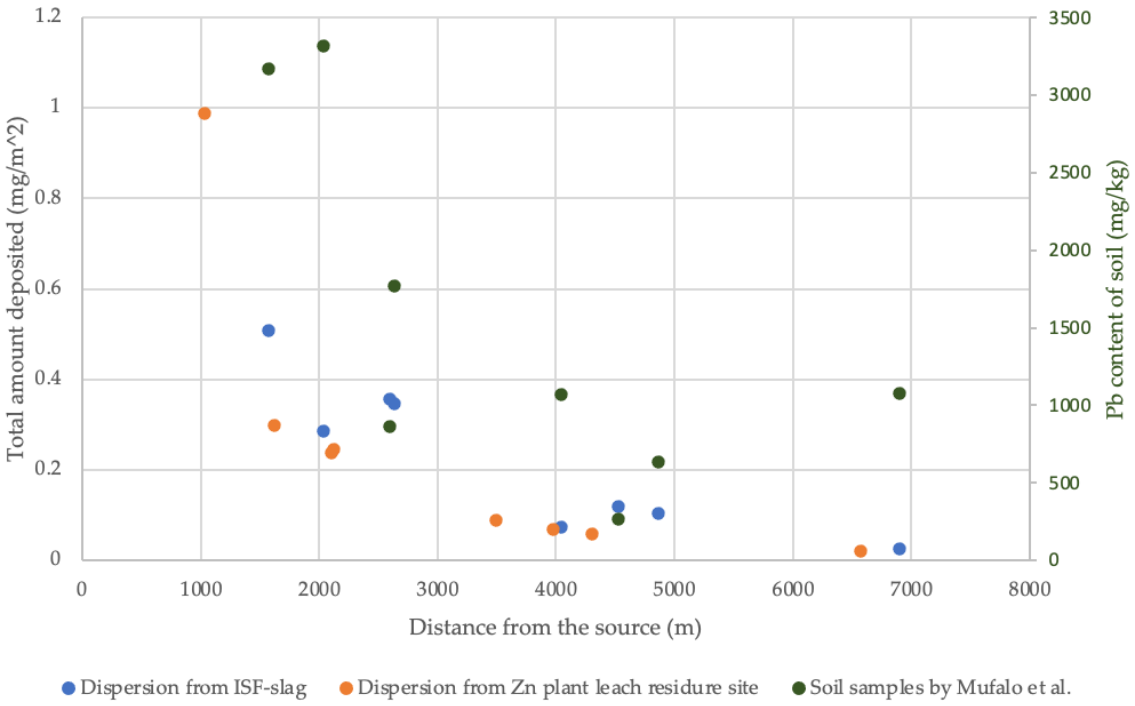

Figure 4- 9. Comparison of simulated results of Pb- and Zn-bearing soils from ISF-slag and Pb-bearing Zn plant leach residue sites and measured Pb content in soils by Mufalo et al. [15]: orange dots show Pb- and Zn-bearing soil dispersion with consideration of water condition on the surface of the source by MNDWI; blue dots show simulated results of Pb-bearing soil dispersion in Chapter 2; and green dots show measured Pb content in soils by Mufalo et al. [15].

For simplifying to understand and evaluate effects of surface water on heavy metal dispersion, simulation by using the average values of weather factors of the rainy and dry seasons of the year 2019 were conducted on the source. The wind direction was fixed as from southeast to northwest which was cleared to have the hugest impacts on heavy metal dispersion to the playgrounds through Chapters 2 and 3.

Table 4- 8. Average values of weather parameters in both rainy and dry seasons in the year 2019.

Value	Wind speed	Solar radiation	Barometric pressure	Humidity	Air temperature
Average of the rainy season	1.43 m/s	2.17 kW/m^2	872.62 hPa	68.65 %	23.08 ℃
Average of the dry season	1.44 m/s	1.88 kW/m^2	877.79 hPa	45.55 %	20.34 ℃

Figure 4-10 shows accumulated amounts dispersed had a trend to be decreased with values of MNDWI to 1. The results indicates that water can be an inhibition for Pb- and Zn-bearing soil dispersion, and MNDWI can be an indicator for evaluating windborne heavy metal dispersion mechanisms.

Figure 4-10 also shows the definite seasonal trends. In the rainy season, accumulated amounts dispersed were decreased with values of MNDWI to 1. Also, accumulated amounts dispersed were lower than the dry season totally. The results indicate that humidity and rain falls which can be other inhibition factors inhibited windborne Pb- and Zn-bearing soil dispersion even though the surface of the source was estimated as dry in the rainy season.

In the dry season, accumulated amounts dispersed were significantly decreased with values of MNDWI to 1. Also, all accumulated amounts dispersed were positive. The net effects by calculation were eliminated, the impacts of water on Pb- and Zn-bearing soil waste dispersion can be simply understood. Amounts dispersed were larger when MNDWI indicated water on the surface soils of the source in the dry season. Seasonal gaps of humidity and rain falls might affect on heavy metal dispersion with surface water.

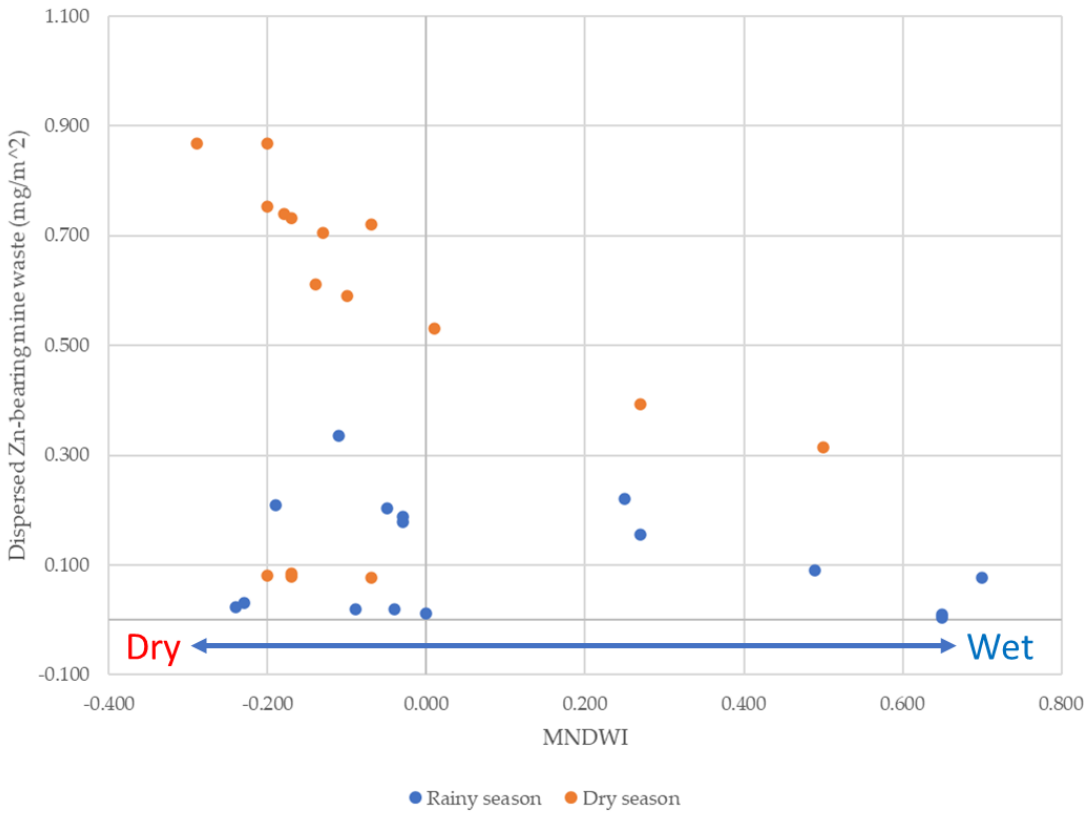

Figure 4- 10. Seasonal difference on correlation between amount of dispersed vs. MDNWI Pb-bearing Zn plant leach residue site.

4.5. Conclusion

For evaluation of dispersing situations and impacts of water at Pb-bearing Zn plant leach residue site where relatively covered by water throughout the year 2019, simulation of Pb- and Zn-bearing soil dispersion was performed with MNDWI under the actual and average weather conditions in the year 2019. The following results were found.

1. MNDWI was an indicator for monitoring the surface soil condition of the source and it is one of the parameters necessary for estimating Pb- and Zn-bearing soil dispersion.
2. Water is an effective inhibiting factor on windborne heavy metal dispersion. Pb-bearing Zn plant leach residue site covered by water was inhibited its abilities as the source for heavy metal dispersion.
3. Wind speeds and directions had huge impacts on windborne Pb- and Zn-bearing soil dispersion when the values of MNDWI were negative.
4. Lead- and Zn-bearing soil dispersion is affected from the seasonal and complex of local environmental conditions including weather and water in waste soils.

Water had impacts to inhibit Pb- Zn-bearing soil dispersion by wind, and the places where were covered by water as like as areas #3 and #4 of Pb-bearing Zn plant leach residue site were difficult to be the source for windborne dispersion. Even if water was estimated as an effective inhibition for the dispersion, soils containing heavy metals under the water was recognized as a reason of acidic mine drainage, which also had huge impacts on the environment around the mine area [16, 17]. In-depth understanding about environmental condition which can be factors of heavy metal dispersion is another of key parameters to propose effective countermeasures against heavy metal dispersion and remediation of soil contamination.

References

1. Nakamura, S.; Igarashi, T.; Uchida, Y.; Ito, M.; Hirose, K.; Sato, T.; Mufalo, W.; Chirwa, M.; Nyambe, I.; Nakata H.; Nakayama, S.; Ishizuka, M. Evaluation of dispersion of lead-bearing mine wastes in Kabwe District, Zambia. *Minerals*, 2021, *11*(8), 901.
2. Tembo, B. D.; Sichilongo, K.; Cernak, J. Distribution of copper, lead, cadmium and zic concentrations in soils around Kabwe town in Zambia. *Chemosphere*, 2006, *63* (3), 497-501.
3. Punia A. Role of temperature, wind and precipitation in heavy metal contamination at copper mines: a review. *Environmental Science and Pollution Research*, 2021, *28*, 4056 – 4072.
4. Ministry of Economy, Trade and Industry of Japan. Technical Manual of Ministry of Economy, Trade and Industry Low rise Industrial Source dispersion model (METI-LIS) ver. 3.02, March 2012. Available online: https://www.jemai.or.jp/tech/meti-lis/detailobj-6117-attachment.pdf (accessed on 30 May 2019).
5. Luhar, A.K. Analytical puff modelling of light-wind dispersion in stable and unstable conditions. *Atmos. Environ.* 2011, *45*, 357–368.
6. Japan Environmental Management Association for Industry; Ministry of Economy, Trade and Industry. Low Rise Industrial Source Dispersion MODEL. 2021. Available online: http://www.jemai.or.jp/tech/meti-lis/detailobj-6117-attachment.pdf (accessed on 28 October 2020).
7. Alaska Satellite Facility. ASF Radiometrically Terrain Corrected ALOS PALSAR products Product guide. ***2015***. Available online: https://asf.alaska.edu/wp-content/uploads/2019/03/rtc_product_guide_v1.2.pdf (accessed on 14 December 2021).
8. McFeeters, S. K. The use of the normalized difference water index (DNWI) in the delineation of open water features. *International Journal of Remote Sensing*, 1996, *17* (7).
9. Titolo, A. Use of time-series NDWI to monitor emerging archaeological sites: case studies from Iraqi Artificial Reservoirs. *Remote Sensing*, 2021, 13, 786.
10. Xu, H. Modification of nformalized difference water index (NDWI) to enhance open water features in remotely sensed *Imaginary. International Journal of Remote Sensing*, 2006, *27* (14), 3025 – 3033.
11. European Committee. Copernicus: Europe's eyes on Earth.https://www.copernicus.eu/en (accessed on 6 May 2020).
12. Jubilee Metals Group. Operations Lead, Zinc & Vanadium. Available online: https://jubileemetalsgroup.com/operations/lead-zinc-vanadium/ (accessed on 28 November 2021).

13. Bangira, T.; Alfieri, S. M.; Menenti, M.; van Niekerk, A. Comparing Thresholding with machine Learning Classifiers for Mapping Complex Water. *Remote Sensing*, 2019, 11, 1351.
14. European Space Agency. Sentinel Online. https://sentinels.copernicus.eu/web/sentinel/user-guides/sentinel-2-msi/product-types/level-1c (accessed on 6 may 2020).
15. Mufalo, W.; Tangviroon, P.; Igarashi, T.; Ito, M.; Sato, T.; Chirwa, M.; Nyambe, I.; Nakata, H.; Nakayama, S.; Ishizuka, M. Characterization and leaching behavior of playground soils in Kabwe, Zambia. In Proceedings of the International Symposium on Earth Science and Technology, Fukuoka, Japan, 26–27 November 2020; pp. 154–157.
16. Anawar, H.M. Sustainable rehabilitation of mining waste and acid mine drainage using geochemistry, mine type, mineralogy, texture, ore extraction and climate knowledge. J. Environ. Manag. 2015, 158, 111–121.
17. Kefeni, K.; Msagati, T.; Mamba, B. Acid mine drainage: Prevention, treatment options, and resource recovery: A review. J. Clean. Prod. 2017, 151, 475–493.

Chapter 5. General conclusion

5.1. Conclusions of all chapters

For analyzing and evaluating the mechanisms of Pb- and Zn-bearing soil dispersion and deposition by winds and other weather factors, three dispersion models and one redispersion model were designed and performed at the Kabwe mine. Also, the local weather conditions and water condition in the dumping site of the Kabwe mine were analyzed, and their impacts on heavy metal contamination were evaluated. The summaries of each chapter were shown below.

In Chapter 1, the importance, methods, and the site of study for the identifying mechanisms of heavy metal dispersion and deposition were described through discussion on environmental impacts and issues by heavy metal contamination in Kabwe by showing the background of mining activities and current situations of heavy mental contamination and its impacts on human health especially children and infants.

In Chapter 2, dispersion of Pb-bearing soils on ISF-slag site was simulated for reproducing Pb contamination of soil in Kabwe. Local weather data of the year 2019 were monitored in situ and used for the simulations. The plume model, weak puff model, and no puff model were adopted for calculation of Pb-bearing soil dispersion under different wind conditions. The results showed that Pb-bearing soil dispersion from the Kabwe mine was directly affected by wind directions and speeds in the dry season although it was not appreciably affected in the rainy season. This may be because the source strength is lower in the rainy season due to higher water content of the surface. This indicates that Pb-bearing soil dispersion patterns depend on the season. In addition, the distribution of the amount of deposited Pb-bearing soils around the mine corresponded to the distribution of Pb contents in soils. These results suggest that Pb contamination in soils primarily results from dispersion of fine mine soils.

In Chapter 3, local weather factors on Pb contamination were analyzed and simulated their impacts on Pb-bearing soil dispersion based on the results in Chapter 2. The weather in Kabwe was calm through the year, but there were significant differences of solar radiation, barometric pressure, humidity, and air temperature between the rainy and dry seasons. Correlation between wind speed and solar radiation was the inversely proportional, and the relationships had effects on the accumulated amounts deposited by simulations. High and low wind speeds did not affect on the accumulated amounts deposited at certain distances from the source. Wind directions had huge impacts on dispersion and deposition areas.

In Chapter 4, for evaluation of dispersing phenomena and impacts of water bodies at Pb-bearing Zn plant leach residue site partially covered with water through a year, simulation of Pb- and Zn-bearing soil dispersion was performed with modified difference water index (MNDWI) under the actual weather conditions in the year 2019. MNDWI

was demonstrated by data analysis of Sentinel-2 datasets which were acquired throughout the year 2019. MNDWI was an indicator for monitoring the surface soil condition of the source and it is one of the parameters necessary for estimating Pb- and Zn-bearing soil dispersion. Water is an effective inhibiting factor on windborne Pb- and Zn-bearing soil dispersion. Water was expected its high abilities for inhibition of the dispersion by winds. Wind speeds and directions had huge impacts on windborne Pb- and Zn-bearing soil dispersion when MNDWI indicated negative values. Pb- and Zn-bearing soil dispersion is affected from the seasonal and complex of environmental conditions including weather and water in waste soils.

5.2. Expected practical utilizations of the study results

In this study, mechanisms of Pb- and Zn-bearing soil dispersion and deposition from the Kabwe mine were clarified, application of three dispersion models and one redispersion model were estimated, and impacts of the local weather and water conditions on the source soils were analyzed and evaluated. In-depth understanding about environmental condition which can be factors of heavy metal dispersion is a key issue to propose effective countermeasures against heavy metal dispersion and remediation of heavy metal contamination.

In this study, data quality and volumes were limited. As issues for next step for improving simulations of the Pb- and Zn-bearing soil dispersions in Kabwe, the following items must be performed:

1. Preparing the networks and infrastructure for observations of local weather, soils, terrain, land coverage and human activities, and
2. Tuning parameters of simulation formula for improving accuracy of the results.

Enrichment of datasets are important activities to understand local conditions around the Kabwe mine, and fill gaps between simulation results and the real. As the next step, the author will consider applying land coverage to the simulation for Pb- and Zn-bearing soil deposition surrounding the Kabwe mine by analyzing satellite datasets and soil samples.

Through this study, dispersion simulation models were developed with Python and database as a small system on one laptop PC. All collected weather datasets, satellite images, geographical information of Kabwe and calculated results were archived and managed on an open-free database, and all analyses about weather data, terrain features, MNDWI and dispersion simulations were processed by Python, an open-free computer script. The ability to develop systems without high-specification servers has advantages of being easy to implement with low cost and apply into other countries for monitoring and mitigating heavy metal contaminations and environmental issues as like this study in Kabwe.

Developing remediation plans around the mine site will be discussed for determination of the priority areas by evaluating impacts of the local wind direction and

speed seasonal patterns through simulation of heavy metal dispersion. Although acidic mine drainage has to be an issue and managed, inhibition by water coverage is effective for reduction of windborne heavy metal dispersion. MNDWI is another indicator to monitor the waste site condition. Effective and economical remediation contributes not only promoting sustainable mine development but also mitigating health risks of infants and children in Kabwe caused by heavy metal contamination.

For example, the methods of this study can be applied and followed to Kabwe Mine Pollution Amelioration Initiative (KAMPAI) as a part of Science and Technology Research Partnership for Sustainable Development (SATREPS) founded by Japan International Cooperation Agency (JICA) and Japan Science and Technology Agency (JST) and Demonstration and Risk-based Implementation of New lead remediation approach in Kabwe (DRINK) as a part of Accelerating Social Implementation for SDGs Achievement (aXis) founded by JST. The University of Zambia and Hokkaido University have cooperated to monitor the lead contamination and apply remediation methods for mitigating environment around the Kabwe mine since 2015. The methods for Pb- and Zn-bearing soil dispersion simulation can detect and evaluate the remediation effectiveness by monitoring the environment around the Kabwe mine, and the suggest kaizen plans for remediation to lead better environment for the future.

Moreover, many mine sites like the Kabwe mine which disperses heavy metals and causes of contaminations are in the world. Each site has unique terrain, climate as well as types of mineral development. The results of this study can be the trigger for applying simulations with considering these factors into the mine activities in the world. Through the development of heavy metal dispersion with local environmental data, the author would like to work on research and resolving issues which aim to social implementation in various places as the next step.

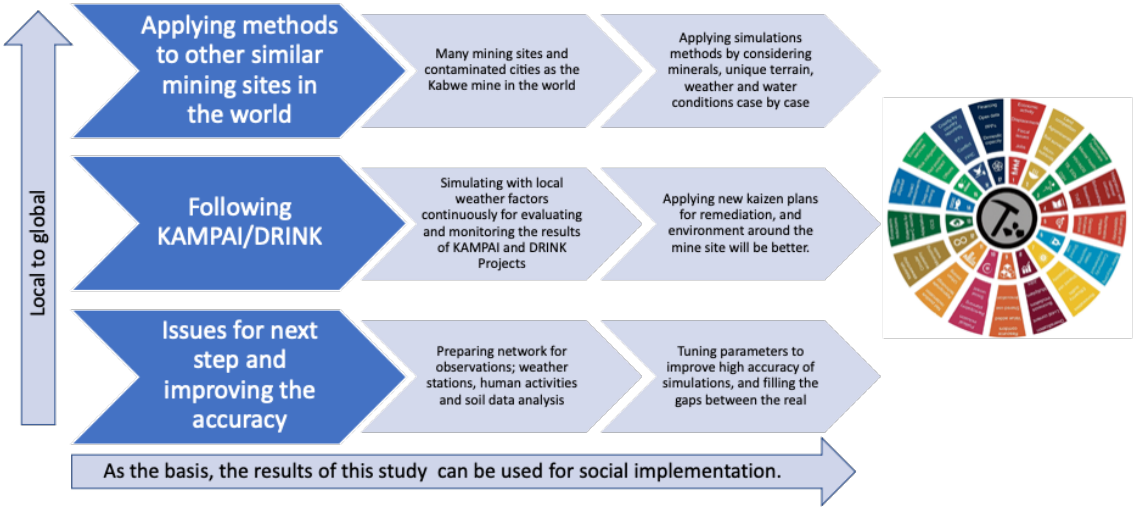

Figure 5- 1. Implication

Acknowledgement

First of all, I would like to thank my supervisor, Professor Toshifumi Igarashi to make this dissertation possible and for all their reviews and supports.

Also, I would like to thank Professor Tsutomu Sato and Associate Professor Mayumi Ito to review and give me helpful comments as deputy investigators for my study.

I am glad to join the research projects, "Kabwe Mine Pollution Amelioration Initiative" as one of JST/JICA SATREPS and "Demonstration and Risk-based Implementation of New lead remediation approach in Kabwe" as one of JST aXis. I would like to thank to Professor Mayumi Ishizuka, Associate Professor Shota Nakayama and other Japanese and Zambian members of these projects and JST and JICA staff for supporting my research in Kabwe, Zambia.

Moreover, I would like to thank all members of Japan Space Systems for their supports in conducting this study in parallel with assignments at Japan Space Systems.

Finally, I would like to thank my family, and I conclude.